AZOBENZENE-LIQUID CRYSTAL COMPOSITE FOR FABRICATION OF OPTICAL STORAGE DEVICES

GAN SIEW MEI

UNIVERSITI MALAYSIA PAHANG

AZOBENZENE-LIQUID CRYSTAL COMPOSITE FOR FABRICATION OF OPTICAL STORAGE DEVICES

GAN SIEW MEI

Thesis submitted in fulfilment of the requirements for the award of the degree of
Master of Science in Advanced Materials

Faculty of Industrial Sciences and Technology
UNIVERSITI MALAYSIA PAHANG

OCTOBER 2015

SUPERVISOR'S DECLARATION

I hereby declare that I have checked this thesis and in my opinion this thesis is satisfactory in term of scope and quality for the award of the Master of Science in Advanced Material.

Signature:
Name of Supervisor:
Position:
Date:

Signature:
Name of Co-Supervisor:
Position:
Date:

STUDENT'S DECLARATION

I hereby declare that the work in this thesis is my own except for quotations and summaries which have been duty acknowledged. The thesis has not been accepted for any degree and is not concurrently submitted for award of other degree.

Signature:
Name: GAN SIEW MEI
ID Number: MSM14001
Date:

My special dedication
to my beloved parents; Mr. Gan Jok Hui and Mrs. Lim Geck Sim, and
to all of my loving and understanding family members.

ACKNOWLEDGEMENTS

This thesis work is both a challenge and an experience to cherish for a lifetime. Although a lot of hard work and sacrifices did come from my part, there are many without whom this work would not come to completion.

First and foremost, I am grateful and would like to express my sincere gratitude to my supervisor Dr. Gurumurthy Hegde for his germinal ideas and invaluable guidance in making this project possible. I appreciate his consistent support from the first day I start this work to these concluding moments. I am truly grateful for his tolerance of my naive mistakes. I also would like to express very special thanks to Yuvaraj A R for his suggestions and co-operation throughout the project.

Secondly, my sincere thanks go to Shoriya Aruni binti Abdul Manaf, my best friend in the laboratory who has continuously accompanied and helped me in my project. Sincere thanks also go to all my lab mates and staffs of Faculty of Industrial Sciences and Technology (FIST) who helped me in many ways and made my stay at Universiti Malaysia Pahang pleasant and unforgettable. Many special thanks go to all laboratory assistants for their excellent co-operation and supports during my work in the laboratory.

Finally, I acknowledge my deepest gratitude to my parents for their love, dreams and sacrifices throughout my life. I cannot find the appropriate words that could properly describe my appreciation for their support and faith in my ability to achieve my goals.

ABSTRACT

The primary purpose of this research is to characterized four series of azobenzene with different substituents to be employed as azobenzene-liquid crystal composite mixture in optical storage devices. Firstly, the azobenzene substituents effects on liquid crystallinity were observed under polarising optical microscope and their phase transition temperatures were confirmed by calorimetric study. After that, photoisomerisation studies were conducted in solution form by using UV–Vis spectrophotometer in order to measure the time required for *cis–trans* isomerisation in thermal back relaxation process. In azobenzene with fluorine addition, monofluoro azobenzene with ester functional group gave smectic-A and nematic phases with thermal back relaxation around 22 hours. Better results were obtained by azobenzene with olefinic terminal chain; the presence of alkene enhanced the thermal back relaxation to 45 hours due to the unsaturated bonding in the molecule, capable of photo-crosslinking. However, incorporation of group-17 elements such as fluorine, chlorine, bromine and iodine in the olefinic azobenzene shorten the thermal back relaxation time although smectic-A and nematic phases were generated. Prototype of optical storage devices created showed good stability with high contrast display due to their thermal back relaxation and mesophases. This study is a bold step to tailor the property of light-sensitive azobenzene to make them suitable for optical storage device applications. Presented data give rich information about structure property relations where one can able to control the molecular structure using light.

ABSTRAK

Tujuan utama kajian ini adalah untuk mengkaji empat siri azobenzena dengan peganti yang berbeza untuk digunakan sebagai bahan komposit azobenzena–hablur cecair dalam penghasilan peranti storan optik. Perbezaan dalam pengantian azobenzena memberikan kesan ke atas keupayaannya membentuk hablur cecair yang mana ditentukan melalui mikroskop optik, manakala suhu peralihan fasanya pula ditentukan melalui kajian kalorimetri. Seterusnya, kajian pengisomeran foto telah dijalankan dengan menggunakan spektrofotometer UV–Vis bagi menentukan masa yang diperlukan untuk proses pengisomeran *cis–trans* atau lebih dikenali sebagai proses pengenduran balik haba. Dalam azobenzena dengan kehadiran fluorin, azobenzena monofluoro dengan kumpulan berfungsi ester menunjukkan fasa smektik-A dan nematic, manakala proses pengenduran balik haba mengambil masa selama 22 jam. Keputusan yang lebih baik telah diperolehi oleh azobenzena olefinik di mana kehadiran alkena telah meningkatkan masa proses pengenduran balik haba, iaitu selama 45 jam berikutan ikatan tidak tepu dalam molekulnya berkebolehan untuk pempolimeran foto. Walau bagaimanapun pengantian unsur-unsur kumpulan-17 seperti fluorin, klorin, bromin dan iodin dalam azobenzena olefinik telah memendekkan masa pengenduran balik habanya walaupun berkebolehan membentuk fasa smektik-A dan nematik. Prototaip peranti storan optik yang dibentuk menunjukkan kestabilan tinggi dengan paparan kontras yang jelas dengan kehadiran ciri-ciri hablur cecair bersamaan dengan proses pengenduran balik haba yang lama. Oleh itu, kajian ini merupakan satu langkah bagus bagi menala molekul sensitif-cahaya untuk menghasilkan peranti storan optik. Data yang diperolehi memberikan maklumat berguna mengenai hubungan antara struktur molekul dengan cir-ciri bahan bagi membolehkan struktur bahan dikawal dengan menggunakan cahaya.

TABLE OF CONTENTS

LIST OF TABLES

LIST OF FIGURES

ABBREVIATIONS

CE	Conversion efficiency
CHN	Carbon, nitrogen, and hydrogen
Cr	Crystalline
DMSO	Dimethyl sulfoxide
DMAP	4-(N, N-dimethylamino) pyridine
DSC	Differential scanning calorimetry
DCC	1,3-dicyclohexylcarbodiimide
E	*Trans*
EPH	*p*-(*p*-ethoxyphenylazo)phenyl hexanoate
FT-IR	Fourier transform infrared
h	Hours
ITO	Indium tin oxide
Iso	Isotropic
LC	Liquid crystal
LCDs	Liquid crystal displays
MBAA	p-methoxybenzylidene-p-n-butylaniline
MS (FAB+)	Mass spectrometry - Fast atom bombardment
Min	Minutes
m	multiplet
m.p.	Melting point
NMR	Nuclear magnetic resonance
N-I	Nematic-Isotropic
N	Nematic

POM	Polarising optical microscope
q	Quadrate
Rf	Retardation factor
Sec	Seconds
s	Singlet
S_0	Ground state
S_1	First excited singlet state
S_2	Second excited singlet state
SIS	Styrene-isoprene-styrene
$T_{N\text{-}I}$	Nematic–isotropic transition temperature
T_c	Clearing temperature
T_m	Melting temperature
t	Triplet
TMS	Tetramethyl silane
TLC	Thin-layer chromatography
Sm-A	Smectic-A
UV–Vis	Ultraviolet and visible light
Z	*Cis*

CHAPTER 1

INTRODUCTION

1.1 THE INTERMEDIATE STATE BETWEEN SOLID AND LIQUID

The state of crystalline solids comprise of long-ranged ordered molecules while isotropic liquids are of disordered molecules. Liquid crystals are matter in a state exist between the crystalline solid and isotropic liquid state (Chandrasekhar, 1977; Collings and Hird, 1997 and Demus et al., 2011). As the intermediate phases, they are more order than liquid but less order than crystal. The some extend of order among the molecules make them exhibits several physical properties of crystals but having fluidity comparable to liquids. For this reason, they are called liquid crystals, and can be properly named as mesomorphic phases.

The two most commonly encountered liquid crystals are thermotropic liquid crystals, in which the phase transitions are realised by varying temperature, and lyotropic liquid crystals, in which the phase transitions are obtained by the action of solvents. In addition, certain systems that possess the ability to form both thermotropic as well as lyotropic mesomorphism are called as amphotropic. The thermotropic liquid crystals have become more commonly known owing to their employment in photo-optic technology such as liquid crystal displays (LCDs) and photonic devices. The lyotropic liquid crystals on the other hand, are responsible for many chemical and biological processes. Since this thesis deals with only thermotropic liquid crystals, discussion about other type of liquid crystals are not included here.

The common characteristic between thermotropic and lyotropic liquid crystals is the shape anisotropy of their structural units make up of elongated molecules, with a rigid central region and flexible ends. Such anisotropic molecules, called mesogens, are the primary factor for the formation of liquid crystalline phases. The interactions between these anisotropic mesogens lead to orientational order in the system. Molecules in orientational order tend to orient their long molecular axes in specific direction on a long-range basis. The preferred direction is known as director, denoted by the unit vector n. The amount of orientational order in a liquid crystalline material can be determined by calculating its order parameter. In an isotropic liquid, the order parameter is equal to zero, whereas in crystalline solid, it is one. On the other hand, the order parameter of liquid crystals ranged between 0.3 and 0.9. So, having the small degree of order produces anisotropic nature in liquid crystal systems.

Due to the anisotropic nature, the properties of the liquid crystals depend on direction they are measured. That is to say, the optical, electrical, magnetic and other properties of the material vary when measure in different direction, either parallel or perpendicular to their length. The same holds true for liquid crystal materials in crystalline solid state. In contrast, liquid crystal molecules in liquid state are energetic and found to be in constant random motion. This causes them to lose the anisotropic nature, and thus become isotropic. This means their properties are uniform in all direction although the molecules are anisotropic. Hence, with this difference it is possible to distinguish between the liquid crystalline state and the liquid state.

The anisotropy of reflective index is one of the optical properties of liquid crystal characteristic that give birefringence colour and texture to the materials. Light passes through liquid crystal materials are broken into two components, travel with different velocities. Thus, a beautiful birefringence colours and textures can be observed under a polarising optical microscope. The difference in colour and texture can provide a lot of information about the macroscopic structure, useful for identification of liquid crystal phases. Manipulating the unique optical properties of liquid crystals by external fields enable them to be used in many applications.

Apart from orientational order, liquid crystals also show positional order. Positional order refers to the extent an average molecule or group of molecules shows a periodic order with translational symmetry as crystalline state shows. However, not all liquid crystal phases possess positional order. If they exhibit positional order, the molecules are constrained to occupy specific sites in the three dimensional lattice and form layers structure. An example of liquid crystal phase exhibiting the positional order is given in the following section.

1.2 PHASE TRANSITION IN THERMOTROPIC LIQUID CRYSTAL

Basically, there are different types of thermotropic liquid crystals exist, classified based on the anisotropic shape of mesogens. The traditionally know thermotropic liquid crystals are rod-shape molecules. Such liquid crystals are called calamitic liquid crystals. However, it has been found that bent-core molecules whose shape resemble a banana shape, results in a new class of liquid crystals, called banana liquid crystals (Niori et al., 1996; Pelzl et al., 1999; Jákli et al., 2002; Elamain, Hegde and Komitov, 2013). Each of these classes exhibit different intermediate phases with the changes in amount of order under the influence of temperature.

As the temperature increases, liquid crystals in crystalline solid state undergo transition to isotropic liquid state. During the process of transition, the thermal motion in the molecular lattice increase until reach a point where orientational and positional order are completely destroyed. Thus, result in the transition from the bright birefringence crystalline state to dark isotropic state. It is between this order and disorder states that liquid crystalline phases can be found (figure 1.1). Liquid crystalline phases are stable within specific temperature range before they become the disordered liquid. The intermediate phases present in thermotropic liquid crystals can include nematic and smectic-A phases, depending on the amount of orientational and/or positional order as the temperature increases. These intermediate phases are collectively known as mesophases.

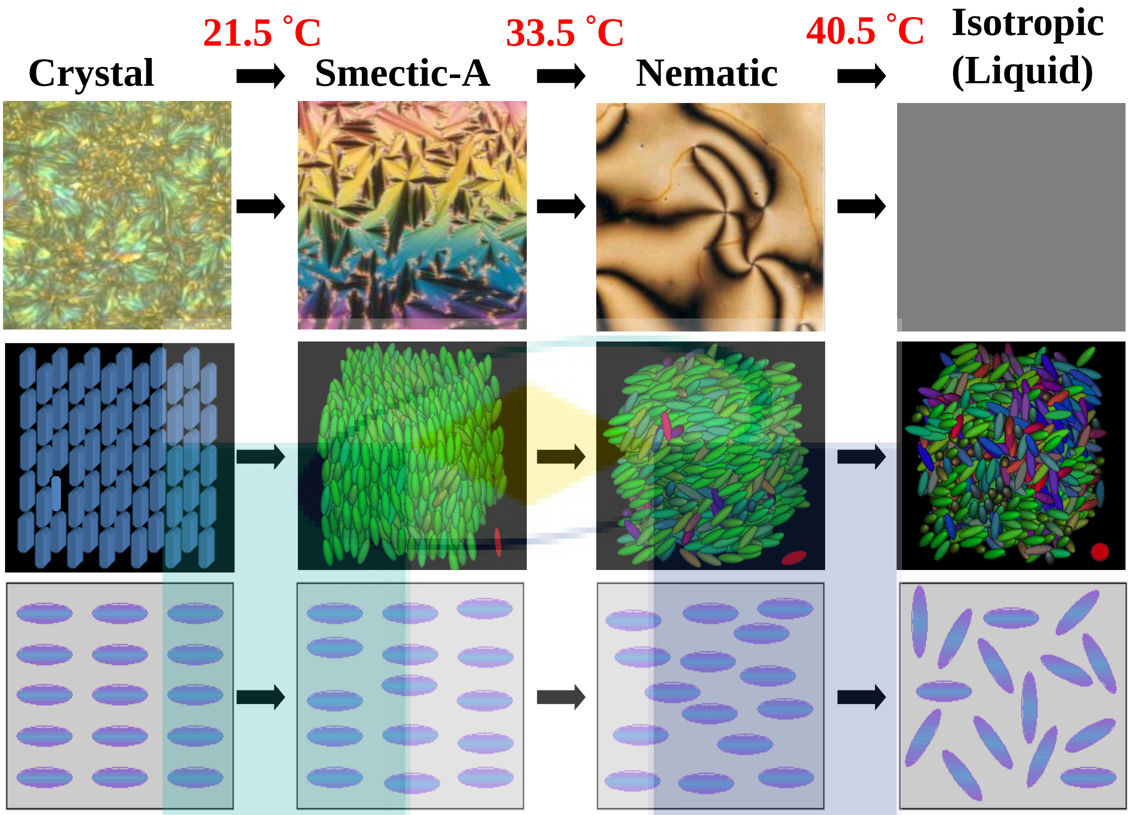

Figure 1.1: Phase transition of thermotropic liquid crystals.

1.2.1 Nematic

Nematic mesophase is the simplest liquid crystal phase of all, yet technologically most important phase. This phase is near to isotropic state, in which the molecules are the least order but maintained a preferred orientational order. In figure 1.2, it can be noticed that the molecules have no positional order, but the long molecular axes align vertically along the director. With only the orientational order means that the nematic phase has high degree of fluidity. This fluid nematic phase has a low viscosity, and when combined with the anisotropic nature is the basis for the operation of LCDs. The anisotropy in fluid nematic materials are designed so that molecular orientation can be switched by application of a low-magnitude electric field, results in large optical effects that make displays application possible (Tilton, 1992).

Under the polarising optical microscope, in general, the nematic phase can be identified by bright birefringent colour with schlieren texture. However, there may be small areas of birefringence with black tread-like defects. The dark regions occur when the orientation of the director is completely parallel or perpendicular to one of the polarisers. Thus, in these regions the light passing through the sample only experience one refractive index, and so behaves as if it were passing through an isotropic liquid.

1.2.2 Smectic-A

The smectic-A mesophase can be identified under the polarising optical microscope by a focal conic fan texture, arises because of the layers structure. The molecules maintained the general orientational order of nematic, but have also positional order forming layers structure. The thickness of each layer is about one to two molecules size. When the smectic-A phase is heated, the positional order is lost, and subsequently produces the nematic phase. Additionally, when orientational order is lost as well, it gives rise to the isotropic liquid. On average, the orientation of the molecules in smectic-A phase is normal to the layer planes with their centres irregularly spaced within each layers. The motions of molecules are restricted to within this layer where they behave in fluid-like fashion (figure 1.3). In fact, the fluidity in the layer is an essential characteristic of all smectic layers for commercial applications.

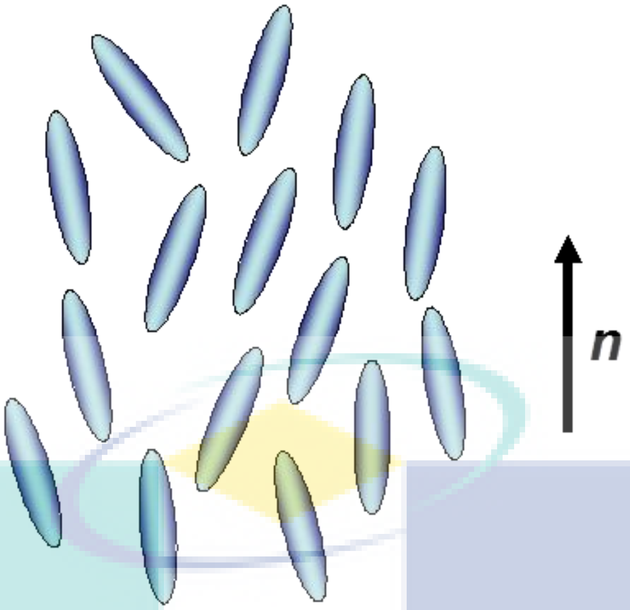

Figure 1.2: Molecular arrangement in the nematic phase, *n* denotes the director.

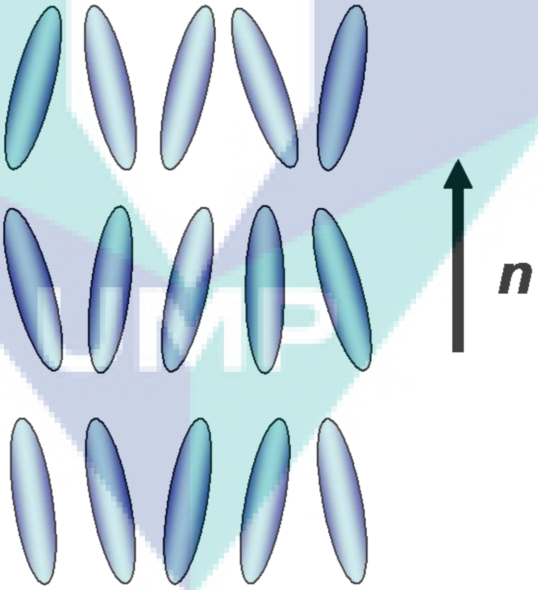

Figure 1.3: Molecular arrangement in the smectic-A phase, *n* denotes the director.

1.3 PHOTOISOMERISATION OF AZOBENZENE

On the other hand, azobenzene is a large class of compounds with the characteristic azo linkage (–N=N–) connecting two phenyl rings. In recent years, much interest has been taken in their photoisomerisation property. Azobenzene may exist as two geometric isomers, the *trans* and *cis* forms, also referred to as *E* and *Z* forms, respectively. The two configurations differ in the direction of the central azo bonds. In the energetically more stable *trans* state, the two bonds linking the azo group to the aromatic rings are parallel, resulting in an elongated shape of the molecule (Schulze et al., 1977). In the metastable *cis* state, the angle between the two bonds is 120 degrees and the molecule adopts a bent shape.

Upon absorption of ultraviolet (UV) light at wavelength around 365 nm, the energetically more stable *trans* isomer transforms to the *cis* isomer. The reverse transformation of the *cis* to *trans* isomerisation can be brought about by irradiation with visible light (in the range of 400 – 500 nm). As an alternative, the latter change can also occur spontaneously in the dark by a process known as thermal back relaxation. A schematic representation of the reversible *trans*–*cis* isomerisation process is given in figure 1.4.

The most important property that changes as a result of the photo-driven isomerisation is the geometry of the azobenzene molecule. While the *trans* isomer has a rod-like shape, the *cis* isomer is bent-shaped molecule. As the shape changes, the geometrical dimension of the azobenzene molecule also changes. For example, in a typical azobenzene, *p*-(*p*-ethoxyphenylazo)phenyl hexanoate (EPH), it has been found that the length (or end-to-end distance) of the *trans* isomer is 2.2 nm, whereas the *cis* isomer is substantially smaller being about 1.6 nm as shown in figure 1.5 (Nair et al,. 2004). The conversion decreases the distance between the 4 and 4’ ring position from 9.0 to 5.5 Å (Sato et al., 1988). It is this combination of dramatic change in the shape and length of the molecule in conjunction with the high photochemical stability of azobenzene, which lies at the heart of the phenomenon of photo-induced phase transitions.

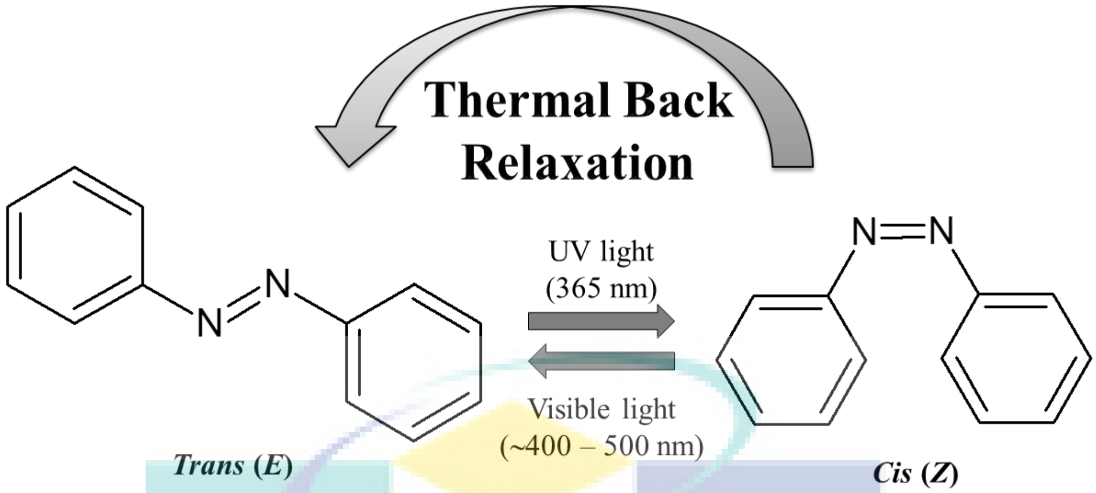

Figure 1.4: A schematic representation of the *trans–cis* (*E – Z*) isomerisation.

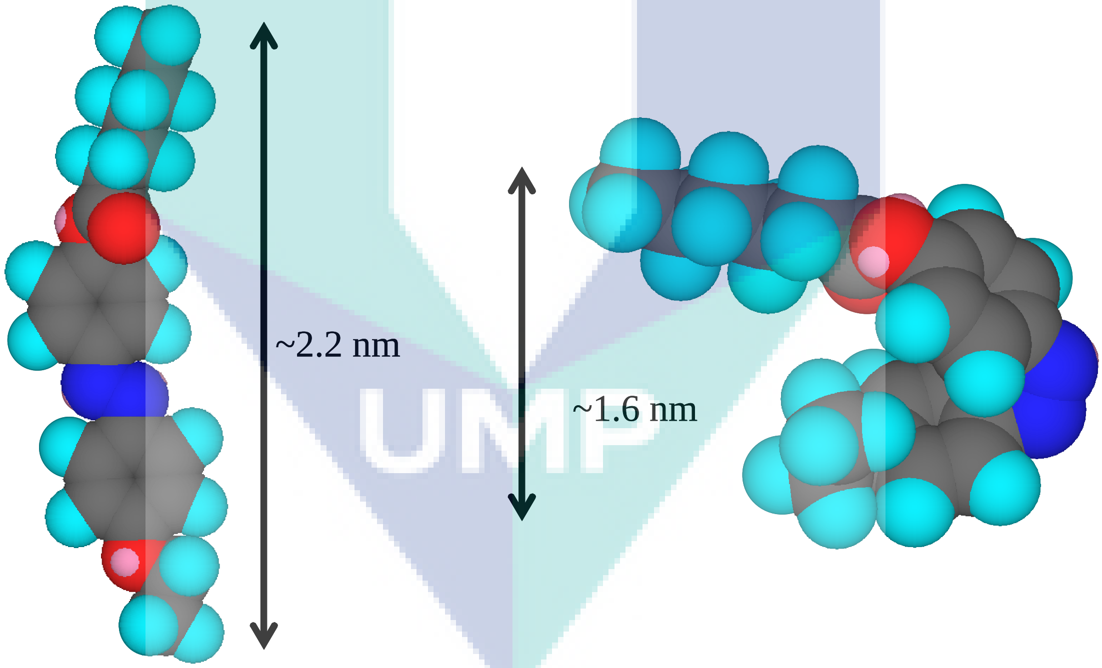

Figure 1.5: An example of the isomer dependent dimension of an azobenzene derivative, EPH, for photo-induced phase transition.

1.4 PHOTO-INDUCED PHASE TRANSITION

Soft materials such as liquid crystals are well-known for their self-assembling nature, in which the microscopic molecular interactions induce a large change in macroscopic properties (Fuji et al., 2014). If a small portion of liquid crystal molecules changes their orientation in response to an external stimulus, such as electric or optical field, molecules in bulk also follow the changes. The reorientation of the molecules causes them to dramatically alter the properties of light reflected from or transmitted through them. This in turn affects the birefringence of the system. It has been shown that even in non-photo absorbing liquid crystals, optical fields, although large in magnitude is required, can be used to reorient the molecules and thus causing the same optical effect (Santomato et al., 1986). So what happen when a small amount of photoactive molecules, such as azobenzene, are incorporated as a dopant into the non-photo absorbing liquid crystals? The answer is, it allows the guest-host mixture to exhibit photo-induced phase transitions when light of particular wavelength is shined, thus reducing the magnitude of light requirement.

As mentioned earlier, the heart of photo-induced phase transition phenomenon in the self-assembling system is the changes in geometrical dimension of azobenzene molecules under exposure of light. Having a rod shape, the *trans* isomer of the azo dopant is favourable for the stabilization of liquid crystalline phase, due to the shape compatibility with the host mesogens (Prasad et al., 2004). Therefore, it supports the orientational order of the host molecules, and the material appears as birefringence under the microscope. When the UV light is shined, the photoactive molecules undergo shape transformation to bent-form, acting like an ‘impurity’ and thus destabilized the system. Hence, the *trans–cis* photoisomerisation introduce a local region of reduced orientational order, as compared to the regions of the host molecules. If the reduction is large enough, it may result in the formation of isotropic domains, and thus leads to an order-to-disorder transition at the irradiated sites to appear as dark regions under the microscope. This is very interesting because the influence of the conformation changes in azobenzene molecules could become very large, making the entire liquid crystal system to demonstrate photo-induced transition from order to disorder (Ikeda, 2003).

1.5 PROBLEM STATEMENT

The optical storage devices are devices for storing and processing optical images in recyclable operating systems. Optical technology is used to record and store images on the device. The principle of image-storing involves selective controlled birefringence of the liquid crystal media prior to photoisomerisation of azobenzene as described earlier (Jayalakshimi et al., 2009). Optical storage devices that demonstrate i) high sensitivity to light such that it can be reversibly driven between two states, ii) high stability over long periods of time, iii) high rewriting-ability and switchable between states with a reasonable efficiency and iv) energy and cost saving are always desirable.

Due to the ever growing demand for photonic devices, the present optical storage technology suffers from an absence of functional organic materials and synthesizing light sensitive molecules becomes a daunting task. Azobenzenes, due to their unique light sensitive properties is being exploited in many areas of photonics, but their metastable state in *cis* configuration give them short thermal back relaxation, which is a disadvantage for optical storage applications. Thus, the main issue concerning is their stability whereby they unable to withstand for a long time due to their photoisomerisation nature. In fact, a necessary condition in creating optical storage devices is to employ materials with slow thermal back relaxation, that is, the *cis* isomers have lifetime long enough so that the optically generated information can be stable for the required period of time. However, the simple fact is that present optical storage industry suffers from an absence of functional organic materials that can apply to the next generation optical rewriting technology. For this reason, the creation of optical storage devices is a challenging subject.

1.6 OBJECTIVES

The aim of this research is to study several novel azobenzene compounds which were used as an attempt to create optical storage devices. The novel materials satisfy the conditions for creating optical storage devices with high stability, better sensitivity to light and cost effective are investigated. With appropriate ring substitution azobenzene may lead to minor or major changes in mesogenic properties as well as their thermal back relaxation time. Azobenzene compounds with different substitution were studied to determine their liquid crystalline behaviour and also their light-induced isomerisation activity in liquid crystalline guest-host system. This eventually provides a path for the exploration of systems for obtaining long-term storage devices.

Specifically, the objectives of conducting this research are as follow:

i. To investigate the structure property relationship between azobenzene molecules and liquid crystalline property using POM and DSC.
ii. To characterize the light sensitive azobenzene with different substituent for their photosensitive isomerisation behaviour using UV–Vis spectrophotometer.
iii. To fabricate and evaluate the prototype of optical storage device using observed data.

1.7 SCOPE OF STUDY

1.7.1 Scope

Basically, this thesis consists of study and characterisation of new azobenzene derivatives for the purpose of creating optical storage device. The investigation reported in this work based on different azobenzene derivatives with different functional group substitution; which substituents constitute of spacer substitution, amide linkages, fluorine addition, electron-withdrawing group, and then photo-crosslinking units. The findings could enrich the knowledge in the field of photonics where one can tune the materials in a proper way.

Systematic characterization on their mesophase behaviour was done using polarising optical microscope (POM) coupled with hot stage, elucidated the importance of liquid crystallinity present in the molecules. Next, thermal investigations were done using differential scanning calorimetry (DSC) studies suggested the range of mesophases which is crucial for these studies. Using these data one can alter the mesophase ranges and systematically apply them for the device applications.

The obtained data suggested that these materials are compatible to be use as composite mixture for making optical storage devices. Due to the different substitution, varying from rigid core to flexible spacers, revealed novel information about thermal back relaxation time where one can able to systematically tune the photoswitching parameters using UV illumination system along with UV–Vis spectrophotometer. Using the materials investigation and findings, prototypes of optical storage devices were presented. Prototype fabrications mainly done on composite mixtures between light sensitive materials with liquid crystals suggested the flexibility to control them effectively and could be utilized in variety of applications.

The presented study showed broad scope in the area of photonics where by changing the amide linkage, fluorine substitutions, spacer addition, and photo-crosslinking molecular substitutions can help to improve the optical storage devices.

1.7.2 Limitations

In a broad sense, it is difficult to make the optical storage device based on data obtained from this thesis alone. This study may be suggestive of which materials may be found promising for applications to optical storage devices, but additional research would be needed to verify whether the findings could be generalize elsewhere. The present study did not examine the materials stability in a real life situation such as indoor and outdoor situation. The photoisomerisation behaviour might be different under the hot weather and influence of sun light, and it would alter the devices performance. Moreover, the device built here is still considered a prototype and the development is still in its very early stages. For the devices to be competitive in the age of information technology, attractive design will be required so that the devices built not only for user-friendly usage, but also to make them robust and extensible.

1.8 RATIONALE AND SIGNIFICANCE OF RESEARCH

The proposed materials will reduce the cost of fabrication and will boost the information technology sector. These materials can be utilized in development of memory storage devices for creating cost effective name cards, advertising board and also UV rewritable board. This project can be a good work to find new and economical ways of energy saving solutions in the information storage technology. The novel azobenzene derivatives will undoubtedly play a significant role in these developments.

CHAPTER 2

LITERATURE REVIEW

2.1 PHOTOCHROMIC MATERIALS FOR REWRITABLE STORAGE

Looking into the development of optical storage media itself, it is obvious that the read only media, CD-ROM and CD-AUDIO, steadily losing their dominant position. They are being replaced by those rewriteable or recordable media, CD-R and CD-RW. In the past, organic photochromic materials have not been considered as viable material for optical storage technology because of insufficient reliability. However, the situation is now dramatically changing. With the worldwide acceptance of rewritable storage device, which uses photochromic compound as the memory medium, organic photochromic materials are now anticipated as promising candidates for rewritable storage media. The rewritable recording media have been realised using additional functional recording layers into the discs, which consist of photochromic compounds, such as cyanines, phthalocyanines, or azobenzenes in the case of CD-R, and inorganic materials such as Te-Se-Sn in the case of the CD-RW.

Indeed, organic photochromic materials have provided the systems with unique possibilities; lighter weight, higher flexibilities, easier way to process and lower cost in comparison with inorganic materials. Most importantly, the deposition of photochromic materials into the storage devices allows the use of laser light to write the information onto the media as well as to remove it for reuse. Using the optical technology for data storage can greatly enhance the data processing speed because light travels at ten times faster than the speed of electric current. Thus, it is possible for the devices to process data using light faster than the speed of conventional storage devices that use electric current. In this way, the consumption of electric power can be reduced.

Furthermore, light also allows for clean remote operation without the need for direct contact to the materials (García-Amorós and Velasco, 2012).

Generally, photochromic compounds are compounds that undergo a major reversible photochemical process on exposure to light at appropriate wavelength. This lead to transformation of the compound between two distinct states having different absorption bands, λ_{max}. The changes in λ_{max} is associated with the conformational changes occur as they are photo-induced. Not only the absorption spectra, but also various other properties changed during the transformation such as the optical, electrical, and other physical properties. These properties are being manipulated for making various optical storage media that process information using optical technology.

The important photochromic processes can be classified into four categories on the basis of process mechanism: *trans–cis* isomerisation, heterolytic cleavage, homolytic cleavage, and tautomerism. The *trans–cis* isomerisation is the main focus in this thesis. Several organic materials with *trans–cis* isomerisation properties have been found to be promising for optical storage devices. These include bacteriorhopsin, stilbenes, and azobenzene.

2.1.1 Bacteriorhodopsin

Bacteriorhodopsin, a key protein in halobacterial photosynthetic system, is one of the compounds from nature that utilising *trans–cis* transformation (Hampp, 2000). It is closely related to rhodopsin protein in the retina of the eye, as a photoresponsive element that enables visual perception (Henderson and Schertler, 1990; Barrett et al., 2007). Apart from its biological importance, the photosensitive nature of bacteriorhopsin has found uses in optical applications such as the construction of spatial light modulators and optical storage devices (Mahimwalla et al., 2012).

However, the biological photochromic protein has intrinsic problems because the reverse relaxation to its initial state is complicated, and thus direct application to optical technology is difficult. Moreover, exposure to light also destroys the stored information because the material subject to degradation (Stuart et al., 2002). Its availability and high price are also among the big concerns which hindered the development of optical memory devices.

2.1.2 Stilbenes

On the other hand, the photoisomerisation of stilbenes has also been extensively investigated. The stilbenes isomerisation involves a considerable torsion of the C=C group and therefore it is associated with a high energetic barrier. The experimental data obtained by Dou and Allen (2003) indicates an energy barrier of ~0.15 eV found in the *trans–cis* reaction, whereas a barrier of no more than 0.05 eV is in *cis–trans* reaction. This means photoisomerisation proceeds much faster in reverse reaction (*cis–trans*) than forward reaction (*trans–cis*). As a result, a long writing time is required to record information to the storage devices.

In addition, the application of stilbene derivatives has been restricted due to unwanted side reactions (Waldeck, 1991; Jørgensen, 2010). The stilbene photoisomerised from *trans* to *cis* when subjected to UV light, but then it changes to phenatherene through dehydrogenation using dissolved oxygen as the oxidant (figure 2.1). The side reaction is certainly a great disadvantage for making optical storage devices.

2.1.3 Azobenzene

Among all, azobenzene is the best candidate as the molecule is stable with clean and reversible photoisomerisation reactions. The isomerisation is one of the cleanest photoreaction known as it does not generate any side-products, or decomposition, even with innumerable isomerisation cycles (Rau, 1990; Bandara and Burdette, 2012). This applies to azobenzene dissolved in solvent, as well as in liquid crystal hosts. Besides that, the photosensitive feature of azobenzene can be used to induce phase transition, due to the significant conformational changes able to affect the orientation of liquid crystal mesogens at large. In fact, it is often used as probe to determined phase transition in liquid crystals. The phenomenon is more interesting when associated with mesogenic properties of azobenzene molecules (Ikeda and Tsutsumi, 1995 and Nair et al., 2000). Obviously, azobenzene characteristics met most of the requirements for application in optical storage devices.

2.2 PHOTOPHYSICAL PROPERTIES OF AZOBENZENE

2.2.1 Electronic properties

Azobenzene is a π-conjugated system, which consist of azo linkage (–N=N–) connecting two aromatic rings. The charge and electrons in the system are delocalized, spread energy around, and make the molecules more stable. The azo linkage is an unsaturated group, provides π bonding electrons and a nonbonding electron pair (n) to the system. Spectroscopic measurement of the system leads to two absorption bands, λ_{max}. The *trans* isomers exhibits a strong absorption band in the visible region (range 350 – 370 nm) due to the $\pi\rightarrow\pi^*$ electronic transition. There is another weak absorption band at visible region around 450 nm due to the $n\rightarrow\pi^*$ transition for the *cis* isomers. According to transition rule, electron transition from one quantum state to a different quantum state is forbidden. Since the $n\rightarrow\pi^*$ electronic transition is forbidden in *trans* isomer, the absorption tends to be much lower than for $\pi\rightarrow\pi^*$ transition, that is allowed by the transition rule. Therefore, it forms a very weak absorption peak in the visible region of the spectrum (figure 2.2).

Many studies have shown that adding substituents of increasing electronic interaction to the azobenzene rings affects both the *trans* and *cis* absorption spectra of the compound (Barrett et al., 2007). For instances, substitution at *ortho*- or *para*-position with an electron-donating group (such as an $-NH_2$ amino) produce an aminobenzene type, exhibiting the $\pi\rightarrow\pi^*$ and $n\rightarrow\pi^*$ band very close to each other, or overlapped in near-visible region. This is due to an increase in the π orbital energy and decrease in the π* orbital energy. Meanwhile, substitution at the 4 and 4’ position with both electron donor and electron acceptor (such as an amino and NO_2 nitro group), produces a stable push-pull system, which shift the $\pi\rightarrow\pi^*$ band toward UV region (bathochromic shift). Nevertheless, the azobenzene chromopores exhibit colour around yellow and red, depending upon the substituent effect.

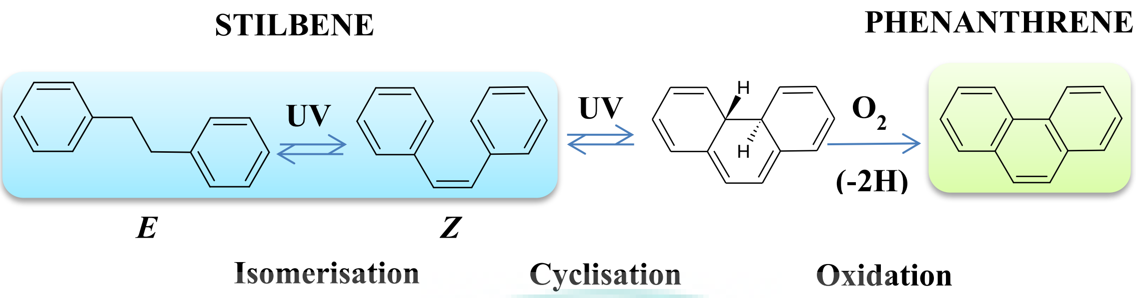

Figure 2.1: Photoisomerisation and cyclisation reaction of stilbene.

Source: Matsuzawa et al. (2011)

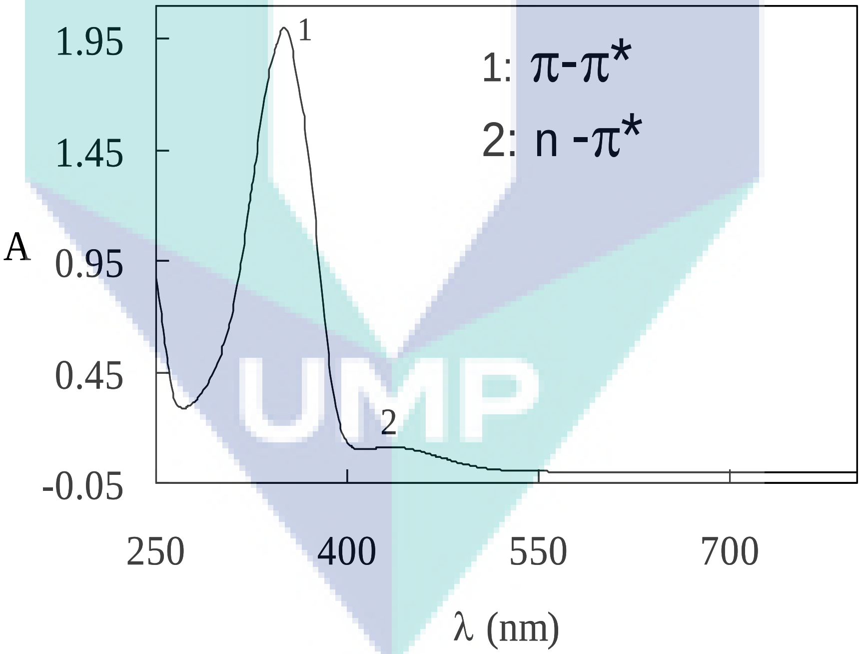

Figure 2.2: Absorbance spectrum of the trans-azobenzene showing two peaks marked as 1 and 2.

Samanta and coworkers (2012) have synthesized bisazobenzene with a piperazine centre links to two azobenzene chromophores. Molecular modelling indicates that the bisazobenzene molecules undergo large change in end-to-end distance upon *trans–cis* isomerisation. Spectroscopic data shows that λ_{max} has shifted toward visible region, around 420 nm. The central piperazine unit in this structure is expected to disconnect the π-delocalization between the two azobenzene chromophores completely, while providing nitrogen lone electron pair for n→π* transition in each independent azo unit. In this way, UV light is not required to induce the photoisomerisation process. The compound can be suitably used for manipulating biological target, including photo-control of folding in protein conformation. In such biological system, where UV light is highly scattered by biomolecules, it can be very harmful.

Trans-azobenzene undergoes photoisomerisation to *cis*-azobenzene, which can isomerise back to the *trans* isomer either photochemically or thermally (Merino and Ribagorda, 2012). Upon UV irradiation, the azobenzene isomerisation reaches a point where photostationary state achieved, which is the equilibrium state for *trans–cis* conversion. The extent of *trans–cis* isomerisation, or the amount of *cis* present in the photostationary state, can be measured indirectly by spectroscopic method and summarized by the *cis* concentration, [*cis*]. In most cases it is impossible to obtain a sample with 100 % of [*cis*] (Wazzan, 2009). In the dark, [*cis*] usually lies below the limit of detection and the system can be considered to comprise of 100 % *trans* molecules (El Halabieh et al., 2004).

For cases when the absorption spectra of the two isomers overlap significantly, a single wavelength of light activates both the forward and reverse reactions, leading to a mixed stationary state and continual inter-conversion of the molecules. This can be a disadvantage for making rewriteable optical storage devices in which “writing” and “erasing” process have to be done using different wavelength of light.

2.2.2 Mechanism of photoisomerisation

The mechanism of azobenzene isomerisation cycle has attracted much attention and this subject has undergone considerable debate among researchers (Bortolus and Monti, 1979; Merino and Ribagorda, 2012). Upon photoexcitation from the *trans* isomer, the valence electron is excited from its ground state (S_0) orbital to an excited state orbital. Since there is no influence of oxygen or heavy atom observed during the photoisomerisation of azobenzene, the electron is most likely to be excited to its first singlet excitation state (S_1), in which the electron retains its spin under an $n \rightarrow \pi^*$ excitation condition, or its second singlet excitation state (S_2), in which the electron retains its spin under an $\pi \rightarrow \pi^*$ excitation condition (figure 2.3). Consequently, the azobenzene undergo conformational changes whereby the phenyl rings move about the azo bond, converting the molecule between rod-shaped *trans* isomer and bent-shaped *cis* isomer (Garcia-Amorós and Velasco, 2012).

Two generally agreed mechanism for *trans*–*cis* isomerisation has been proposed. One is through the rotation around N=N double bond, which happen when the π-bond is broken by optical excitation of an electron, causing $\pi \rightarrow \pi^*$ electronic transition ($S_0 \rightarrow S_2$ excitation) to allow free rotation take place. The second mechanism is through inversion pathway, where the π-bond remain intact, but instead, the nonbonding electron pair of nitrogen atom lead to $n \rightarrow \pi^*$ electronic transition ($S_0 \rightarrow S_1$ excitation) – enabling the inversion of the N–C bond (figure 2.4).

The likelihood occurrence of photoisomerisation through rotational or inversion pathway in azobenzene depend on host environment, such as in gas phase, solvent, liquid crystal, or polymer, where the mechanism can be different. For photo-isomerisation in solvent environment, both mechanisms are most probably competing (Tiberio et al., 2010). Pure rotation and pure inversion mechanism are less likely to occur because it seems to be hindered by steric solvent interaction. Push-pull azobenzenes, for example, the reaction mechanism is found to change from inversion in non-polar solvents to rotation in polar solvents (Dokic et al., 2009). In some conditions, pure rotation or pure inversion is preferred. For example, the inversion mechanism usually has much smaller free volume requirement than the rotation. It has been

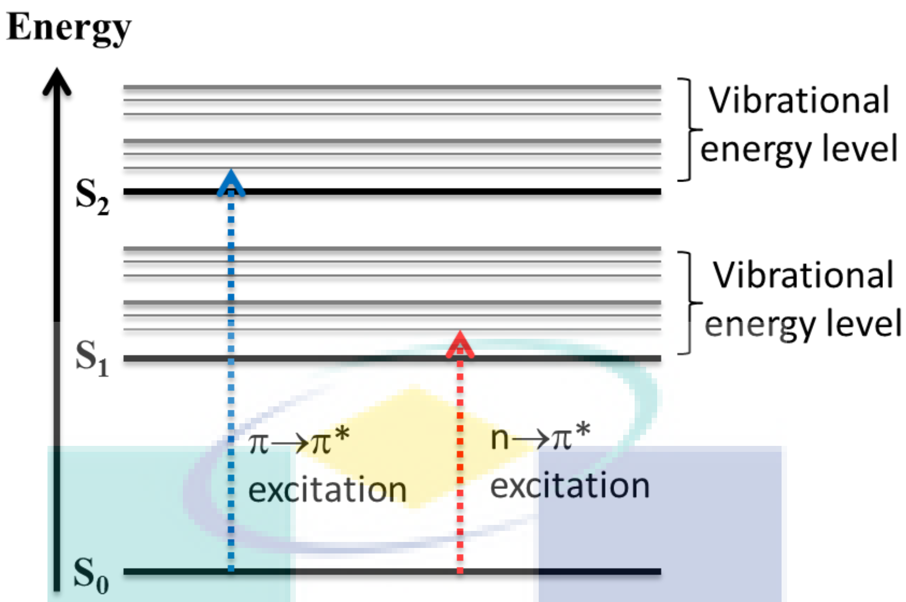

Figure 2.3: Energy diagram representing the electronic excitation for the mechanism of azobenzene photoisomerisation.

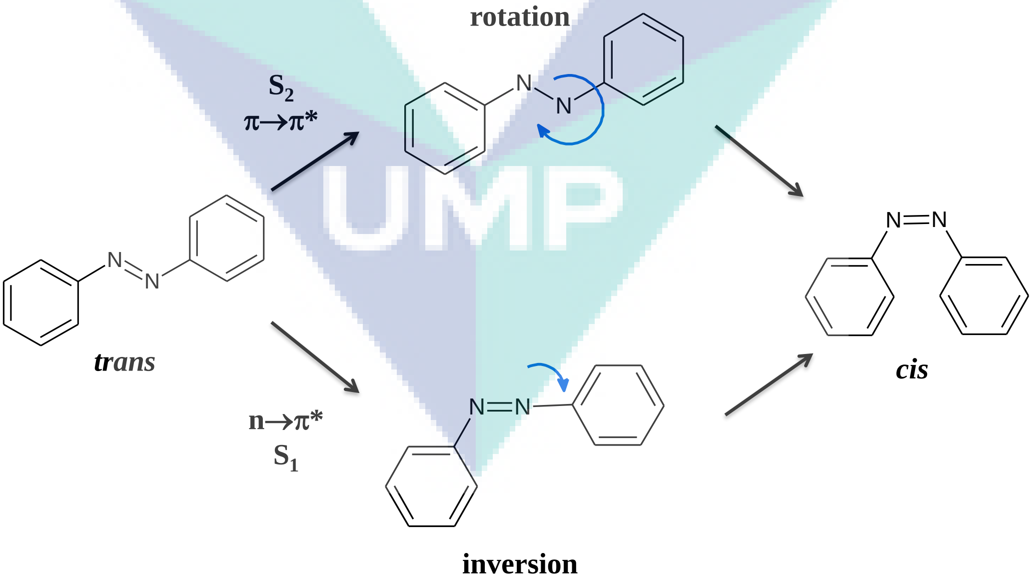

Figure 2.4: Schematic mechanistic proposals for the isomerisation of azobenzene.

estimated that the minimum free volume required to allow isomerisation to proceed through inversion is 0.12 nm^3, and approximately 0.38 nm^3 for rotation (Mahimwalla et al., 2012). Thus, in rigid host matrices with molecular constraints, such as in glassy polymers, isomerisation through inversion mechanism is favourable. Meanwhile, the thermal back relaxation reaction in dark condition is generally agreed to proceed through pure rotation pathway.

2.3 FACTORS AFFECTING AZOBENZENE PHOTOCHEMICAL ACTIVITIES

There are several factors affect the photochemical activity of azobenzene. The rate of thermal isomerisation may be influenced by ring-substitution pattern, temperature of the environment and solvent used. In case of photoisomerisation, since it is a light-induced process, wavelength and intensity of light exert influence to the photoisomerisation rate, in addition to other factors.

2.3.1 Light

Photoisomerisation is induced by irradiation of light with a wavelength within the absorption spectrum of azobenzene, preferably close to λ_{max}. The extent of *trans–cis* isomerisation depends on the irradiation intensity and wavelength of the irradiated light (García-Amorós and Velasco, 2012). For example, in a non-substituted azobenzene, irradiation at 313 nm gives approximately 80 % of [*cis*], whereas at 365 nm only 40 % of [*cis*] achieved (Feringa, Jager and de Lange, 1993).

The choice of light source also depends on the absorption spectrum of the azobenzene molecules. The most common light source is UV light of 250 – 400 nm wavelengths from mercury lamp or visible light from Xenon lamps giving light emission in the range of 450 nm to 550 nm. The source of light gives a significant influence to the photochemical activity. It is known that the energy transfer from a laser source to the molecules is far more efficient than from a conventional source. Therefore, the *trans–cis* isomerisation proceeds much faster when azobenzene is subjected to pulsed laser source than to a conventional UV source. For example, the time required for photoisomerisation using convention light source is of the order of a few seconds, whereas with a pulsed laser source, an instant of time of sub microsecond level can be achieved (Nair et al., 2004). However, the high power laser emission may lead to degeneration of azobenzene compound.

Hu and coworkers (2011) have studied the rewriting-ability of bisazobenzene-containing films. They found that the recording data points can be erased by linearly polarised light, whose polarisation direction is perpendicular to that of the recording beam. Then, in the same region, new data can be rewritten after erasing. In addition, the recorded data can also be erased completely by circularly polarised light. Compared with linearly polarised beam, the circularly polarised light is a better choice for erasing as no main orientation is regained after erasing.

2.3.2 Temperature

Temperature influences the rates of thermal back relaxation. In general, the higher the temperature the faster the process will proceed. This suggests that elevating the reaction temperature provides a larger number of molecules with sufficient energy to cross the barrier, which increases the rate of thermal back relaxation. Essentially, the rates of thermal back relaxation can be calculated from the change in absorbance at a certain wavelength with time.

The thermal back relaxation of azobenzene is generally a first-order kinetic process (Barrett, Natansohn and Rochon, 1995). The thermal back relaxation is carried out at constant temperature and changes in absorption are measured against time. Thus, a first-order kinetic relationship will yield a straight line if the logarithm of absorbance changes is plotted against time, where the slop gives the rate constant of thermal back relaxation. A first-order rate implies that for a given temperature a *cis–trans* isomerisation will proceed at a constant logarithmic rate until the *cis* isomer is fully converted to *trans* isomer. This linear relationship can be used to predict how long it will take for an azobenzene thermal back relaxation to occur. Knowing the rate of the process allows it to be used to predict time to completion.

2.3.3 Solvents

The photochemical activity of azobenzene dissolved in solvent depends strongly on the solvent–solute interaction and the nature of solvent. Kojima et al. (2005) reported that the half-life for thermal isomerisation of *cis*-4-hydroxyazobenzene to its *trans* isomer is highly dependent on the solvent used. For non-aromatic solvents, the *cis* isomer is extremely unstable at 19.85 °C, with half-life of less than 1 min in methanol and acetonitrile, and 6 min in cyclohexane. Instead, the *cis* isomer is more stable in benzene with 125 min half-life.

By studying the effect of different solvent on the shift in absorption maxima, λ_{max}, it was found that the polarity and hydrogen bonding properties of the solvents give strong salvatochromic effect on the λ_{max} of azobenzene (Yari, Sedaghat, and Hekmait, 2008). Modi and coworkers (2012) shows that tris(heteroaryl)bisazo dyes exhibits strong polarity dependence of visible λ_{max} on the polarities of solvents. The λ_{max} increases with the increase in polarities of solvent in the order of chloroform < acetone < methanol < DMF. Compared to azobenzene, the hetorocyclic azo compounds tend to be more strongly affected by solvent.

Besides that, it has also long known that, from the Arrhenius activation energy studies, the activation energy decreases with the increase in polarity of the solvent (Nishimura et al., 1976). Therefore, the rate of thermal *cis–trans* isomerisation of azobenzene increases when the solvent polarities increase.

2.3.4 Ring-substitution pattern

It is well-known that modification of the substitution pattern on the azobenzene ring-structure is one of the main factors that change the isomerisation behaviour, but not always in a predictive manner. Any substitution in the aromatic rings, in particular their type, number, and positioning, can produces substantial change in geometrical and photochemical properties of azobenzene system.

For instance, the rate of thermal back relaxation of azobenzene can be accelerated by introduction of substituent in *para* position. Nishimura and coworkers (1976) showed that for *para*-donor and *para'*-acceptor substituted azobenzene such as 4-nitro-4'dimethylaminoazobenzene, the rate was distinctly accelerated.

Pu and coworkers (2005) have studied the substituent effects on the *trans–cis* isomerisation and the stability of azobenzene. From the results obtained, it shows that the variation of the isomerisation barrier can be attributed to fluctuation of atomic charge in the –N=N– bond induced by the substituent. It means that high electronegative and strong electron-withdrawing substituents can significantly reduce the *trans–cis* isomerisation barrier of azobenzene. They also conducted an isodesmic reaction, a type of hypothetical reaction, to quantify the structure-stability relationship for azobenzene molecule in the isomerisation reaction by enthalpy calculation. The study suggests that the π-donating ability of substituent dominates the stability of the azo moiety.

The effect of the size of photochromic group in optical storage properties has been studied by Ho and coworkers (1995). Since a larger local free volume should be needed for the isomerisation of molecules with a bulkier displacing group, the rates of photoisomerisation should be significantly influenced by the size of the isomerising chromophore. However, results showed that there is no significant difference in the relaxation rate when comparison made between a bulkier Poly[(4-nitronaphthyl)[4-[[2-(methacryloyloxy)ethyl]ethyl-amino]phenyl]-diazene] (pNDR1M) with the less bulky Poly[(4-nitrophenyl)[4-[[2-(methacryloyloxy)ethyl]ethylamino]phenyl]diazene] (pDR1M).

2.4 AZOBENZENE LIQUID CRYSTALLINITY

In addition to their photochemical property, another interesting feature of azobenzene is their rigidity and anisotropic natures thereby render them with liquid crystalline property. Liquid crystallinity of a material generally requires rigid mesogenic groups and sufficient conformational freedom to allow the mesogenic units to form an organized domain. That means, the rigid core and flexible chain is often the prerequisite for mesomorphic property of liquid crystalline molecules. In this regard, azobenzene made up of rigid and anisotropic core provides this group of compound ideal mesogenic units to form mesomorphic phases (El Halabieh et al., 2004).

In 1995, Ikeda and Tsutsumi showed that azobenzene liquid crystal films exhibit nematic phase in *trans* isomers but not mesophase in *cis* isomer. *Trans–cis* photoisomerisation of the azobenzene gave a rapid optical response of 200 microseconds with a pulsed laser, resulted in a nematic–isotropic transition. Hence, the combined advantages of photochromic properties with those of liquid crystallinity offer useful and versatile characteristics for development of optical storage devices.

According to Al-Hamdani and coworkers (2010), introduction of a substituent in a side position of mesogenic molecule has two opposing effects on the thermal stability of mesophase. Firstly, the substituent changes the molecular polarisability and this may increase the thermal stability of the mesophase. Meaning that, the more electronegative atom pulls the electrons from neighboring atom toward itself creating some bond polarity that help to stabilize the mesophase at high temperature range. In spite of this, the size of the substituent broadens the molecule and as a result decreases the length-to-breath ratio. This affect the anisotropic nature of the molecule and hence the mesophase thermal stability also being affected. The later effect is often more dominant than the effect of molecular polarisability. However, it can be minimized by substituting small molecule like fluorine.

The chances of azobenzene to generate a smectic or nematic mesophase depend on the degree of difference between the terminal and lateral attractions. Smectic properties are always occurred when the lateral-to-terminal ratio is high, and on the contrary nematic phase occurred when the ratio is low. Another requirement for generating smectic mesophase is to introduce additional dipole moment across the long axis of the molecule which enhances the intermolecular lateral attraction. In other words, the intermolecular lateral attraction stabilized the smectic phase structure.

Meanwhile, Yang and coworkers (2013) found that the phase transition behaviour of liquid crystalline polymers containing monosubstituted azobenzene moiety depend strongly on the position of the substituent on the azobenzene moiety. They investigated the effects of *para*-, *meta*-, and *ortho*-monosubstituted azobenzene moiety in the side chain on the liquid crystalline behaviours of the polymer. The results showed that the glass transition temperature (T_g), isotropic temperature (T_i) and liquid crystalline range (ΔT, from T_g to T_i) of the polymers decrease in the order, *para* > *meta* > *ortho*. And the associated enthalpy changes of these polymer are also in the same order, *para* > *meta* > *ortho*. This suggests that the substitution in *para* position help to enhance the liquid crystalline behaviour of the polymer.

2.5 TUNING OF AZOBENZENE MOLECULES

In order to improve the optical storage features in azobenzene chromophore, a considerable number of researches have been conducted, by molecular modification of azobenzene molecule to generate mesogenic behaviour, along with good photochemical properties. The first possibility in this process concerns the chemical synthesis whereby different terminal moiety, lateral substituents or spacer group can be attached (Prasad et al., 2002). Many examples of azobenzene liquid crystals have been developed, in which azobenzene moieties serve as both mesogens and photosensitive chromophores.

2.5.1 Bent-shaped Azobenzene

Calamitic liquid crystalline phases such as nematic phase and smectic-A phase are usually found to be rod-shaped in nature. However, these calamitic phases can also be manifested by materials that make up of bent-core molecules, given that the bending is not too extreme, and the length of molecule is adequate for demolishing the destructive nature of the bending (Hird, 2005). However, banana liquid crystals with the bent core unit are rather rare. Since the discovery, not many compounds have been synthesized because chances for getting liquid crystalline phases are unlikely to succeed.

Banana liquid crystals have been known for many years, dated back to 1929, when Vorländer reported the first example of liquid crystal with bent-shaped molecules. As a matter of fact, most of the successful generation of liquid crystalline phases from a bent-core molecule is by minimising the degree of bending, so that it behaves as rod-like mesogen. This can be done by employing multiple rings and flexible ester-linking group in the structure. Recently, Lutfor and coworkers (2013) have synthesized banana-shaped monomers with naphthalene as central units, and azobenzene in side arms with terminal alkenes having double bonds. Such bent-core liquid crystalline monomers with double bonds at both ends are used for polymerisation to form main-chain liquid crystal polymers. Results obtained shows that the molecules able to exhibit liquid crystalline phase, and also the photostationary state achieved at 45 sec with a long thermal back relaxation of 28 h and 30 min. In some way, the photochemical activity is similar to the previously reported bent-shaped monomers that contain resorcinol as central unit and terminal double bonds as polymerisable functional groups, which exhibit strong photoisomerisation behaviour in solution. Here, the *trans–cis* isomerisation took about 50 sec whereas the reverse process took almost 31 h (Lutfor et al., 2009). Needless to say such a strong photochemical behaviour is an advantage for creation of optical image storage devices.

According to Keith et al. (2010), nematic phases are relatively rare among mesophases of bent-core compounds. The occurrence of nematic phases in banana liquid crystals are exclusive to molecules with extended aromatic cores and relatively short terminal chains, or a reduction of the molecular bent. Cvetinov and coworkers (2013) have studied a nematogenic biphenyl bent-core molecule with 1-undecen terminal end. They calculated the total molecular length of the compound to be 4.65 nm; the linear length of the half rigid molecular core is 1.4 nm and the linear length of each alkyl chain is 1.44 nm. The two arms of the molecule bend at the centre at 121.32 ° angle. However, since the material is a non-azo compound, no photoisomerisation property has been reported on this compound. Nevertheless, by knowing the size and geometry of the molecule, one can design azobenzene molecule with the similar liquid crystalline property.

2.5.2 Azobenzene with amide group

The hydrogen bonding of amide linkage is a strong bond and it is known to play a significant role in the formation and stabilization of protein secondary structure in biological system. In a biological environment, the main competitor for the hydrogen donor (N–H) on the amide are the nearby carbonyl linkage (C=O) as well as oxygen atom of nearby water molecules. The hydrogen acceptor (C=O linkage) and hydroxyl O–H of water compete for the hydrogen donor (N–H) on amide for the formation of amide–amide (C=O···H–N) hydrogen bond, or amide–water ($H–N···OH_2$) hydrogen bond. Considering the central role hydrogen bonding plays in protein folding, examining the effect of hydrogen bond of amide group on mesomorpic property and photochemical activity of azobenzene is of great interest.

A few researchers have utilized the amide group to enhance the mesomorphic properties and thermal back relaxation in azobenzene molecule. Li and coworkers (2012) have synthesized a series of photoresponsive side-chain liquid crystalline polymer with amide group-substituted azobenzene mesogens. They discovered that introduction of an amide group into the azobenzene mesogens led to the formation of strong hydrogen bonding among the side chains of polymers, which played a decisive role in forming and stabilizing the liquid crystalline mesophase of the polymers. Indeed, a very important consequence of amide structure is the extensive molecular association of amides through hydrogen bonding. The relatively negative oxygens acted as the hydrogen acceptors while the N–H hydrogens served as the hydrogen donors.

Another property observed in azobenzene derivatives with hydrogen bonding is the self-assembly nature. Miao and coworkers (2012) have studied the self-assembly of azobenzene derivatives with various lengths of alkyl chains ($C_nAzCOOH$) by scanning tunnelling microscopy on highly oriented pyrolytic graphite surface. Though there is no amide group presence, they observed that $C_nAzCOOH$ molecules formed hydrogen-bonded dimers with “head-to-head” fashion. The self-assembly pattern was achieved by the intermolecular multiple hydrogen bonding interactions. So, it is clear that the formation of hydrogen bonding plays a major role to drive about self-assembly of azobenzene derivatives.

In 2010, Bandara and coworkers synthesized and studied AzoAMP-1 (2,2'-bis[N-(2-pyridyl)methyl]diaminoazobenzene), which possesses two aminomethyl-pyridine groups at *ortho* position to the azo group. The molecules exhibit minimal *trans*–*cis* photoisomerisation and extremely rapid *cis*–*trans* thermal recovery. The remarkable properties arise as a result of two strong intramolecular hydrogen bonds between aniline protons and pyridyl and azo nitrogen atom. With this knowledge, it is interesting to study the effect of hydrogen bonding arise from amide linkage on the photoisomerisation behavior of azobenzene.

2.5.3 Azobenzene with fluorine addition

Fluorine has a unique effect on molecular properties attributed to its high electronegativity and lone pair electrons (Namazian and Coote, 2009). Electronegativity is a well-known chemical property that describes the tendency of an atom or a functional group to attract electron density toward itself. An atom's electronegativity is affected by both its atomic number and the distance at which its valence electrons reside from the charged nucleus. The higher the associated electronegativity number, the more an element or compound attracts electrons towards it.

The electronegative substituent are thought to withdraw electron density from the bonding π-type orbitals of the photochromic azo bridge (–N=N–) in the centre of the molecule. A weakened –N=N– double bond reduces the barrier for rotation around this bond, which should allow for more efficient interconversion since rotation is one of the two pathways (the other one being inversion) for isomerisation. Pu et al. (2005) have stated that the atomic charge on nitrogen atom in –N=N– bond bearing substituent does not show electron-withdrawing or -donating ability. Rather, substitutions either by electron donating or electron-withdrawing groups decrease the electron density on the nitrogen atom. So, it is notable that the electron density on the nitrogen atom decreases as the group electronegativity increases, signifying a considerable dependence on the electronegativity.

In addition, fluorine substituted azo compounds exhibit greater thermal stability than other substituents such as chlorine or methyl group (Al-Hamdani et al., 2010). This is because the smaller size of fluorine as compare to other substituents does not increase the width of the molecule and so the ratio of lateral to terminal attraction force is higher and hence results in thermal stability. Furthermore, Rahman and coworkers (2013) found that as the number of fluorine atom increase, transition temperature decrease.

This signify that the size of the molecule increase as more fluorine atoms is added and hence destabilized the compound which reduced the phase transition temperature. Besides, substitution of fluorine into the azobenzene molecule introduces a dipole moment across the long axis of molecules which strengthen the intermolecular lateral attraction so that it generates mesophases, in particular the smectic phase.

The rapid development in the area of optical storage devices leads to significant interest in liquid crystalline materials from fluorobenzene derivatives. It has been reported by Rahman and coworkers (2013) on fluoro-substituted azobenzene moiety and their liquid crystalline behaviour along with photoswitching property. In the studies they observed nematic phase in monofluoro-substituted azobenzene ester and smectic-A phase in difluoro-substituted azobenzene ester.

According to Al-Hamdani et al. (2010), there are three possible reasons for the absence of smectic properties in monofluoro-substituted azobenzene. Firstly, the dipole of fluorine substituent is partly cancelled by the dipole of the ester group, which lies with its carbonyl group (C=O) at opposite orientation to the fluorine atom. Secondly, there is no other dipole acting across the long axis of the molecule. And lastly, due to the increase in molecular breadth, the rod-shape molecule is forced to further apart, thus reducing the strength of the intermolecular lateral attraction, and hence reducing the strength of the intermolecular lateral attractions.

This explained why the monofluoro-substituted azobenzene ester does not exhibit smectic-A phase. Despite the fact the fluorine substituent give dipole moment which acts through the long axis of the molecule, it is cancelled by the dipole moment due to the ester group, so the terminal–lateral attractive force become weaker. In case of diflouro-substituted azobenzene, the dipole moment from two fluorine substituents is so strong that it cannot be diminished by the dipole moment from ester group, and thus smectic-A phase appears.

2.5.4 Azobenzene with olefinic terminal

Olefins, also called alkenes, are organic compounds made up of hydrogen and carbon that contain one or more pairs of carbon atoms linked by double bond. They are unsaturated compound because the carbon atom in the –C=C– bond do not fully bonded to hydrogen atom. Organic molecules with double bond usually predominantly undergo photoisomerisation from *trans* to *cis* isomer upon irradiation with light, as in azobenzene molecules which have –N=N– bond with phenyl rings on either side. The main $\pi \rightarrow \pi^*$ absorption of simple alkene, such as ethylene, is located at λ_{max} 163 nm, thus limiting the usefulness of most conventional light sources. Introduction of substituent on the C=C moiety of alkene, however, can lead the absorption to longer wavelength or bathochromic shift, so that absorptivity from light source can occur.

Other than that, photo-crosslinking is other photochemical process takes place in olefins. Photo-crosslinking is initiated by direct irradiation of the polymerisable double bond with light in UV–Vis spectral region or through energy transfer to form reactive intermediates, such as free radical or reactive cations. In general, photo-crosslinking includes the photo-initiated crosslinking among molecules by formation of interchain bonds and leading to the increase of molecular weight caused by light. For example, recently Javani and coworkers (2014) has investigated the photo-crosslinking of styrene-isoprene-styrene (SIS) triblock copolymer in the presence of benzoin and a dimethacrylate monomer. Benzoin was used as photoinitiator because it contains chromophore group that could absorb UV radiation whereas ethylene glycol dimethacrylate was used as crosslinking agent, since it has alkene functional groups that could react with the alkene group of SIS.

The most commercially important and simplest photo-crosslinkers are chalcone and cinnamate due to their high sensitivity to UV radiation. The photosensitivity of these materials is mainly attributed to the π electron density of the photoactive chromophre (Choe and Ban, 2001). The materials are either added as pendant group or incorporated in polymer backbone. There are a great number of literatures described about photoresponsive polymers. In order to make to polymer responsive to light, they are necessary to possess photosensitive functional groups such as azobenzene for photoisomerisation and photo-crosslikable material for crosslinking property. Jayalatha and coworkers (2009) have studied on thermotropic main chain liquid crystalline polymers bearing photo-crosslinkable chalcone and photoisomerisable azobenzene moieties. The liquid crystalline polymers show fast photo-crosslinkability due to chalcone unit and *trans–cis* isomerisation due to the azobenzene moiety in the polymer backbond.

However, photo-crosslinking as an approach to produced long thermal back relaxation in azobenzene has yet to be studied. If alkene is substituted into azobenzene molecule then the resulting azobenzene derivative may possess photo-crosslinking property. Besides the photoisomerisation by azobenzene moiety, the unsaturated double bond in alkene unit might undergo photo-crosslinking under the influence of light to form interchain bond with nearby molecules. The consequence intermolecular network may produce a unique photochemical behaviour in the molecular system.

2.6 PHOTO-INDUCED PHASE TRANSITION STUDY

The photo-induced isothermal transitions have been observed in a variety of systems exhibiting different liquid crystalline phases (Legge and Mitchell, 1992; Coles et al., 1993 and Prasad et al., 2002). For instance, photo-induced effects have been well studied in systems exhibiting nematic–isotropic, smectic-A–nematic (Ikeda and Tsutsumi, 1995; Nair et al., 2000; Biswas and Umapathy, 2003; Ikeda, 2003 and Prasad et al., 2002) and also from the re-entrant nematic–smectic-A systems; the latter is a rare example of a photo-induced disorder-to-order phase transition (Prasad and Nair, 2001). Various photonic applications, other than LCDs, can be realised if the phase transition can be driven by light. However, not all liquid crystal materials are responsive to optical field.

The subsequent demonstration of the influence of dopant photoactive molecules in reducing the required optical field has triggered a significant numbers of research activities (Janossy, Csillag and Lioyd, 1991; Janossy, 2000; Simoni and Francescangeli, 1999). Tazuke et al. in 1987 reported the first explicit example of the nematic–isotropic phase transition induced by *trans–cis* photoisomerisation of azobenzene guest molecules dispersed in a nematic liquid crystal host. Figure 2.5 shows the schematic representation of the photo-induced nematic–isotropic transition takes place in azobenzene-liquid crystal guest-host system. It can be seen that the molecular-scale change expands spatially into the micro- or milli-scale region. This kind of spatio-temporal structural changes in response to UV light can be observed by means of nanoscopic or microscopic observation.

More recently, Fuji and coworkers (2014) has studied the photo-induced molecular dynamic in liquid crystal polymer film with azobenzene dopant, by heterodyne transient grating method combined with the transient absorption technique. They successfully observed the dynamic over a wide time range, and examined the molecular motions which precede the macroscopic structural change. It gives a better understanding of the photo-induced phenomenon happen in the mixture of azobenzene and liquid crystals polymer.

2.7 REQUIREMENTS FOR CREATION OF OPTICAL STORAGE DEVICES

From the practical point of view, although the liquid crystallinity from azobenzene is not a necessary condition for driving phase transition, yet it makes the photo-induced orientation even easier to achieve when the azobenzene and liquid crystal are in the same phase. The liquid crystallinity of azobenzene promotes a homogeneous distribution in the guest-host system. If a material exhibits a nematic–isotropic transition and UV irradiation is done in the nematic phase, the lowering of nematic–isotropic transition temperature, $T_{N\text{-}I}$, can induce an isothermal nematic–isotropic transition. Nair et al. (2000) have observed that even with a low concentration of photoactive material, UV light, as small as 0.1 mW/cm^2 in intensity, is capable to lower the nematic–isotropic transition temperature, $T_{N\text{-}I}$, by 15 °C.

Indeed, one of the requirements for optical storage applications is the appreciable lowering of the $T_{N\text{-}I}$. As the azobenzene change their molecular shape upon photo-irradiation, the $T_{N\text{-}I}$ of the mixture with the *cis* form is much lower than with the *trans* form (Ikeda and Tsutsumi, 1995; Shishido, 2010). So as soon as the $T_{N\text{-}I}$ is lowered than the irradiation temperature, phase transition happens. From another perspective, it can be said that the time required for the photo-induced nematic–isotropic transition to occur depends on the rate the *trans–cis* photoisomerisation as well as the temperature at which the UV irradiation is done.

The [*cis*] in photostationary state also influence the photo-induced phenomena. Legge and Mitchell (1992) have studied the effect of photostationary state of doped materials achieved by *cis–trans* isomerisation upon the transition temperature of the mixture and response time of the system. They have discussed the implications of the photostationary state with regards to the reversibility of the photo-induced phase transition.

Another requirement of creating optical storage device is a slow recovery time for the photo-induced isotropic state relaxed back to nematic phase, so that the optically generated image can stay longer. So, if the time required for *trans–cis* isomerisation is faster whereas the thermal back relaxation time for restoring the nematic phase take much longer, this can be a good advantage for making an optical storage.

Nair et al. (2004) have investigated the influence of adding octadecane, a long-chain alkane, on the photo-induced nematic–isotropic transition of a liquid crystal having a small amount of photoactive compound. They found that addition of octadecane helps to extend the time needed for restoration of nematic phase from the induced isotropic phase, thereby increase the thermal back relaxation time. Octadecane has only flexible units and prefer the coil form, thus, do not support the formation of liquid crystalline phases. Even when added to materials that already exhibit liquid crystalline phases, they tend to destabilize the liquid crystallinity due to incompatible rod-like form of the liquid crystal molecules and the coil form of octadecane, thus making the isotropic phase stay longer. They also found that, in the system studied, the addition of 15 % of octadecane brings down the temperature range of the nematic phase by as much as 16 °C, as compared to that for the host material. With such occurrence, it can be said that the addition of octadecane helps to lower the T_{N-I} and increase the thermal back relaxation time.

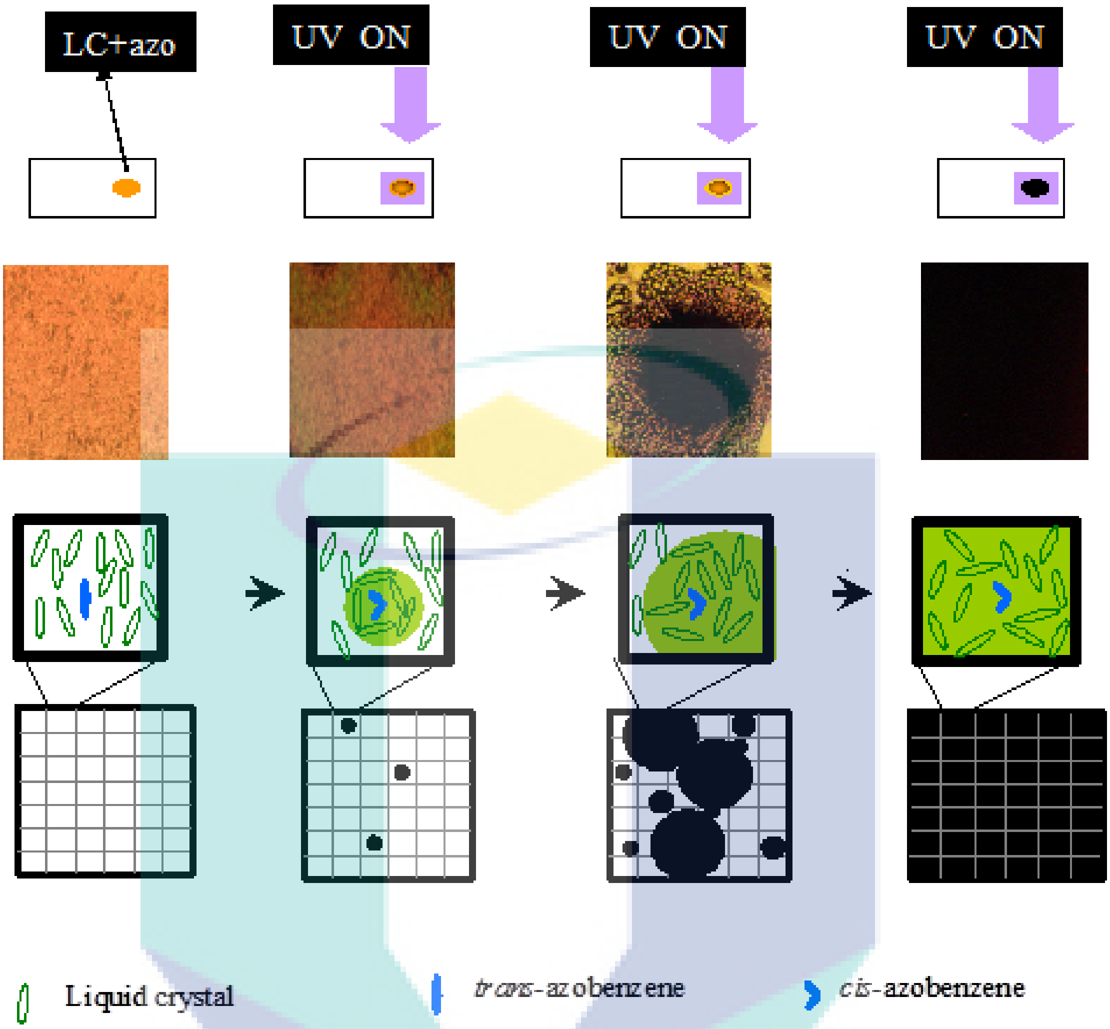

Figure 2.5: Optically induced birefringence mechanism in azobenzene-liquid crystal systems.

Source: Ikeda (2003)

CHAPTER 3

METHODOLOGY

3.1 MATERIALS AND REAGENT

All the azobenzene derivatives were supplied by Dr. Gurumurthy Hegde, formerly worked for Universiti Malaysia Pahang. These compounds were synthesized and their chemical structures were determined by means of FT-IR spectroscopy, ^{1}H NMR, ^{13}C NMR, and elemental analysis (CHN), by a PhD student in chemistry, Yuvaraj A R. For informational purposes, experimental details about the synthetic procedure of the compounds are included in this section and the FT-IR and NMR spectra are in APPENDICES.

Ethyl 4-amino benzoate, sodium nitrite, 1-bromohexane, potassium hydroxide, potassium iodide, hydroquinone, aniline, 1,3-dicyclohexylcarbodiimide (DCC), 4-(N, N-dimethylamino) pyridine (DMAP), 4-nitroaniline, 5-bromo 1-pentene, 4-fluoro phenol, 4-chloro phenol, 4-bromo phenol, 4-iodo phenol, and sodium hydroxide were supplied by Fluka. Phenol, 4-amino acetophenone, 4-fluoro benzoic acid, 3,5-difluoro benzoic acid, hydrochloric acid and silica gel-60 were purchased from Merck. Potassium carbonate was purchased from Aldrich. Commercial reagents and solvents were used as supplied with following exception. Acetone was dried over phosphorus pentaoxide (Merck), dichloromethane was dried over calcium hydride (Fluka) and distilled out before use. IR spectra were recorded using a Perkin Elmer (670) Fourier Transform Infrared (FT-IR) spectrometer. ^{1}H NMR (400 MHz) and ^{13}C NMR (100 MHz) were recorded using Bruker Nuclear Magnetic Resonance (NMR) spectroscopy, and chemical shifts are reported as values in ppm relative to tetramethyl silane (TMS) as standard at $\delta = 0.00$ ppm. Elemental analysis was done by CHN elemental analyser (Leco & Co).

3.2 SYNTHETIC PROCEDURE

3.2.1 Synthesis of bent-shaped azobenzene

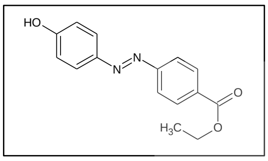

Ethyl 4-(4-hydroxyphenylazo) benzoate (A): Compound **A** was prepared by dissolving ethyl 4-amino benzoate (46.0 mmol, 1 equiv.) in methanol (40 mL), cooled to 2 °C. After 8.672 mL of 25 % hydrochloric acid was added drop wise at 2 °C, sodium nitrite dissolved in water (44.6 mmol, 1 equiv.) was also added drop wise and stirred for 15 min. Then, the prepared phenol solution in methanol (44.6 mmol, 1 equiv.) was added slowly to the reaction mixture at 2 °C and the pH was raised to 8.5 – 9.0 by using 1 N sodium hydroxide, stirred for 4 h. The resulting mixture was added with methanol (250 mL) and ice, and then pH was reduced to 4 with diluted hydrochloric acid. The reddish yellow product precipitate was filtered and dried. The crude product was recrystallized twice from methanol. A reddish yellow coloured solid; Rf = 0.42 (40 % CH_2Cl_2-EtOH); yield: 62 %; m.p. 160.2 °C; IR (KBr, ν_{max}, cm^{-1}): 3321, 1728, 1602, 1484, 1248, 1140, 829; ^1H NMR ($CDCl_3$) δ: 8.17 (d, 2H, J = 8.2 Hz, Ar-H), 7.92 (d, 2H, J = 7.5 Hz, Ar-H), 7.88 (d, 2H, J = 7.5 Hz, Ar-H), 7.01 (d, 2H, J = 8.2 Hz, Ar-H), 5.54 (s, 1H, OH), 4.42 (q, 2H, J = 7.2 Hz, $–CH_2CH_3$), 1.44 (t, 3H, $–CH_2CH_3$); MS (FAB+): m/z for $C_{15}H_{14}N_2O_3$, Calculated: 270.28. Found: 270.08.

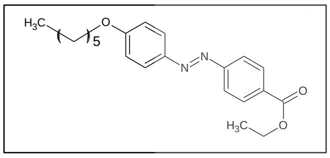

Ethyl 4-[4-(4-hexyloxy) phenylazo] benzoate (B): Compound **A** (18.5 mmol, 1 equiv.) and 1-bromohexane (37.1 mmol, 2 equiv.) were dissolved in dry acetone (300 mL). Potassium carbonate (18.5 mmol, 1 equiv.) was added drop wise followed by catalytic amount of potassium iodide (50 mg). Then, the reaction mixture was refluxed for 24 h under nitrogen atmosphere, monitored by thin-layer chromatography (TLC). After completion of the reaction, solvent was removed and the product obtained was taken as such for the next step.

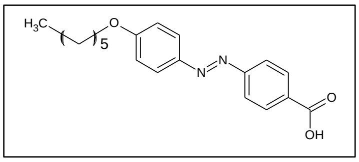

4-[4-(4-hexyloxy)phenylazo] benzoic acid (C): Compound **B** was dried and dissolved in 100 mL of methanol. The reaction mixture was cooled to 5 °C and potassium hydroxide (62.2 mmol, 3 equiv.) in water (20 mL) was added drop wise. Then the reaction mixture was refluxed for 4 h and monitored by TLC to confirm the completion of reaction. The reaction mixture was washed with n-hexane (25 mL) twice to remove nonpolar impurities and pH was adjusted to 6 with diluted hydrochloric acid. The compound was extracted in ethyl acetate, followed by brine wash. The ethyl acetate layer was dried over anhydrous sodium sulphate for 1 h. Then, filtered and ethyl acetate was removed to collect the solid product and recrystallized from ethanol: chloroform (2:1). A dark yellow coloured solid; yield: 46 %; IR (KBr, ν_{max}, cm^{-1}): 3004, 2918, 2849, 1711, 1588, 1493, 1248, 1220, 1130, 1092, 835; ^{1}H NMR (CDCl$_3$) δ: 10.46 (s, 1H, COOH), 7.94 (d, 2H, J = 8.05 Hz, Ar-H), 7.89 (d, 2H, J = 8.10 Hz, Ar-H), 7.52 (d, 2H, J = 8.01 Hz, Ar-H), 6.61 (d, 2H, J = 7.98Hz, Ar-H), 2.13 – 0.92 (m, 13H, –C_6H_{13}); MS (FAB+): m/z for $C_{19}H_{22}N_2O_3$, Calculated: 326.39. Found: 326.09.

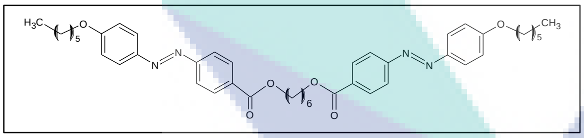

1,6-Hexylene bis-{4-[4-(4-hexyloxy) phenylazo]benzoate} (D): Compound **C** (15.3 mmol, 1 equiv.) was dissolved in 50 mL of dry dichloromethane and DMAP (1.40 mmol, 0.1 equiv.) were added and stirred. After 30 min, a solution of 1,6-dibromohexane (7.6 mmol, 0.5 equiv.) in dry dichloromethane (10 mL) and DCC (23.0 mmol, 1.5 equiv.) in 10 mL of dry dichloromethane was added. The mixture was stirred for 24 h and monitored by TLC. After completion of reaction, the precipitate was removed by filtration and the filtrate was quenched with 1.5 N hydrochloric acid. The compound was extracted twice with dichloromethane followed by washing with 1 N sodium hydrogen carbonate and with brine solution. Then, water content was removed the by adding anhydrous sodium sulfate. The solid crude product was collected by evaporating dicholoromethane using rotatory evaporator. Obtained product was purified by column chromatography using chloroform: methanol (20:1) as eluent. The product was recrystallized from methanol: chloroform (2:1) to get the target compound **D**. A pale yellow coloured solid; yield: 35 %; m.p. 154.2 °C; IR (KBr, ν_{max}, cm^{-1}): 1730, 1625, 1579, 1248, 1238, 1130, 1092, 835; ^{1}H NMR (CDCl$_3$) δ: 8.37 – 6.90 (m, 16H, Ar-H), 0.92 – 1.85 (m, 38H, aliphatic-H);

^{13}C NMR ($CDCl_3$) δ: 161.6, 144.3, 157.0, 132.3, 114.7 123.6, 122.9, 130.2, 165.9, 68.7, 64.8, 29.6, 31.7, 25.6, 25.5, 22.7, 14.1; MS (FAB+): m/z for $C_{44}H_{54}N_4O_6$, Calculated: 734.92. Found: 734.40; Elemental analysis: Calculated (found) %: C 71.91 (71.65), H 7.41 (7.22), N 7.62 (7.48), O 13.06 (12.87).

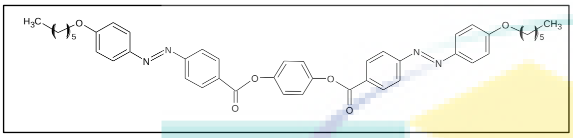

1,4-Phenylene bis-{4-[4-(4-hexyloxy) phenylazo]benzoate} (E): Compound **E** was synthesized by following similar procedure for synthesizing compound **D** except hydroquinone was used instead of 1,6-dibromohexane. A pale yellow coloured solid; yield: 35 %; m.p. 124.3 °C; IR (KBr, ν_{max}, cm^{-1}): 1735, 1578, 1538, 1248, 1130, 1022, 1092, 835; ^{1}H NMR ($CDCl_3$) δ: 8.28 – 7.00 (m, 20H, Ar-H), 0.84 – 1.78 (m, 26H, aliphatic-H); ^{13}C NMR ($CDCl_3$) δ: 146.2, 161.6, 144.3, 157.9, 129.6, 122.0, 123.6, 122.9, 130.6, 144.7, 165.2, 68.7, 29.6, 25.6, 31.8, 22.7, 14.1; MS (FAB+): m/z for $C_{44}H_{46}N_4O_6$, Calculated: 726.86. Found: 726.32; Elemental analysis: Calculated (found) %: C 72.71 (72.82), H 6.38 (6.29), N 7.71 (7.63), O 13.21 (13.12).

3.2.2 Synthesis of azobenzene with amide group

4-[(4-hexyloxyphenyl)diazenyl]-N-phenylbenzamide (F): Compound **C** (15.3 mmol, 1 equiv.) was dissolved in 50 mL of dry dichloromethane before DMAP (1.40 mmol, 0.1 equiv.) was added. The mixture was stirred for 30 min. A solution of aniline (15.3 mmol, 1 equiv.) in dry dichloromethane (10 mL) and DCC (23.0 mmol, 1.5 equiv.) in 10 mL of dry dichloromethane were added slowly. The mixture was stirred for 24 h, monitored by TLC. After completion of the reaction, the precipitate formed was removed by filtration and the filtrate was quenched with hydrochloric acid (1.5 N). The compound was extracted with chloroform forming a chloroform layer. The layer was washed with 1 N sodium hydrogen carbonate followed by brine wash. Then, chloroform was dried over anhydrous sodium sulphate for 1 h. Finally, the solid crude product was collected by evaporation and purified by column chromatography using chloroform: methanol (20:1) as eluent. The product was recrystallized from methanol: chloroform (2:1) to get the target compound **G**. The similar procedure was followed to synthesize the compound **H**, **I** and **J**.

Compound G: A pale yellow coloured solid; yield: 60 %; m.p. 184.5 °C; IR (KBr, v_{max}, cm^{-1}): 3325, 3004, 2930, 2852, 1640, 1538, 1500, 1449, 1248, 1130, 1094, 1092, 835. ^{1}H NMR (CDCl$_3$) δ: 7.95 (d, 1H, CONH), 7.94 – 7.89 (m, 9H, Ar-H), 7.52 (d, 2H, *J* = 8.01 Hz, Ar-H), 6.61 (d, 2H, *J* = 7.98 Hz, Ar-H), 2.13 – 0.92 (m, 13H, -C_6H_{13}); ^{13}C NMR (CDCl$_3$) δ: 162.39, 148.61, 132.22, 127.61, 125.12, 122.69, 114.81, 32.36, 31.57, 30.94, 30.79, 29.14, 26.25, 25.69, 25.36, 25.24, 24.51, 22.60, 14.04; MS (FAB+): m/z for $C_{25}H_{27}N_3O_2$, Calculated: 401.50. Found: 401.18; Elemental analysis: Calculated (found) %: C 74.79 (74.86), H 6.78 (6.69), N 10.47 (10.38) and O 7.97 (7.86).

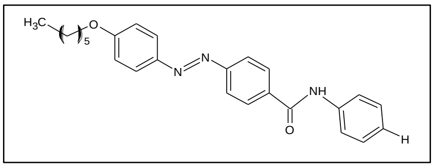

Compound H: A pale yellow coloured solid; yield: 60 %; m.p. 183.5 °C; IR (KBr, v_{max}, cm^{-1}): 3328, 3004, 2930, 2851, 1640, 1538, 1520, 1500, 1449, 1310, 1248, 1130, 1106, 1092, 835; ^{1}H NMR (CDCl$_3$) δ: 8.11 (d, 2H, *J* = 8.02 Hz, Ar-H), 7.98 (d, 1H, *J* = 8.00 Hz, CONH), 7.93 – 7.79 (m, 6H, Ar-H), 7.26 (d, 2H, *J* = 8.01 Hz, Ar-H), 6.81 (d, 2H, *J* = 8.02 Hz, Ar-H), 2.01 – 0.85 (m, 13H, –C_6H_{13}); ^{13}C NMR (CDCl$_3$) δ: 161.19, 145.81, 130.29, 126.83, 126.74, 124.33, 124.06, 123.41, 121.41, 121.94, 121.57, 121.46, 113.84, 113.76, 67.42, 48.16, 47.83, 32.94, 32.24, 30.54, 28.12, 24.67, 24.60, 24.56, 23.92, 21.57, 13.00; MS (FAB+): m/z for $C_{25}H_{26}N_4O_4$, Calculated: 446.50. Found: 446.16; Elemental analysis: Calculated (found) %: C 67.25 (67.34), H 5.87 (5.81), N 12.55 (12.16) and O 14.33 (14.19).

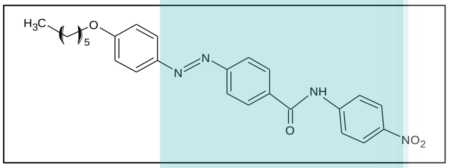

Compound I: A pale yellow coloured solid; yield: 60 %; m.p. 212.3 °C; IR (KBr, v_{max}, cm^{-1}): 3328, 3002, 2930, 2851, 1732, 1640, 1538, 1520, 1448, 1248, 1130, 1106, 1099, 1092, 835; ^{1}H NMR (CDCl$_3$) δ: 8.29 (d, 2H, *J* = 8.03 Hz, Ar-H), 7.99 (d, 1H, *J* = 8.01 Hz, CONH), 7.79 – 7.94 (m, 4H, Ar-H), 7.64 (d, 2H, *J* = 8.01 Hz, Ar-H), 7.37 (d, 2H, *J* = 8.04 Hz, Ar-H), 6.81 (d, 2H, *J* = 8.02 Hz, Ar-H), 3.41 (m, 5H, –$COOC_2H_5$), 0.85 – 2.00 (m, 13H, –C_6H_{13}); ^{13}C NMR (CDCl$_3$) δ: 161.55, 130.29, 126.74, 126.62, 124.33, 124.06, 123.44, 122.03, 121.66, 121.58, 121.49, 113.84, 113.79, 48.16, 32.94, 31.33, 30.54, 29.76, 28.11, 25.22, 24.67, 24.60, 24.33, 24.21, 23.92, 23.49, 21.58, 13.01; MS (FAB+): m/z for $C_{28}H_{31}N_3O_4$, Calculated: 473.56.

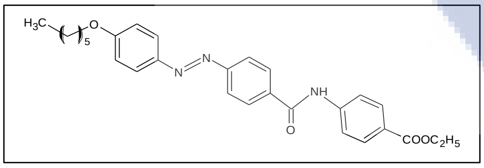

Found: 473.40; Elemental analysis: Calculated (found) %: C 71.01 (71.22), H 6.60 (6.48), N 8.87 (8.77), O 13.51 (13.39).

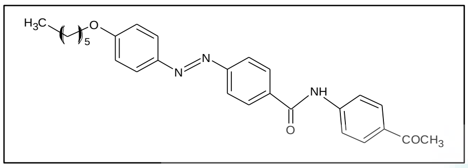

Compound J: A pale yellow coloured solid; yield: 60 %; m.p. 185.5 °C; IR (KBr, v_{max}, cm^{-1}): 3326, 3004, 2929, 2852, 1700, 1640, 1609, 1578, 1449, 1248, 1130, 1092, 835; ^1H NMR ($CDCl_3$) δ: 8.29 (d, 2H, *J* = 8.00 Hz, Ar-H), 7.99 (d, 1H, *J* = 8.00 Hz, CONH), 7.80 – 7.93 (m, 4H, Ar-H), 7.64 (d, 2H, *J* = 8.02 Hz, Ar-H), 7.38 (d, 2H, *J* = 8.04 Hz, Ar-H), 6.95 (d, 2H, *J* = 8.01 Hz, Ar-H), 3.41 (s, 3H, –$COCH_3$), 0.85 – 2.00 (m, 13H, –C_6H_{13}); ^{13}C NMR ($CDCl_3$) δ: 161.19, 153.37, 145.81, 130.29, 126.74, 124.33, 124.06, 121.57, 113.85, 113.77, 67.42, 48.15, 47.82, 32.94, 32.24, 30.54, 28.12, 24.67, 24.60, 23.92, 21.57, 13.00; MS (FAB+): m/z for $C_{27}H_{29}N_3O_3$, Calculated: 443.54. Found: 443.18; Elemental analysis: Calculated (found) %: C 73.11 (73.23), H 6.59 (6.46), N 9.47 (9.33) and O 10.82 (10.73).

3.2.3 Synthesis of azobenzene with fluorine addition

***Para*-Substituted azobenzene:** Ethyl 4-amino benzoate or aniline (46.00 mmol, 1 equiv.) was dissolved in methanol (40 mL) cooled the solution to 2 °C. Then, 8.672 mL of hydrochloric acid (25 %) was added drop wise at 2 °C to the reaction mixture followed by sodium nitrate dissolved in water (44.6 mmol, 1 equiv.). The reaction mixture was stirred for 15 min. Phenol solution prepared with methanol (44.6 mmol, 1 equiv.) was added slowly while maintaining the temperature at 2 °C. After the pH was elevated to 8.5 – 9.0 by using 1 N sodium hydroxide, the reaction mixture was agitated for 4 h. The reaction mixture was then diluted with methanol (250 mL) and ice before reducing the pH to 4. The reddish yellow precipitate was filtered and dried. The crude product was recrystallized twice from methanol to obtain compound **K** and **L**.

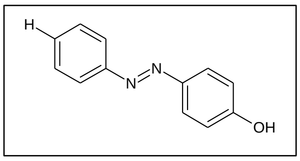

Compound K: A red coloured solid; Rf = 0.42 (40 % CH_2Cl_2-EtOH); yield: 62 %; m.p. 158.5 °C; IR (KBr, v_{max}, cm^{-1}): 1728, 1602, 1484, 1248, 1140, 829; ^1H NMR ($CDCl_3$) δ: 7.26 (t, 1H, *J* = 7.68 MHz, Ar-H), 7.50 (t, 2H, *J* = 7.52 MHz, Ar-H), 7.88 (t, 2H, *J* = 8.11 MHz, Ar-H), 7.44 (d, 2H, *J* = 8.36 MHz, Ar-H), 6.95 (d, 2H, *J* = 8.32 MHz, Ar-H), 7.88 (s, 1H, OH); Calculated: 198.22. Found: 198.01; Elemental analysis: Calculated (found) %: C 72.71 (72.83), H 5.08 (4.89), N 14.13 (14.02), O 8.07 (7.98).

Compound L: A red coloured solid; Rf = 0.42 (40 % CH_2Cl_2-EtOH); yield: 62 %; m.p. 160.2 °C; IR (KBr, ν_{max}, cm^{-1}): 3321, 1728, 1602, 1484, 1248 , 1140, 829; ^{1}H NMR ($CDCl_3$) δ: 8.17 (d, 2H, *J* = 8.2 Hz, Ar-H), 7.92 (d, 2H, *J* = 7.5 Hz, Ar-H), 7.88 (d, 2H, *J* = 7.5 Hz, Ar-H), 7.01 (d, 2H, *J* = 8.2 Hz, Ar-H), 5.54 (s, 1H, OH), 4.42 (q, 2H, *J* = 7.2 Hz, CH_2CH*3*), 1.44 (t, 3H, CH_2CH_3); MS (FAB+): m/z for $C_{15}H_{14}N_2O_3$, Calculated: 270.28. Found: 270.08; Elemental analysis: Calculated (found) %: C 66.66 (66.74), H 5.22 (5.16), N 10.36 (10.21), O 17.76 (17.67).

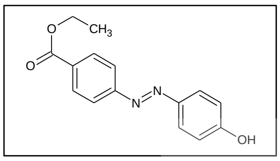

Fluorinated azobenzene: Compound **M** and **N** having single fluorine atom was obtained by coupling compound **K** or **L** with 4-fluoro benzoic acid in the presence of DCC and DMAP as coupling agent. The synthesis of compound **O** and **P** with two fluorine atoms were performed by coupling compound **K** or **L** with 3,5-difluoro benzoic acid by DCC and DMAP. Firstly, 4-fluoro benzoic acid or 3,5-difluoro benzoic acid, (15.3 mmol, 1 equiv.) was dissolved in 50 mL of dry dichloromethane. DMAP (1.40 mmol, 0.1 equiv.) were added and the mixture was stirred for 30 min. The solution of compound **K** or **L** (15.3 mmol, 1 equiv.) in dry dichloromethane was then added into the mixture, followed by adding DCC (23.0 mmol, 1.5 equiv.) in dry dichloromethane (10 mL) slowly. The mixture was stirred for 24 h and monitored by TLC. After completion of reaction, the precipitate was removed by filtration and the filtrate was quenched with 1.5 N hydrochloric acid. The compound was extracted twice with dichloromethane and washed with 1 N sodium hydrogen carbonate, followed by brine wash. Water content was removed by adding anhydrous sodium sulfate. Finally, the solid crude product was collected by evaporating dicholoromethane using rotatory evaporator. Obtained product was purified by column chromatography using chloroform: methanol (20:1) as eluent. The product was recrystallized from methanol: chloroform (2:1) to get the target compound **M**, **N**, **O**, and **P**.

Compound M: A pale yellow coloured solid; yield: 35 %; m.p. 151.2 °C; IR (KBr, v_{max}, cm^{-1}): 2922, 2857, 1732, 1605, 1508, 1238, 1075, 884, 759, 604; ^1H NMR ($CDCl_3$) δ: 8.29 – 8.25 (m, 4H, Ar-H), 8.06 – 8.03 (M, 4H, Ar-H), 7.96 – 7.94 (m, 5H, Ar-H); ^{13}C NMR ($CDCl_3$) δ: 167.32 (ester C=O), 165.29 – 117.80 (Ar-C); MS (FAB+): m/z for $C_{19}H_{13}FN_2O_2$, Calculated: 320.32. Found: 320.13; Elemental analysis: Calculated (found) %: C 71.24 (71.29), H 4.09 (3.97), F 5.93 (5. 97), N 8.75 (8.68), O 9.99 (9.91).

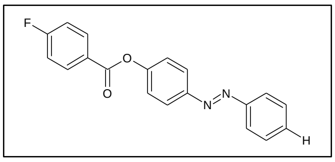

Compound N: A pale yellow colored solid; yield: 35 %; m.p. 168.7 °C; IR (KBr, v_{max}, cm^{-1}): 1742, 1706, 1602, 1508, 1278, 1196, 1067, 1015, 875, 755, 684; ^1H NMR ($CDCl_3$) δ: 8.22 – 7.21 (m, 12H, Ar-H), 4.45 (q, 2H, OCH_2), 1.46 (t, 3H, CH_3); ^{13}C NMR ($CDCl_3$) δ: 166.07 (ester C=O), 163.86 – 115.87 (Ar-C), 61.32 (OCH_2), 14.35 (CH_3); MS (FAB+): m/z for $C_{22}H_{17}FN_2O_4$, Calculated: 338.09. Found: 338.19; Elemental analysis: Calculated (found) %: C 67.45 (67.58), H 3.58 (3.49), F 11.23(11.16), N 8.28 (7.98), O 9.46 (9.29).

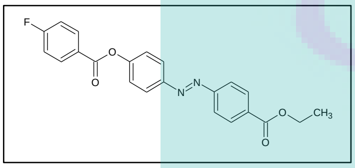

Compound O: A pale yellow coloured solid; yield: 35 %; m.p. 167.35 °C; IR (KBr, v_{max}, cm^{-1}): 1742, 1595, 1442, 1335, 1212, 1116, 983, 864, 802, 687; ^1H NMR ($CDCl_3$) δ: 8.06 – 7.39 (m, 12H, Ar-H); ^{13}C NMR ($CDCl_3$) δ: 166.08 (ester C=O), 163.86 – 109.11 (Ar-C); MS (FAB+): m/z for $C_{19}H_{12}F_2N_2O_2$, Calculated: 392.38. Found: 391.23; Elemental analysis: Calculated (found) %: C 67.34 (67.48), H 4.37 (4.23), F 4.84 (4.78), N 7.14 (6.98), O 16.31 (16.24).

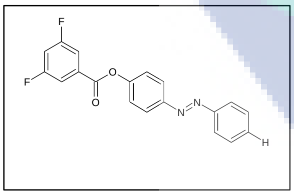

Compound P: A pale yellow coloured solid; yield: 35 %; m.p. 170.1 °C; IR (KBr, v_{max}, cm^{-1}): 1737, 1705, 1625, 1596, 1447, 1337, 1280, 1222, 1124, 1024, 870, 800, 642; ^1H NMR ($CDCl_3$) δ: 8.24 – 7.02 (m, 11H, Ar-H), 4.45 (q, 2H, OCH_2), 1.26 (t, 3H, CH_3); ^{13}C NMR ($CDCl_3$) δ: 166.05 (ester C=O), 161.97 – 109.38 (Ar-C), 61.34 (OCH_2), 14.53 (CH_3); MS (FAB+): m/z for $C_{22}H_{16}F_2N_2O_4$, Calculated: 410.37. Found: 140.05; Elemental analysis: Calculated (found) %: C 64.39 (64.71), H 3.93 (3.49), F 9.26 (9.14), N 6.83 (6.72), O 15.60 (15.21).

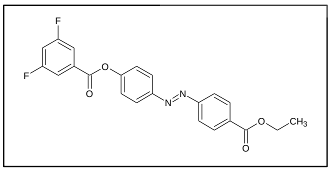

3.2.4 Synthesis of azobenzene with olefinic terminal

Ethyl 4-{(E)-[4-(pent-4-en-1-yloxy)-phenyl]diazenyl}benzoate (Q): Compound **A** (18.5 mmol, 1 equiv.) and 5-bromo 1-pentene (37.1 mmol, 2 equiv.) were dissolved in dry acetone (300 mL). Then potassium carbonate (18.5 mmol, 1 equiv.) was added drop wise using addition funnel followed by a catalytic amount of potassium iodide (50 mg). The reaction mixture was refluxed for 24 h under nitrogen atmosphere and monitored by TLC. The solvent was evaporated in the fume hood. The dried reaction mixture was taken as such for the next step (Ester hydrolysis reaction).

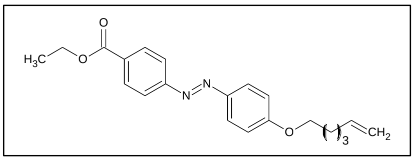

4-{(E)-[4-(pent-4-en-1-yloxy)phenyl]diazenyl}benzoic acid (R): Compound **Q** was dissolved in 100 mL of methanol. The reaction mixture was cooled to 5 °C in ice bath. A solution of potassium hydroxide (62.2 mmol, 3 equiv.) in water (20 mL) was added drop wise and the reaction mixture was reflux for 4 h, monitored by TLC. The reaction mixture was taken in a separating funnel. It was washed two times with n-hexane to remove nonpolar impurities. Then the aqueous solution was acidified with dilute hydrochloric acid and pH was adjusted to 6. The compound was extracted with ethyl-acetate, followed by brine wash. Anhydrous sodium sulphate was added to remove the water content present in the ethyl-acetate layer. The solid product was collected from the solution by evaporating ethyl-acetate using rotatory evaporator and recrystallized from ethanol: chloroform (2:1). A dark yellow coloured solid; yield: 46 %; m.p. 156.2 °C; IR (KBr, v_{max}, cm^{-1}): 3004, 2918, 2849, 1711, 1588, 1493, 1248, 1220, 1130, 1092, 835; ^{1}H NMR (DMSO) δ: 11.10 (s, 1H, COOH), 7.13 – 8.12 (m, 8H, *J* = 8.15 Hz, Ar), 4.22 (t, 2H, *J* = 12.35 Hz, OCH_2), 4.99 – 5.10, 5.85 – 5.93 (m, 3H, olefinic), 2.42 – 2.59 (m, 4H, CH_2).

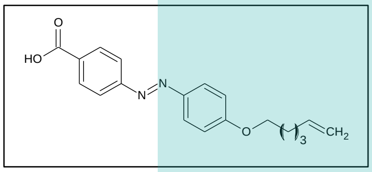

Phenyl 4-{(E)-[4-(pent-4-en-1-yloxy)phenyl]diazenyl}benzoate derivative (S): Compound **R** (15.3 mmol, 1 equiv.) was dissolved in 50 mL of dry dichloromethane. DMAP (1.40 mmol, 0.1 equiv.) was added and the mixture was stirred for 30 min. A solution of *para*-substituted halogen phenol (7.6 mmol, 0.5 equiv.) and DCC (23.0 mmol, 1.5 equiv.) in dry dichloromethane (10 mL) were added to the mixture. The mixture was stirred for 24 h, and monitored by TLC. After completion of reaction, the precipitate was removed by filtration and the filtrate was quenched with 1.5 N HCl. The compound was extracted two times with DCM. Then it was rinsed with 1 N sodium hydrogen carbonate, followed by brine wash. Water content was removed by adding anhydrous sodium sulphate to the DCM layer. Finally, the solid crude product was collected by evaporating DCM by using rotatory evaporator and obtained product was purified by column chromatography using chloroform: methanol (20:1) as eluent. The product was recrystallized from methanol: chloroform (2:1) to get the target compound **S**. The similar procedure was followed to synthesize the other target compound **T**, **U**, **V** and **W**.

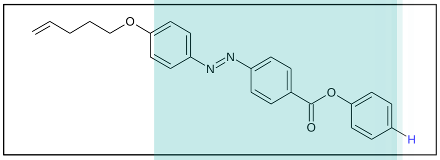

Compound S: A pale yellow coloured solid; yield: 35 %; m.p. 119.1 °C; IR (KBr, v_{max}, cm^{-1}): 3004, 2918, 2849, 1732, 1261, 1200, 1143, 1096, 1072, 859, 838; ^{1}H NMR ($CDCl_3$) δ: 7.13 – 8.32 (m, 12H, *J* = 8.11 Hz, Ar-H), 5.84 – 5.92, 5.03 – 5.10 (m, 3H, *J* = 12.41 Hz, 7.99 Hz, olefinic), 4.20, 4.11 (t, 2H, *J* = 12.32 Hz, OCH_2), 2.42 – 2.59 (m, 4H, CH_2); ^{13}C NMR (DMSO) δ: 24.93 – 47.97 (aliphatic), 67.96 (ether), 115.03 – 157.08 (aromatic), 115.72 (olefinic), 164.01 (ester).

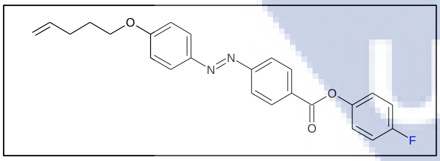

Compound T: A pale yellow coloured solid; yield: 35 %; m.p. 126.2 °C; IR (KBr, v_{max}, cm^{-1}): 3006, 2918, 2848, 1725, 1261, 1186, 1143, 1096, 1072, 858, 838; ^{1}H NMR ($CDCl_3$) δ: 7.13 – 8.32 (m, 11H, *J* = 8.11 Hz, Ar-H), 5.84 – 5.93, 4.96 – 5.10 (m, 3H, *J* = 12.31 Hz, 7.87 Hz, olefinic), 4.20, 4.12 (t, 2H, *J* = 12.22 Hz, OCH_2), 2.42 – 2.58 (m, 4H, CH_2); ^{13}C NMR (DMSO) δ: 24.92 – 47.95 (aliphatic), 67.93 (ether), 115.10 – 157.09 (aromatic), 115.72 (olefinic), 164.01 (ester).

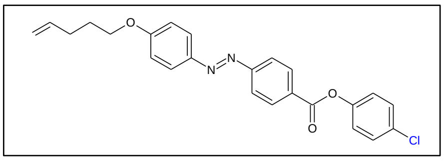

Compound U: A pale yellow coloured solid; yield: 35 %; m.p. 131.4 °C; IR (KBr, v_{max}, cm^{-1}): 3006, 2918, 2916, 2851, 1259, 1208, 1143, 1092, 1066, 837, 809; ^{1}H NMR ($CDCl_3$) δ: 7.16 – 8.33 (m, 11H, *J* = 8.12 Hz, Ar-H), 5.80 – 5.98, 4.92

– 5.15 (m, 3H, *J* = 12.42 Hz, 7.96 Hz, olefinic), 4.20, 4.12 (t, 2H, *J* = 12.12 Hz, OCH_2), 2.42 – 2.59 (m, 4H, CH_2); ^{13}C NMR (DMSO) δ: 24.92 – 47.98 (aliphatic), 67.96 (ether), 115.05 – 157.09 (aromatic), 115.72 (olefinic), 164.01 (ester).

Compound V: A pale yellow coloured solid; yield: 35 %; m.p. 142.1 °C; IR (KBr, v_{max}, cm^{-1}): 3006, 2919, 2848, 1733, 1208, 1143, 1259, 1092, 1066, 837, 809; ^1H NMR ($CDCl_3$) δ: 7.13 – 8.32 (m, 11H, *J* = 8.11 Hz, Ar-H), 5.85 – 5.98, 5.00 – 5.10 (m, 3H, *J* = 12.31 Hz, 7.97 Hz, olefinic), 4.20, 4.12 (t, 2H, *J* = 12.17 Hz, OCH_2), 2.41 – 2.58 (m, 4H, CH_2); ^{13}C NMR (DMSO) δ: 24.92 – 47.97 (aliphatic), 67.98 (ether), 115.05 – 157.09 (aromatic), 115.73 (olefinic), 164.01 (ester).

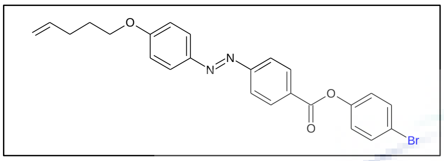

Compound W: A pale yellow coloured solid; yield: 35 %; m.p. 158.2 °C; IR (KBr, v_{max}, cm^{-1}): 3003, 2916, 2848, 1731, 1257, 1205, 1139, 1068, 1052, 859, 836; ^1H NMR ($CDCl_3$) δ: 7.12 – 8.33 (m, 11H, *J* = 8.11 Hz, Ar-H), 5.81 – 5.93, 4.96 – 5.10 (m, 3H, *J* = 12.43 Hz, 7.97 Hz, olefinic), 4.20, 4.12 (t, 2H, *J* = 12.32 Hz, OCH_2), 2.42 – 2.57 (m, 4H, CH_2); ^{13}C NMR (DMSO) δ: 24.91 – 47.98 (aliphatic), 67.95 (ether), 115.02 – 157.09 (aromatic), 115.71 (olefinic), 164.01 (ester).

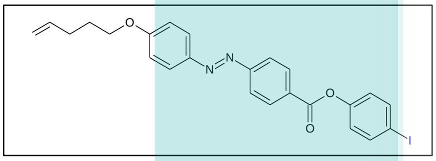

3.3 MESOMORPHIC STUDIES

3.3.1 Polarising optical microscopy (POM)

Mesomorphic properties exhibited by each samples were analysed through an optical Olympus BX 51 microscope, equipped with a digital camera and Linkam hotstage. Microscope glass slides and coverslips were clean with acetone before the sample preparation to avoid contamination. Then, thin samples of azobenzene derivatives were sandwiched between the microscope glass slide and coverslip. The prepared samples were placed in a Linkam hotstage, where the temperature of the materials was controlled between 0 °C and 250 °C. The heating and cooling scan rate was fixed at 10 °C/min. Optical textures of mesosphases exhibited by the materials were observed at 20X magnification under the polarised light. Identified microscopic textures were captured while observation was made.

3.3.2 Differential scanning calorimetry (DSC)

Thermal analysis was conducted at International Islamic University Malaysia (IIUM), Kuantan. All of the azobenzene derivatives were analysed using a differential scanning calorimeter DSC 1 from Mettler Toledo Inc. The samples (5 mg) were weighed into an aluminium sample pan and crimped shut with an aluminium top. An empty pan and cover were used as reference. The prepared samples and reference were placed on sample holder and ready for analyse. Temperature was scanned between 25 ℃ to 190 ℃, at heating and cooling rate of 10 ℃/min in nitrogen atmosphere. Samples were heated twice to make the spectra more accurate.

3.4 PHOTOISOMERISATION STUDIES

Solution samples of novel azobenzene derivatives were prepared using chloroform, in 1 cm quartz cuvette. The concentration of the solution was fixed at 1.1×10^{-5} mol/L. The cuvette was rinsed twice with chloroform before used. Cuvette lid was used to cover the cuvette to avoid evaporation. The solutions were not disturbed once UV light was irradiated to stimulate *trans–cis* photoisomerisation. OmniCure® S2000 UV light source was used to irradiate sample at 365 nm through UG11 filter, and heat filter was inserted to avoid any heating effects. The UV intensity passed through the filter was measured to be 5.86 mW/cm^2 by UV meter. After photostationary state achieved, the samples were then left in the dark for thermal back relaxation. Absorption spectra were recorded from time to time by an Ocean Optics HR-2000+ UV–Vis spectrophotometer, measured under air in the dark condition, at temperature 27 ± 1 ℃. Figure 3.1 shows the experimental set up used to measure and record the absorption spectra before and after irradiation with 365 nm UV light.

3.5 DATA ANALYSIS

3.5.1 Calculation of conversion efficiency

The spectroscopic data was used to calculate the conversion efficiency (CE) in the photostationary state by equation 3.1 (Bandara and Burdette, 2012).

$$CE = \frac{A(t_0) - A(t_\infty)}{A(t_0)} \times 100\% \tag{3.1}$$

where $A(t_o)$ is absorbance before UV and $A(t_\infty)$ is absorbance after UV. The results were summarized as *cis* concentration, [*cis*].

3.5.2 First-order kinetics

The first-order kinetics was calculated from the changes in absorbance at a certain wavelength with time using equation 3.2 (Sasaki et al., 1993)

$$\ln \frac{A_\infty - A_t}{A_\infty - A_o} = -k_\Delta t \tag{3.2}$$

where k_Δ is the thermal rate constant in s^{-1}. A_t, A_o, and A_∞ were the absorbance at peak wavelength at time t, time zero, and infinite time, respectively. The inset gave a negative logarithmic plot with a linear fit, where the slop gave the rate constant of thermal back relaxation.

3.6 DEVICE STUDIES

3.6.1 Photoisomerisation studies in liquid crystal host

Photoisomerisation studies were also performed on liquid crystal cells made up of indium tin oxide (ITO) coated and unidirectionally rubbed glass plates, which had been cleaned by ultra-sonicator. Two glass plates were attached at the edge using UV curing glue and the cell thickness was maintained around 5 µm. Guest-host effect was employed to study the photoisomerisation behaviour of selected azobenzene molecules in liquid crystal host. Here, azobenzene derivatives acted as guest while liquid crystal acted as host. Accordingly, the liquid crystal mixture containing 5 % of azobenzene derivative and 95 % of a commercial nematic liquid crystal MLC6873-100, obtained from Merck, was filled into the prepared liquid crystal cell by capillary force at isotropic temperature (about 100 °C). The liquid crystal cell was cold down slowly to room temperature to attain uniform liquid crystalline phases before used for the photoisomerisation study. The experimental set up that had been used for photoisomerisation study in solvent was also applied for photoisomerisation study in liquid crystal host.

Besides that, in order to test the rewriting ability of the compound, numerous cycles of photoisomerisation was also performed by alternating UV light at 356 nm for inducing *trans–cis* isomerisation, and visible light at 420 nm for *cis–trans* isomerisation. The changes in peak absorption λ_{max} were recorded and plotted in the function of time.

3.6.2 Device fabrication

A prototype of optical image storage device was fabricated using the selected azobenzene derivatives. Similarly, two glass plates with ITO coated and rubbed layers were used for making the prototype, where guest-host mixture consisting 5 % of azobenzene derivative and 95 % of commercially available nematic liquid crystal, MLC6873-100, was filled into the cell by capillary force at isotropic temperature. After the cell was brought back to room temperature, a photo-mask was placed on top. Next, UV light of 365 nm wavelength and 5.86 mW/cm^2 of intensity was shined through the photo-mask for about 10 min to form the image. The image formed was observed using crossed polarisers. The image was then erased by using high intensity visible light of 420 nm wavelength in order to test the rewriting ability.

Ideally, these cell preparation processes should be performed in a clean room and preferably in an enclosure free of humidity or other chemicals in order to prolong the lifetime of the sample. Nevertheless, the liquid crystal cells prepared can last several months and can withstand a numbers of temperature cycling through the nematic–isotropic phase transitional, provided the liquid crystals used are chemically stable.

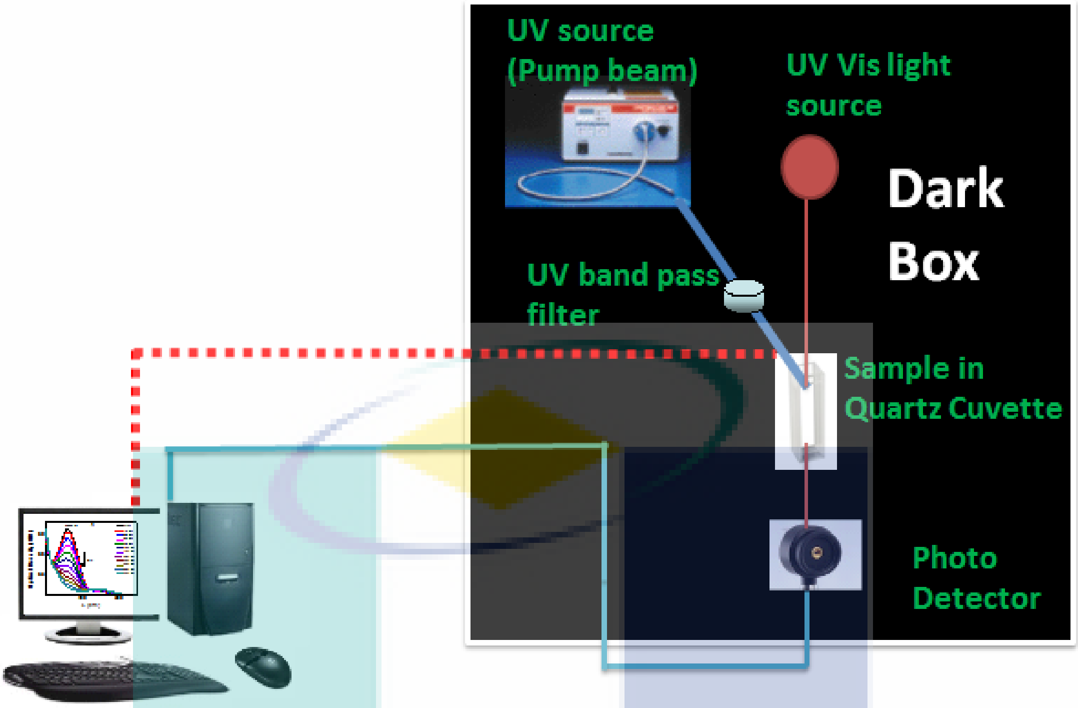

Figure 3.1: Experimental set up for photoisomerisation studies using Ocean Optics HR-2000+ UV–Vis spectrophotometer.

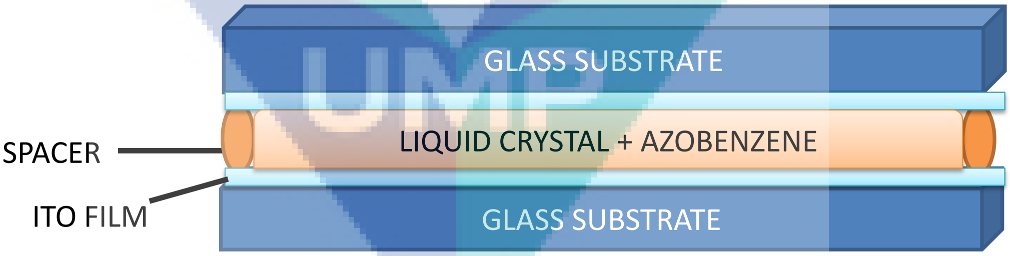

Figure 3.2: Construction of liquid crystal cell.

CHAPTER 4

RESULTS AND DISCUSSION

4.1 MESOMORPHIC STUDIES

The difference between many liquid crystal phases was generally minimal, and such minimal differences in the structure mean that precise classification of the mesophases required several techniques to be employed. Since polarising optical microscopy (POM) technique alone did not supply sufficient information about the liquid crystalline properties, differential scanning calorimetry (DSC) had been used as a complementary tool to the POM.

The mesomorphic texture of all azobenzene derivatives was studied using POM along with a Linkam hotstage enabling *in situ* high temperature observations, and polariser which were crossed at 90° to each other (upper and lower polarisers). The identification of mesophases through POM involved the magnified view of a thin sample of azobenzene derivatives sandwiched between a clean glass microscope slide and a coverslip. The microscope slide of material was placed in the hotstage, which can be accurately temperature controlled.

Technically, POM allows the visual observation of the liquid crystalline optical texture due to the birefringence of mesophase. Since the polarisers in the microscope were perpendicular to each other, light from the lower polariser was extinguished by the second polariser. If no sample was placed in the hotstage, light was extinguised and so darkness appeared. Likewise, if an isotropic liquid was placed, the polarised light could not pass through the analyser (upper polariser) and again darkness appeared.

On the other hand, when an anisotropic, birefringent azobenzene derivative was present, light was not extinguished and an optical texture appeared to give information related to the arrangement of the molecules within the medium. The arrangement of azobenzene molecules within the phase was detected by careful analysis of the microscopic defect texture. Beautiful focal conic images represent smectic-A phase while thread-like apperances represent nematic phase.

Next, calorimetric test was performed by using DSC in order to determine the enthalpy change associated with phase transition in the samples. Accordingly, when the azobenzene sample was heated, the material melted – changing from crystalline state to liquid state. During this process of melting, energy was absorbed from the surroundings and so the process was endothermic. Similarly, when the sample was cooled down, the azobenzene recrystallized and since it was an exothermic process, energy was released to the surroundings. The DSC immediately measured the energy absorbed or released by the sample as it was heated or cooled.

The melting transition from solid to liquid was a relatively drastic transition in terms of the structural change and this was reflected by the relatively high enthalpy changes in the DSC curve. DSC also detects the much more subtle phase transitions that involved in azobenzene materials. Such more subtle structural changes involved in liquid crystal phase transitions were reflected by the relatively small enthalpy changes. The total enthalpy changes ΔH for the process were given by the integral under the DSC peak, above the baseline. However, the DSC could not identify the type of liquid crystalline phases in the azobenzene sample, so it was combined with POM technique which revealed the distinct optical texture generated by the liquid crystalline phases.

4.1.1 Bent-shaped azobenzene

As a matter of fact, bent-shaped molecules with extended aromatic cores and short terminal chains, helped to minimize the bending structure of the molecules, thus facilitated the generation of nematic phase (Keith et al., 2010; Cvetinov et al., 2013). Not all of the bent-shaped azobenzene were liquid crystalline in nature. But spacers that responsible for flexibility and free rotation, acted as the central unit, might affect their mesomorphic properties to a significant extent. Therefore, it was quite interesting to study the mesomorphic properties and photoisomerisation behaviour based on the effect of aliphatic/aromatic spacer in dimeric azobenzene. To date, the dramatic influence of aliphatic/aromatic spacers on the bent-shaped azobenzene has not been studied. Two dimeric azobenzene derivatives were studied, particularly named as compound **D** and compound **E**. Both of the compounds were in bent shape with aliphatic or aromatic spacer placed at the centre connecting two azobenzene moieties with alkyl chains at the terminal ends.

From the microscopic study, the tread-like texture was observed upon cooling of compound **D** and **E** from isotropic state. The optical textures were identified for compound **D** at temperature 245.6 °C, and compound **E** at temperature 236.1 °C. Figure 4.1 shows the typical texture for nematic phase of compound **E**, captured on cooling cycle under the polarised light. No other phase, except crystallisation, was observed on further cooling up to room temperature.

On the other hand, table 4.1 summarized the phase transition temperature and enthalpy changes for both compound in the second heating and cooling cycles, obtained from DSC analysis. One can notice from the table that on heating cycle, crystalline–nematic transition took place at temperature around 103 °C (ΔH = 9.50 mJ) in compound **D**, and around 136 °C (ΔH = 32.11 mJ) in compound **E**. After that, upon reaching 153 °C, compound **D** turned into isotropic state as indicated by the enthalpy changed from the nematic phase. In case of compound **E**, since the calorimetric test was carried out from temperature 25 °C to 190 °C only, the enthalpy change from nematic to isotropic phase, which took placed at temperature above 190 °C, could not be detected. Alternatively, the transition temperature was obtained from POM study.

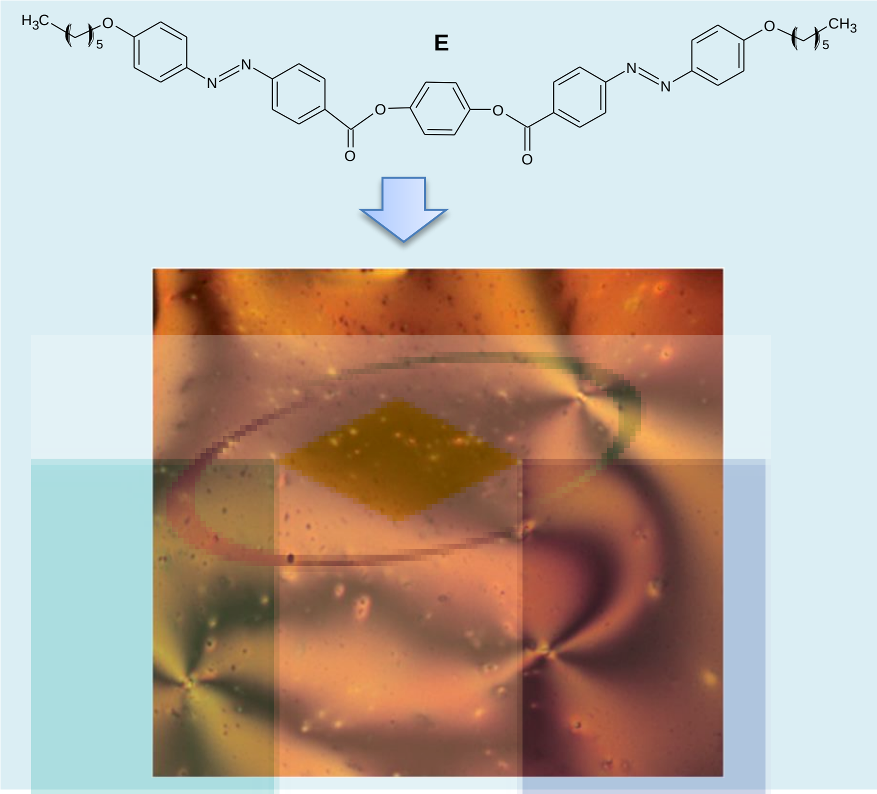

Figure 4.1: Optical micrograph of bent-shaped azobenzene **E** with aromatic spacer captured at temperature 200 °C.

Table 4.1: Phase transition temperature (T/ °C) and associated transition enthalpy values (ΔH/ mJ) in parentheses obtained from second DCS scan of compound **D** and **E**.

Compound designation	DSC (°C)				
	Cr	Heating Cooling	N	Heating Cooling	Iso
D	√	103.86 (9.50) 125.64 (-5.75)	√	153.89 (20.51) 178.30 (-17.09)	√
E	√	135.99(32.11) 155.00 (-27.93)	√	{245.6} {245.6}	√

Abbreviations: Cr = crystalline phase; N = nematic phase; Iso = isotropic phase.
Notes: values in { } was $T_{N\text{-}I}$ obtained from POM; "√" indicates phase exists; "–" indicates no phase exists.

Both the compound **D** and **E** had alkyl as terminal end, but their spacers were different. Compound **D** with n-hexane spacer, while compound **E** with benzene ring spacer. In spite of this, the obtained results showed that both of the compounds exhibited nematic phase only. Though this type of ring-substitution pattern seems to give nematogenic nature to the bent-shaped azobenzene (Keith et al., 2010; Cvetinov et al., 2013), it is noteworthy that with the increased in length and flexibility by using aliphatic spacer, replacing the aromatic spacer, did not make any difference in the liquid crystalline property. One possible reason for this could be that both of the spacers were made up of six carbon atoms, so the different in molecular length was not sufficient to bring about significant difference.

4.1.2 Azobenzene with amide group

Four azobenzene derivatives containing amide group were studied. In all of four compounds, one side arm of the azo bond was made up of an anisole, $(C_6H_5)OCH_3$, and another side arm was made up of benzamide. In order to investigate the effect of adding electron-withdrawing group on the formation hydrogen bonding, the benzamide unit was connected to different electron-withdrawing group, namely benzene, C_6H_5, nitrobenzene, $(C_6H_5)NO_2$, ethyl benzoate, $(C_6H_5)COOC_2H_5$, and phenylethanone, $(C_6H_5)COCH_3$ (as in figure 4.2).

From the microscopic observation, all of the four compounds did not show any liquid crystalline phase. Rather, they were changing from crystalline to isotropic throughout the heating cycle. Later on, when DSC analyses were carried out, the results (table 4.2) showed that there was liquid crystalline phase transition took place during the second heating and cooling cycle. The results were contradicted with the microscopic observation where all of the compound exhibit crystalline-to-liquid crystalline transition at temperature ($T_{C\text{-}LC}$) in the range between 135 – 148 °C on the heating cycle, except compound **G** which showed no enthalpy change for mesomorphic phase. On further heating, the rest of the compounds transformed into isotropic phase at temperature ($T_{LC\text{-}I}$) in the range of 160 – 179 °C.

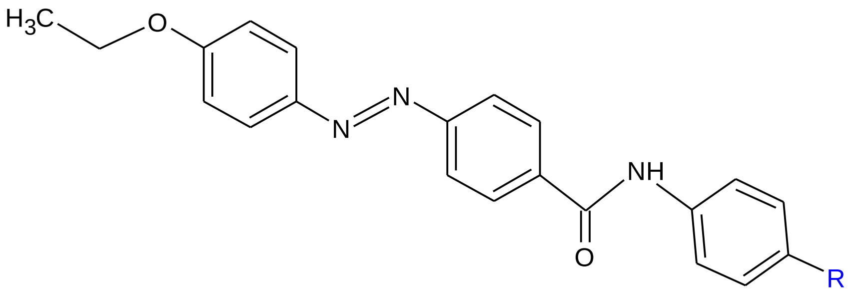

Where **G**: R = H
H: R = NO_2
I: R = $COOC_2H_5$
J: R = $COCH_3$

Figure 4.2: Chemical structures of amide-based azobenzene compound.

Table 4.2: Phase transition temperature (T/ °C) and associated transition enthalpy values (ΔH/ mJ) in parentheses obtained from second DCS scan of compound **G** – **J**.

Compound designation	DSC (°C)				
	Cr	Heating Cooling	LC	Heating Cooling	Iso
G	√	179 (31.02) 197.67 (-6.58)	-	- -	√
H	√	133.01 (7.98) 167.61 (-1.91)	√	160.06 (39.88) 179.58 (-30.43)	√
I	√	137.36 (11.31) 168.78 (-11.62)	√	156.4 (22.60) 182.75 (-28.39)	√
J	√	147.73 (25.12) 168.30 (-0.52)	√	160.25 (38.54) 185.52 (84.20)	√

Abbreviations: Cr = crystalline phase; LC = liquid crystalline phase; Iso = isotropic phase.
Notes: "√" indicates phase exists; "–" indicates no phase exists.

The reasons for none of these mesophases were observed under the microscope might be due to the narrow liquid crystalline temperature range. In compound **J**, for example, the liquid crystalline temperature range ($\Delta T = T_{LC\text{-}I} - T_{C\text{-}LC}$) was about 13 °C, so observation through the optical polarising microscope under heating rate of 10 °C/min was difficult. Meanwhile, one of the reasons for no mesomophic transition detectable in compound **G** might be due to the benzene ring attached to the benzamide did not help the formation of rigid and anisotropic central core in the azobenzene molecule.

4.1.3 Azobenzene with fluorine addition

Next, the third series of azobenzene derivative studied was azobenzene with fluorine addition. Here the azobenzene derivatives added with fluorine atoms as lateral group. In section 2.5.3, there has been stated that fluorine gives a unique effect on molecular properties due to its high electronegativity and lone pair electrons (Namazian and Coote, 2009). In addition, fluorine atom helps to stabilize the azobenzene molecule to a greater extent than other substituent due to its smaller size. Besides that, it is noteworthy that the fluorinated azobenzene compounds give a lower phase transition temperature compare to non-fluoro compounds because the transition temperature decreases with the increase in number of fluorine atom (Rahman et al., 2013). With this knowledge in mind, it is interesting to study mesomorphic and photoisomerisation property of the fluorinated azobenzene derivatives. Then, the effects of fluorine addition were compared with those consist of ethyl benzoate terminus, $-COOC_2H_5$.

Under the optical microscope, liquid crystalline phases were observed in compound **N**. First of all, nematic phase (schlieren texture) was captured at 225.5 °C upon cooling from the isotropic at the rate of 2 °C/min. Figure 4.3a shows the typical nematic phase captured for compound **N**. On further cooling, a broken fan-shaped texture (figure 4.3b) was observed as typical for smectic-A phase. It was found at lower temperature, about 168 °C. And lastly, crystalline phase (figure 4.3c) was observed on further cooling. For compound **P**, a fan shaped texture typical for smectic-A phase was observed (Figure 4.4a) at 181 °C, and it transformed to crystalline phase at 106 °C (Figure 4.4b).

The phase transition temperature of compound **N** was then confirmed by DSC analysis. Table 4.3 summarizes the DSC results. On cooling, there were two peaks observed for compound **N** at 163.92 °C (ΔH = -228.46 mJ) and 156.92 °C (ΔH = -2.98 mJ), which corresponded to the nematic–smectic-A and smectic-A–crystalline transition. However, there was another peak undetectable in DSC analysis as it occurred at temperature beyond the heating scan range. Similarly, a peak corresponding to nematic–smectic-A transition was also missing for the compound **P** on cooling cycle while smectic-A–crystalline transition took place at 128.67 °C (ΔH = -51.58 mJ).

The monofluoro-substituted and difluoro-substituted azobenzene containing benzoate ester terminus, $–COOC_2H_5$, namely compound **N** and **P** respectively, generated smectic-A. Apart from the smectic-A phase, compound **N** also generated nematic phase. Compound **P** did not generate nematic phase but it was observable that its melting temperature, T_m, lower compared to compound **N**; T_m of compound **P** observed at 106.33 °C while that of compound **N** observed at 112.33 °C. In some way, these compounds similar to the previously reported fluorine-substituted benzoate ester incorporated in azobenzene polymer, which also showed smectic-A and nematic phases and thermal stability decreased as the number of fluorine increased (Rahman et al., 2013).

In compound **M** and **O** without the ester terminus (figure 4.5), no liquid crystalline phase detected in microscopic and DSC analysis. The effects of adding lateral fluorine atoms in the two compounds were that electron-withdrawing inductive effect were so weak that its dipole moment could be overwhelmed by the dipole moment exerted by the oxygen atom of the carbonyl moiety on the phenyl ring to which it attached. In this situation, the liquid crystalline properties lost through the loss of conjugation of the molecule or broadening of the molecular size (Al-Hamdani et al., 2010).

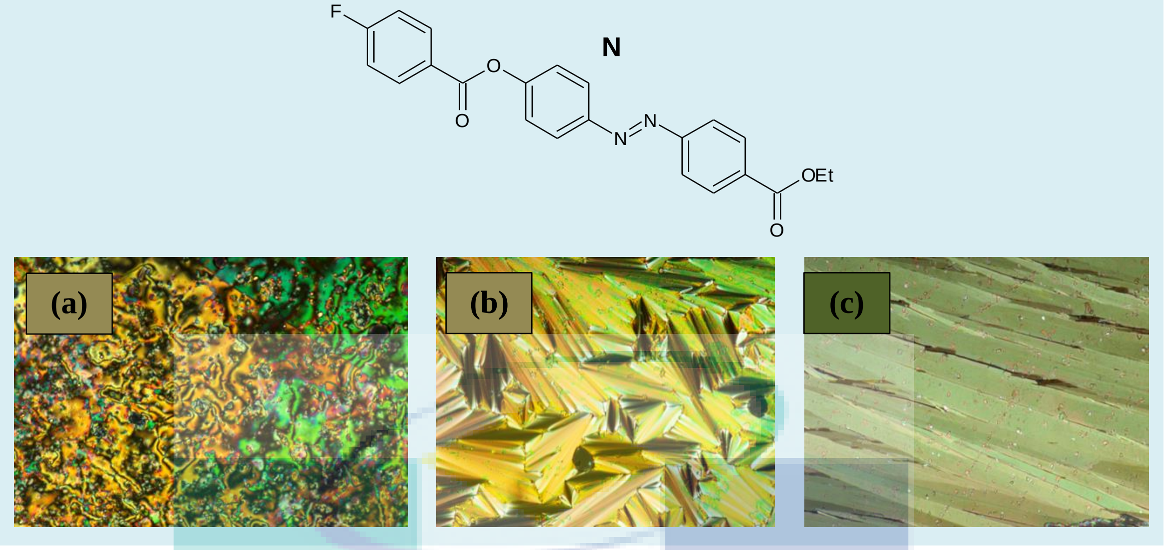

Figure 4.3: Optical micrographs obtained from cooling of azobenzene **N** from isotropic phase; a) – nematic phase at 225.5 °C, b) – smectic-A phase at 168.0 °C, c) – crystalline phase at 160.0 °C.

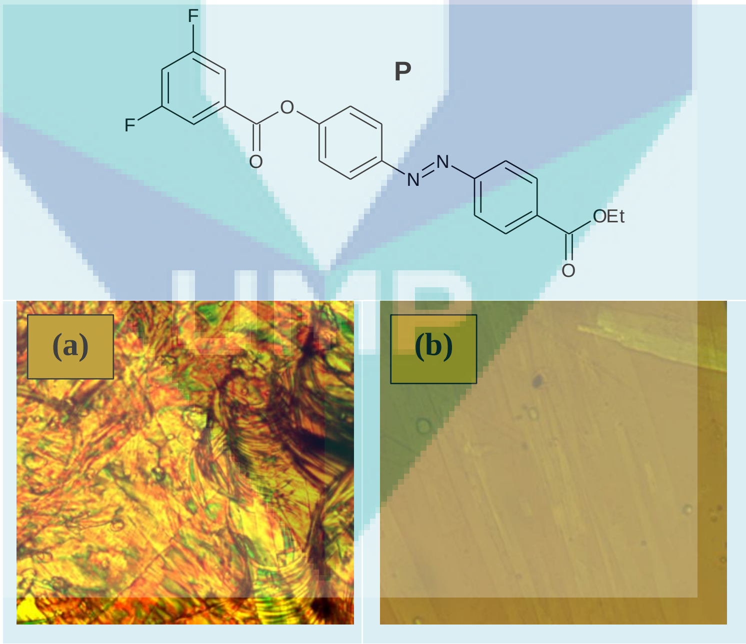

Figure 4.4: Optical micrographs obtained from cooling of azobenzene **P** from isotropic phase; a) – smectic-A phase at 181.0 °C, b) – crystalline phase at 106 °C.

Table 4.3: Phase transition temperature (T/ °C) and associated transition enthalpy values (ΔH/ mJ) in parentheses obtained from second DCS scan of compound **M** – **P**.

Compound designation	DSC (°C)						
	Cr	Heating Cooling	Sm-A	Heating Cooling	N	Heating Cooling	Iso
M	√	104.42 (291.23)	-	-	-	-	√
		146.08 (-317.92)		-		-	
N	√	112.33 (13.56)	√	124.67 (202.58)	√	{230.0}	√
		156.92 (-2.98)		163.92 (-228.46)		{235.5}	
O	√	86.42 (257.87)	-	-	-	-	√
		143.92 (-235.27)		-		-	
P	√	106.33 (126.71)	√	{198.0}	-	-	√
		128.67 (-51.58)		{181.0}		-	

Abbreviations: Cr = crystalline phase; Sm-A = smectic-A phase; N = nematic phase Iso = isotropic phase.
Notes: Values in { } was transition temperature obtained from POM;
"√" indicates phase exists; "–" indicates no phase exists.

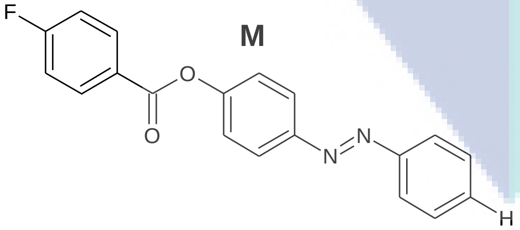
M

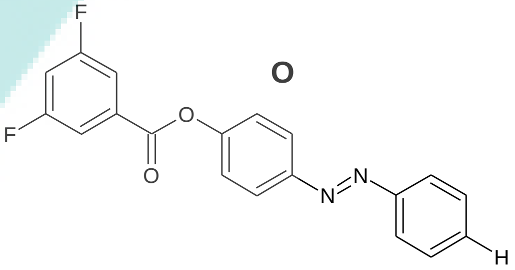
O

Figure 4.5: Chemical structure of fluorinated azobenzene without ester terminal end; compound **M** is monofluoro azobenzene whereas compound **O** is difluoro azobenzene.

In compound **N** and **P**, the addition of ester linkage for dipole moment at the terminal group on the opposite site of fluorine atoms enhanced the induction effect and increased the length-to-breadth ratio. This structure tends to favour liquid crystalline properties. Hence, it is clear that the benzoate ester group played a major role to bring about mesogenic features in these novel fluorinated azobenzene derivatives.

4.1.4 Azobenzene with olefinic terminal

Lastly, several azobenzene derivatives with olefinic terminal group were studied for their possible mesomorphic and photoisomerisation property. The molecules of azobenzene in this series of compound linked to 1-pentene at the terminal end, which contained double bond as polymerisable functional group. In order to investigate the effect of halogen substituent in *para*-position of the benzene ring lateral group, four other compounds derived from 4-fluoro phenol, 4-chloro phenol, 4-bromo phenol, 4-iodo phenol were also studied. The chemical structure of the olefinic azobenzenes with different halogen substituents at lateral group is shown in figure 4.7.

First of all, their liquid crystalline properties were checked. Under the polarising optical microscope, all compounds showed liquid crystalline mesophases. Representative microscopic images for various phases are showed in the figure 4.6 where one could see the beautiful thread-like behaviour as well as focal conic textures. On cooling from the isotropic state, a thread-like appearance which was characteristic of nematic phase appeared in compound **T** – **W**, followed by focal conic texture representing smectic-A phase. But in the case of compound **S** with the absent of halogen group only smectic-A phase was shown. It was observed that the inclusion of halogen group was essential for obtaining multiple liquid crystalline phases, whereas without halogen group only layered smectic-A phase was obtained. Compound **S** – **W** exhibited mesophases both on heating and cooling with enantiotropic in nature.

The transition temperatures and associated peak width values obtained from the DSC studies for the compound **S** – **W** are summarized in table 4.4. DSC thermograms were measured at 10 °C/min for second heating and cooling. The melting temperature, T_m, of the series was observed in the range of 95 – 160 °C and clearing temperature, T_c,

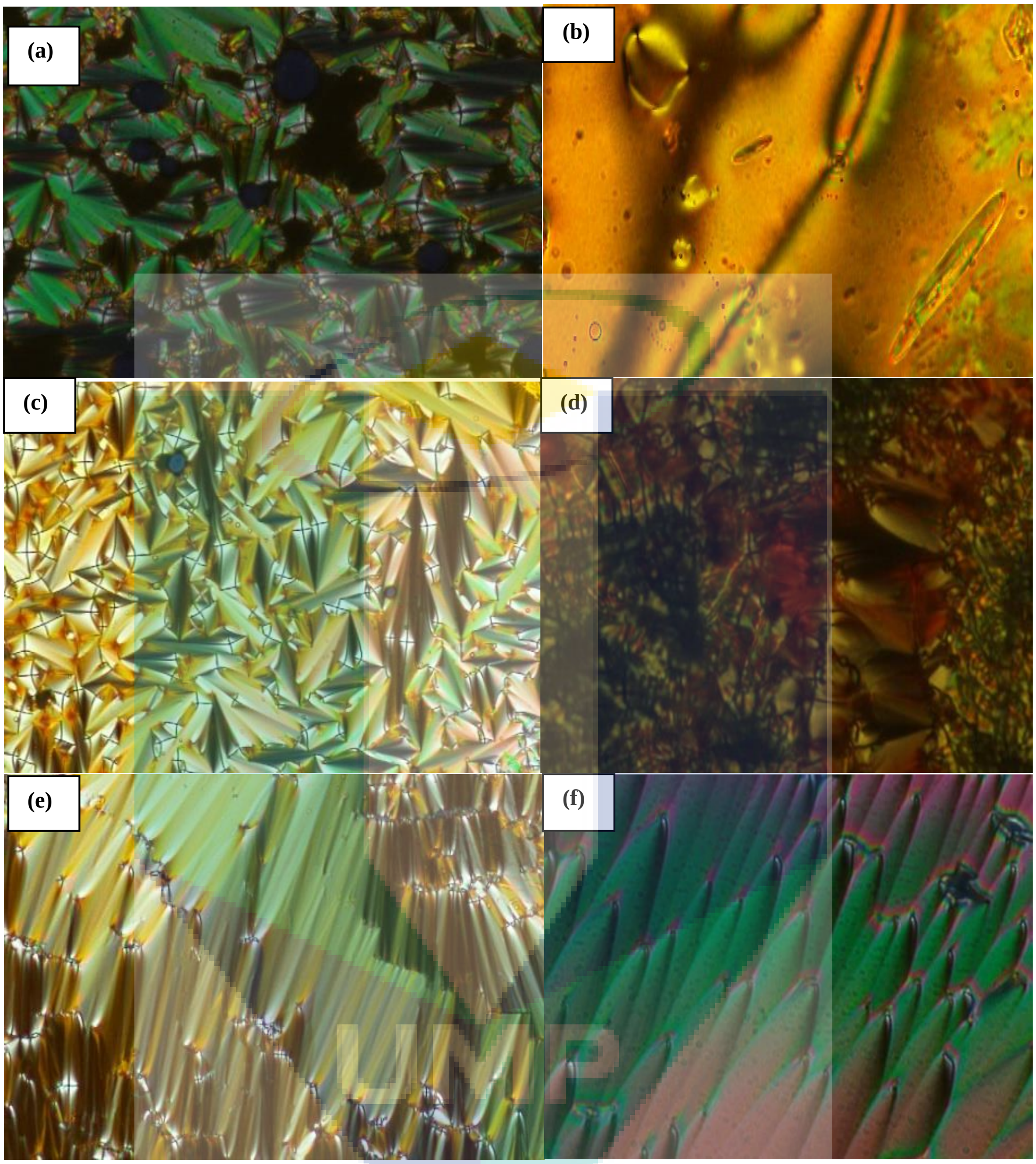

Figure 4.6: Representative optical micrograph obtained when compound **S** – **W** were cooled from isotropic; a) – focal conic texture representing smectic-A phase for compound **S** at 132 °C , b) – thread-like appearance representing nematic phase for compound **T** at 200 °C, c) – smectic-A phase for compound **T** at 152 °C, d) – smectic-A phase for compound **U** at 155 °C , e) – smectic-A phase observed for compound **V** at 172 °C , and f) – smectic-A phase for compound **W** at 180 °C.

Table 4.4: Phase transition temperature (T/ °C) and associated peak width (°C) in parentheses obtained from second DCS scan of compound **S** – **W**.

Sample	R	DSC (°C)						
		Cr	Heating Cooling	Sm-A	Heating Cooling	N	Heating Cooling	Iso
S	H	√	128.50 (2.7) 108.17 (1.9)	√	–	–	205.0 (5.5) 198.20 (4.8)	√
T	F	√	130.67 (2.8) 97.70 (2.9)	√	187.10 (3.8) 180.00 (2.8)	√	208.50 (10.5) 203.10 (8.6)	√
U	Cl	√	143.33 (2.0) 116.83 (2.1)	√	205.70 (1.7) 190.17 (2.2)	√	256.10 (2.8) 254.60 (2.4)	√
V	Br	√	152.83 (2.6) 121.33 (0.7)	√	203.00 (1.5) 200.10 (1.2)	√	254.10 (3.1) 252.30 (2.8)	√
W	I	√	160.00 (1.8) 131.50 (1.1)	√	205.00 (3.1) 203.50 (2.6)	√	238.00 (3.5) 233.33 (3.4)	√

Abbreviations: Cr = crystalline phase; Sm-A = smectic-A phase; N = nematic phase; Iso = isotropic phase.
Notes: "√" indicates phase exists; "–" indicates no phase exists.

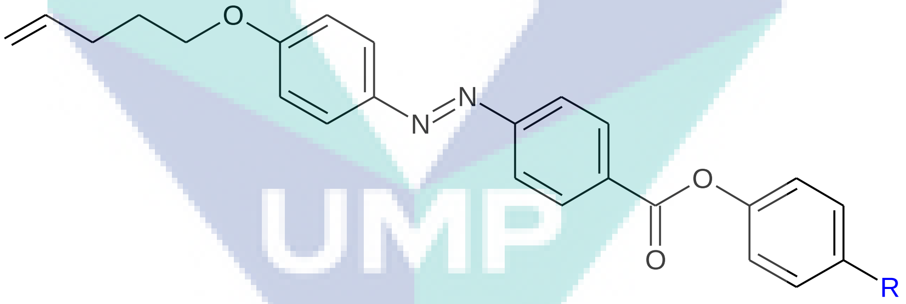

Where
S: R = H
T: R = F
U: R = Cl
V: R = Br
W: R = I

Figure 4.7: Chemical structures of azobenzene with olefinic terminal chain.

was 190 – 260 °C. The DSC analysis revealed that compound **T** – **W** showed nematic and smectic-A phases whereas compound **S** showed only smectic-A phase. All other compound exhibited similar behaviour.

4.2 PHOTOISOMERISATION STUDIES

Photosomerisation studies were performed on quartz cuvette with chloroform, $CHCl_3$, as the solvent to investigate the behaviour of the materials with respect to UV light. *Cis–trans* and *trans–cis* isomerisations were studied by real-time UV–Vis spectroscopy. The present of *trans* or *cis* isomers was detected by the changes in absorption spectra in which the two isomers displayed two different absorption spectra. One was the $\pi \rightarrow \pi^*$ band in the near UV region, and another was the $n \rightarrow \pi^*$ band located in the visible region which was due to the presence of lone electron pairs of nitrogen atom (Nägele et al., 1997). The *trans–cis* isomerisation was observed by a strong decrease of the band at around 320 nm associated with a $\pi \rightarrow \pi^*$ transition, and a coincident increase of the band around 450 nm associated with the $n \rightarrow \pi^*$ transition of the azo chromophore. All azobenzenes underwent *trans–cis* photoisomerisation following the $S_0 \rightarrow S_1$ and $S_0 \rightarrow S_2$ excitation (Wei-Guang Diau, 2004; Bortolus and Monti, 1979).

4.2.1 Preliminary UV intensity test

The rate of photochemical conversion of azobenzene system depends mainly on the intensity of the excitation beam (Feringa, Jager and de Lange, 1993; García-Amorós and Velasco, 2012). Thus, a preliminary UV intensity test was performed in order to determine the relevant intensity used for photoisomerisation of azobenzene derivatives. To check the appropriate intensity, compound **J** was selected for study as a function of UV intensity due to its good photochemical activities. It was shined for 24 sec to achieve photostationary state with UV light at different intensities; 2.38 mW/cm^2, 5.86 mW/cm^2, 9.02 mW/cm^2, 13.2 mW/cm^2 and 17.59 mW/cm^2. The results of these tests are summarized in table 4.5. It was evident that as the intensity increased, thermal back relaxation proceeded faster and the intensity 5.86 mW/cm^2 gave the most preferable thermal back relaxation time (10.58 h) among all other intensities as the thermal back relaxation time was sufficiently long. Thus, this intensity was used for the photoisomerisation studies of all compounds.

4.2.2 Bent-shaped azobenzene

Photoisomerisation studies of compound **D** and **E** showed similar absorption spectra with peaks, λ_{max}, around 357 nm due to their similar molecular structures. The only difference between the two compounds was their spacers at the central unit, which are n-hexane as aliphatic spacer and benzene ring as aromatic spacer. These bent-shaped molecules were symmetric in nature and the symmetry of the molecular system allowed delocalized electronic charge distribution between both sides of the π-system. The absorption spectra of compound **D** and **E** are shown in figure 4.8. The strong absorbance in the UV region corresponds to $\pi \rightarrow \pi^*$ transition of the *trans* isomer, whereas a very weak absorbance in the visible region represents the $n \rightarrow \pi^*$ transition of the *cis* isomer.

Different spacers gave different characteristics to the compounds. The dramatic influence of aliphatic/aromatic spacers on photoisomerisation of the dimeric azobenzene was investigated by UV light illumination at 5.86 mW/cm^2 intensity. The compounds were illuminated at different time intervals and the absorption spectra were recorded immediately as shown in figure 4.9. The absorption at λ_{max} decreased gradually as the *trans* isomers transformed to *cis* isomers (Nayek et al., 2012; Pal et al., 2011). Figure 4.10 shows the *trans–cis* absorption of compound **D** and compound **E** as a function of exposure time. The data were extracted from figure 4.9 by considering the λ_{max} at 358 nm and 356 nm as a function of exposure time. The curve shows that photostationary state of these compounds, when UV light was illuminated, achieved at 17 sec and 18 sec, respectively. Meanwhile, the conversion efficiency (CE) varies in the presence of different spacers where compound **D** gave 76 % and compound **E** gave only 55 % of extent of isomerisation. This effect was due to the nature of the spacers, lengths of the spacers and free rotations.

Table 4.5: The photoisomerisation behaviour with different UV intensity for compound **J**.

Intensity (mW/cm^2)	Photostationary state (sec)	Thermal back relaxation (h)
2.38	29	10.93
5.86	24	10.58
9.02	19	8.95
13.20	16	7.84
17.59	10	6.38

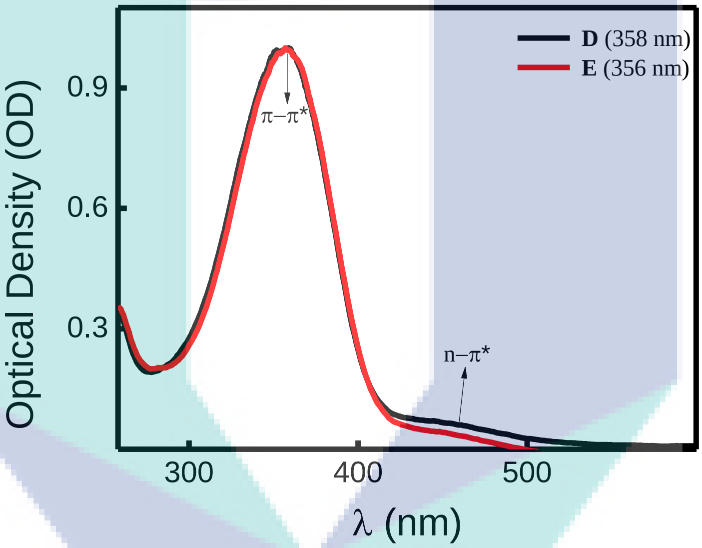

Figure 4.8: Absorption spectra of compound **D** and **E** measured with chloroform solutions by using a UV–Vis.

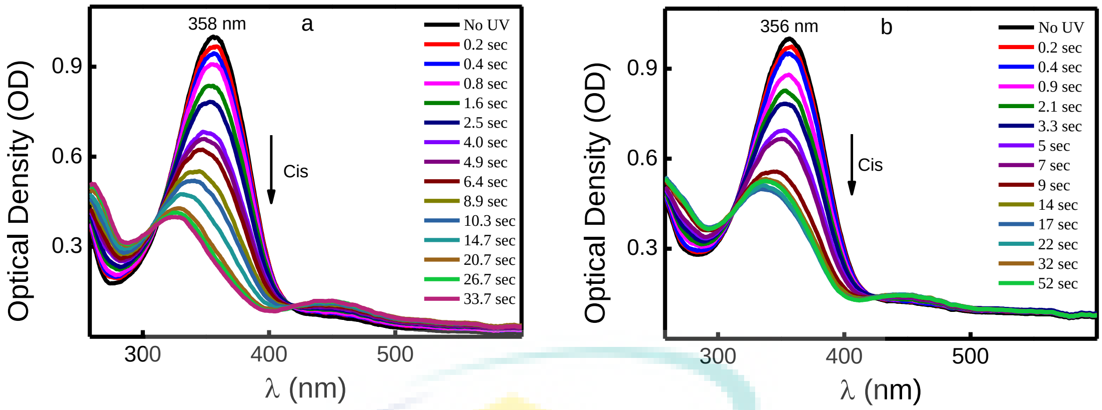

Figure 4.9: *Trans–cis* conversion of: a) – compound **D** and b) – compound **E** in chloroform solution by shining UV light at 365 nm.

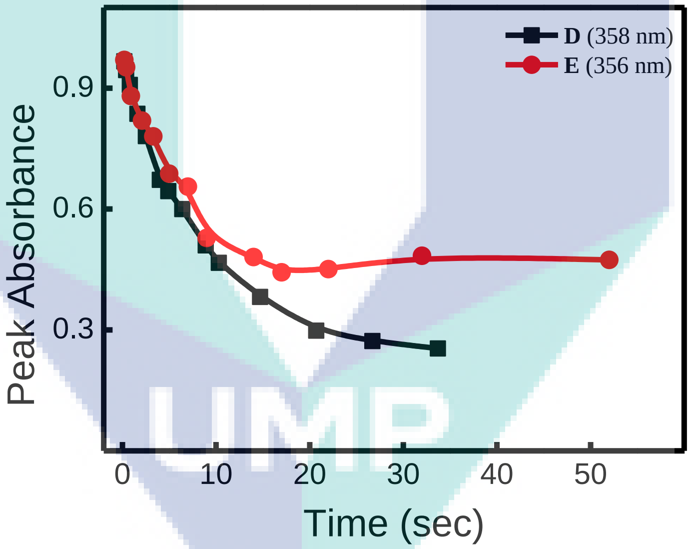

Figure 4.10: The plot of peak absorbance of compound **D** and **E** extracted from figure 4.9 (a and b) in the function of exposure time for *trans–cis* isomerisation.

The reverse transformation not only could be driven by shining visible light of higher wavelength (450 nm), but also occured thermally in the dark by thermal back relaxation, spontaneously. Figure 4.11 shows the thermal back relaxation process in which the solution samples, after achieved photostationary state, were left in a dark condition. The thermal back relaxation of compound **D** and **E** were 13.21 h and 7.25 h, respectively. Meanwhile, figure 4.12 shows the time dependent *cis–trans* spectral behaviour of the compounds, obtained from figure 4.11 by plotting the absorbance at λ_{max} as a function of time. It has been widely accepted that photochemical reaction of azobenzene compounds affected significantly by the spacers (Rahman et al., 2014). Hence, the compounds showed different time requirements for photostationary state and thermal back relaxation (table 4.6).

In order to explain the effect of spacers on the dramatic variation of photoisomerisation, figure 4.13 was constructed. The aromatic/aliphatic spacers affect the free movement of the molecules to a significant extent. For compound **D**, in between the two azobenzene wings there was an aliphatic chain (n-hexane) present. In this situation, the photochemical activities were a little slower compared to compound **E** due to the flexibility of aliphatic spacer. The time required to achieve photostationary state was 17 sec and thermal back relaxation time was 13.25 h. This happened due to bending of the molecules caused by the flexible aliphatic chain, preventing the system from going back to *trans* configuration easily by forming a coiled geometry. Somewhat similar results on long chain alkanes were reported earlier (Nair, Prasad, and Hegde, 2004).

For compound **E**, in between the two azobenzene side wings there was an aromatic benzene ring present. Due to the rigidity of the benzene ring, the molecule did not bend as much as compound **D**. Apart from *trans–cis* isomerisation of the two azobenzene moieties placed at the molecular side wings, there was no appreciable change in the molecular structure of compound **E** after UV irradiation, and thus photochemical activity was relatively faster than compound **D**. The time required to achieve photostationary state was 18 sec, whereas thermal back relaxation time was 7.21 h.

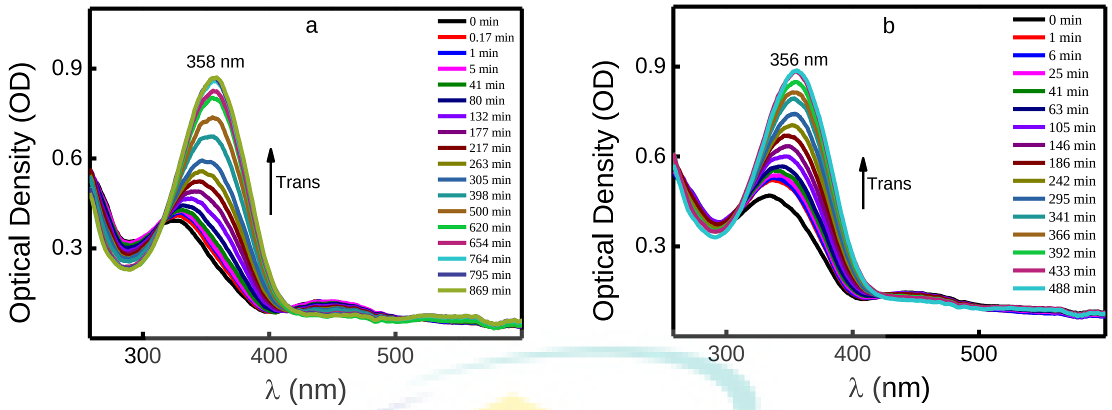

Figure 4.11: Thermal back relaxation spectra for a) – compound **D** and b) – compound **E**.

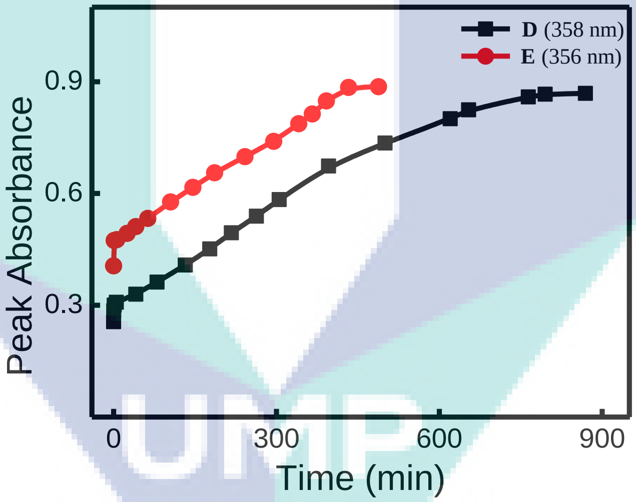

Figure 4.12: The plots of peak absorbance of compound **D** and **E** extracted from figure 4.11 (a and b) in the function of recovery time for *cis–trans* isomerisation.

Table 4.6: Photoisomerisation behaviour and nature of spacers in compound **D** and compound **E**.

Compound structures and spacer locations	Photoisomerisation	Thermal back relaxation
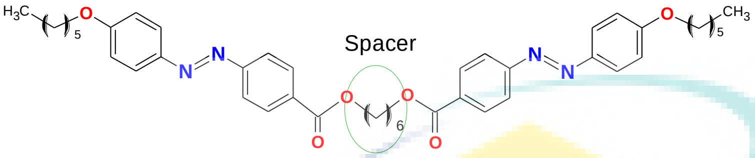 **D**: Aliphatic n-hexane chain spacer	17 sec	13.25 h
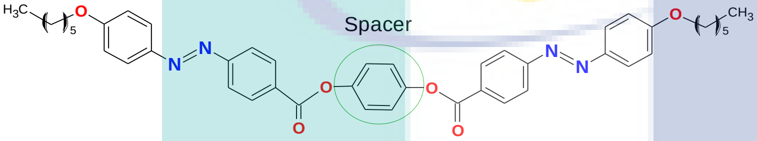 **E**: Aromatic benzene ring spacer	18 sec	7.21 h

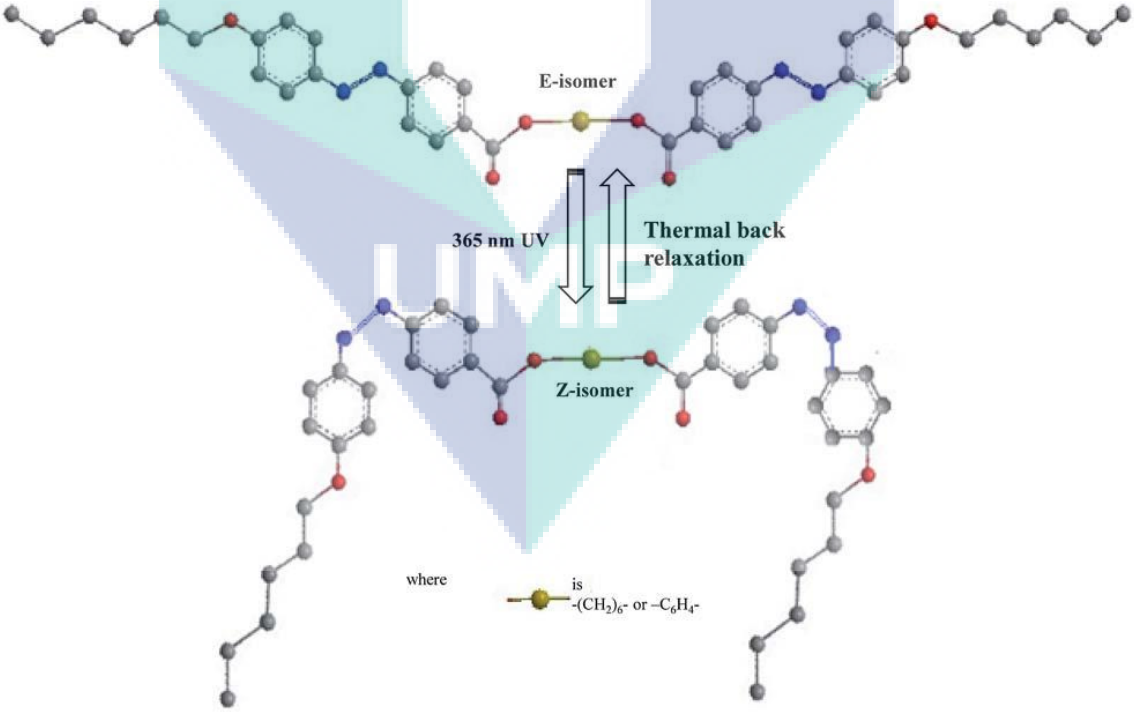

Figure 4.13: Effect of aliphatic and aromatic spacer on photoisomerisation of bent-shaped azobenzene.

It was notable that time taken for the molecules to achieve photostationary state almost same in both compound. This is because, the *trans–cis* photoisomerisation was a radiation-induced process, whereas the thermal back relaxation was a completely radiation-free process, it depended solely on the structural modifications. Therefore, it can be concluded that the aromatic spacers in azobenzene dimer relaxed faster due to their rigidity, whereas the azobenzene dimer with aliphatic spacers relaxed slower due to their flexibility.

4.2.3 Azobenzene with amide group

Before UV illumination, the chloroform solution of compound **G**, **H**, **I**, and **J** exhibited similar absorption band around 355 nm which might be due to the similarity in their molecular structures. As shown in figure 4.14, for each spectrum there exists an intense absorbance in the UV region corresponding to $\pi \rightarrow \pi^*$ transition of the *trans* isomer, and a very weak absorbance in the visible region at 450 nm represents $n \rightarrow \pi^*$ transition of the *cis* isomer (Rau, 1990; Wei-Guang Diau, 2004).

The photoisomerisation of compound **G** – **J** in chloroform solution were studied by irradiation with 356 nm UV light at intensity 5.86 mW/cm^2 and the changes in λ_{max} absorbance were observed. Figure 4.15 depicts the *trans–cis* absorption spectral behaviour of compound **G**, **H**, **I**, and **J** at different irradiation time. When the solutions were irradiated, the *trans* isomers of azo derivatives transformed into *cis* isomers, which was indicated by decreased in the strong *trans* absorption band and increased in weak *cis* absorption band. In brief, the photostationary states for all four compounds achieved at 18 sec, 20 sec, 22 sec and 24 sec, respectively.

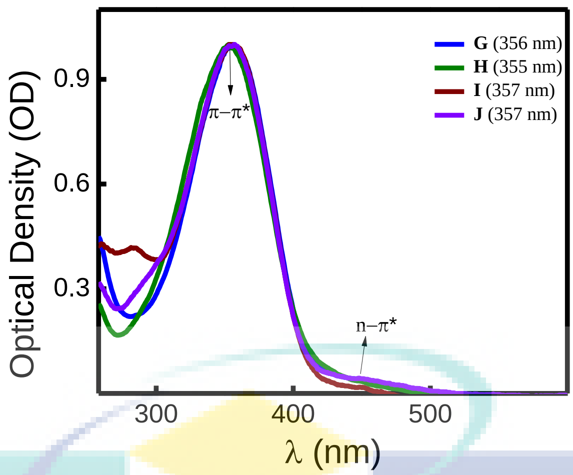

Figure 4.14: The absorption spectra of compound **G** – **J** show same peak absorption due to the similarity in their molecular structures.

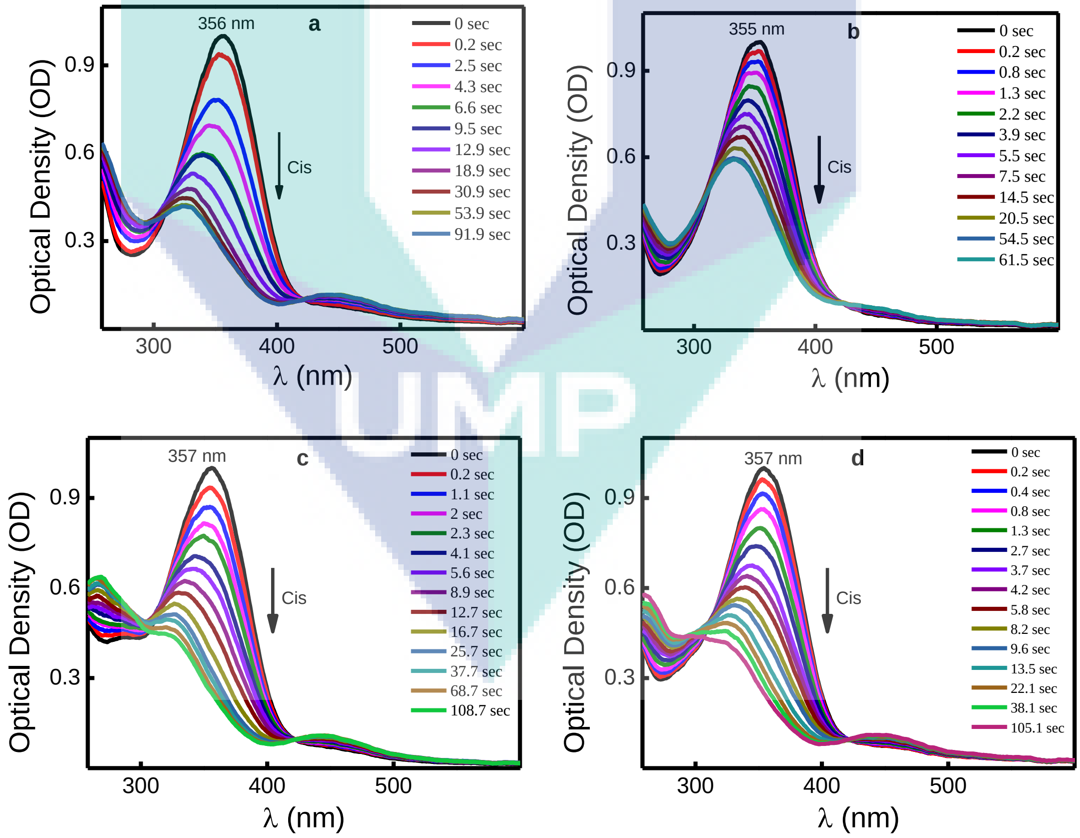

Figure 4.15: *Trans–cis* conversion of a) – compound **G**, b) – compound **H**, c) – compound **I** and d) – compound **J** when UV light at wavelength 365 nm was shined.

On the other hand, figure 4.16 shows the *trans–cis* absorption of compound **G** to **J** as a function of exposure time. The plots of peak absorbance were extracted from figure 4.15 by plotting the peak absorbance as a function of exposure time. The curves clearly show that photostationary state occurred in the range between 20 sec to 24 sec. Calculation of *cis* fraction, [*cis*], in photostationary state showed that compound **I** and **J** gave the highest [*cis*], with 75 % in both samples. The high [*cis*] might be due to the presence of ethyl benzoate $(C_6H_5)COOC_2H_5$ and phenylethanone $(C_6H_5)COCH_3$ connected to the benzamide unit in the respective compounds. The two substituents are weaker electron-withdrawing groups compared to nitrobenzene $(C_6H_5)NO_2$ in compound **H** (with 52 % of [*cis*]). It made the intermolecular hydrogen bonding at benzamide unit weaker and thus the *trans–cis* isomerisation became efficient.

The thermal back relaxation of compound **G** to **J** were 9.21 h, 5.73 h, 10.18 h and 10.58 h, respectively as shown in figure 4.17. The possible reason for the difference in thermal recovery time might be due to mesomeric effect as well as hyperconjugation effect as the different functional group varied the effect on intermolecular hydrogen bonding to a certain extent.

The intermolecular hydrogen bonding gave a profound impact in the azobenzene system. In chloroform solution, it was believed that there existed an intermolecular hydrogen bonding between the azobenzene molecules. Under normal circumstances, as in compound **G**, where no electronic effect from electron-withdrawing group present, the carbonyl group (C=O) served as hydrogen acceptor for the amide group (N–H) of nearby azobenzene molecule, and formed a stable amide-amide (C=O···H–N) hydrogen bond. This hydrogen bonding restricted the free movement of the molecules and so thermal back relaxation last for 9.21 h.

In case of compound **H**, the benzene ring was replaced by nitrobenzene, $(C_6H_5)NO_2$. The strong electron-withdrawing nitro group induced negative mesomeric effect. Once UV was shined, the molecules received energy and withdraw the electrons by delocalization mechanism from the neighbouring benzamide unit. The electron density on the benzamide was decreased and consequently, the intermolecular amide-

amide (C=O···H–N) hydrogen bonding broke. So, molecular movement was easy as there was no hydrogen bond.

On the other hand, compound **I** and **J** was designed with weak electron-withdrawing groups, i.e. ethyl benzoate and phenylethanone, respectively. They have less electron-withdrawing power to withdraw the electron density from the amide group. Nevertheless, there were hyperconjugation effects in the carbonium ions at the alkyl groups of the electron-withdrawing substituents. The σ-electrons of the α-C–H bond in the alkyl groups were delocalized into the adjacent empty p-orbital of the positive carbonium ions contributing to no bond resonance structures. The hyperconjugation effect eventually stabilized the whole molecular systems and the molecular movement was restricted in these two compounds due to the intermolecular hydrogen bonding. As a result, the compound **I** and **J** showed very long back relaxation times more than 10 h.

4.2.4 Azobenzene with fluorine addition

The influence of fluorine on the $\pi \rightarrow \pi^*$ absorption band position was best evaluated from the absorption spectra. Prior to illumination, the *trans* isomers of compound **M** and **N**, which contained a fluorine atom displayed their absorption bands at 322 nm whereas compound **O** and **P** which were substituted with two fluorine atoms produced absorption band at 331 nm. As shown in figure 4.18, a strong peak appeared at UV region corresponding to $\pi \rightarrow \pi^*$ transition of *trans* isomer and weak peak at visible region corresponding to $n \rightarrow \pi^*$ transition of *cis* isomer. Compound **O** and **P** showed bathochromic shifts with respect to compound **M** and **N** in the spectra. This implies that the addition of fluorine on the molecular structure of azobenzene affect the electronic spectra of the compounds which probably due to the lone pair electrons presented in the fluorine atom had considerable interaction with the π system of the aromatic ring to alter photophysical behaviour of the compound (Rahman et al., 2013).

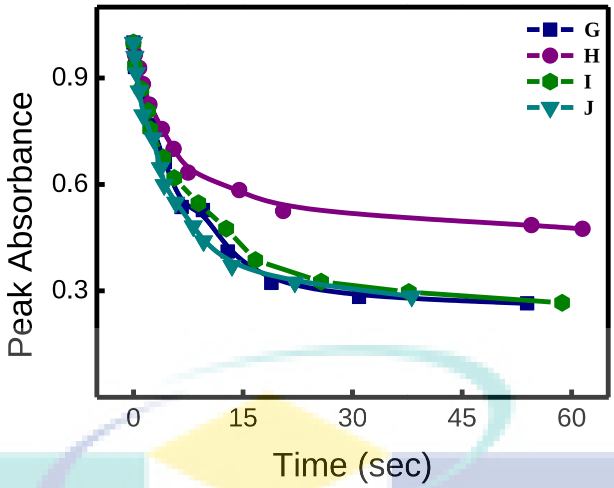

Figure 4.16: The plots peak absorbance of compound **G** – **J** with respect to the function of recovery time for *trans–cis* isomerisation. Data were extracted from figure 4.15.

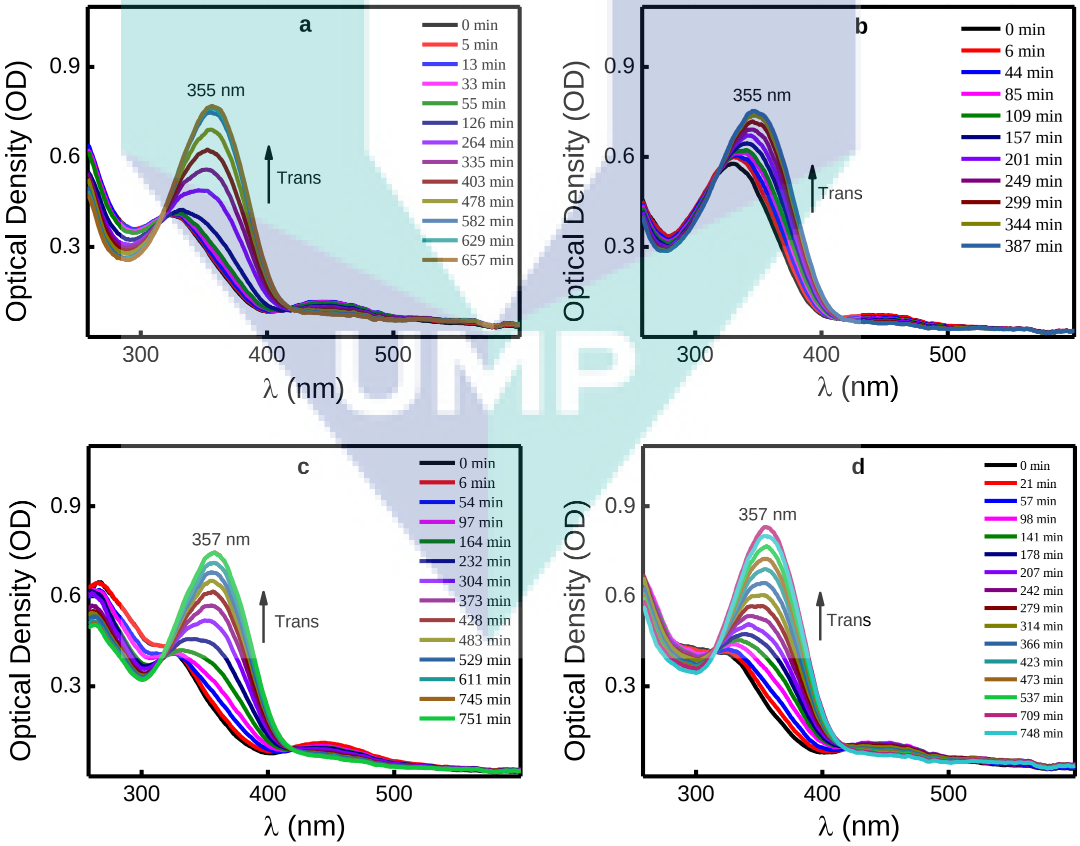

Figure 4.17: Thermal back relaxation of a) – compound **G**, b) – compound **H**, c) – compound **I** and d) – compound **J**. Samples were shined until photostationary state and then thermal back relaxation time were recorded in dark condition.

The wavelength at which azobenzene photoisomerisation occurred depend on the particular structure of azobenzene molecules which could be attuned synthetically with substituent groups to the chromophores (El Halabieh et al., 2004). Azobenzene molecules undergo *trans–cis* isomerisation when irradiated with light attuned to an appropriate wavelength (Pavia et al., 2008). Upon UV illumination of monofluoro- and difluoro-azobenzene compounds, though absorption were observed at different peak wavelengths, there were notably no changes in their *trans–cis* isomerisation time where all four compounds took 4 min to reach photostationary state (figure 4.19). The results showed that the limitation in wavelength tuning did not influence the speed of *trans–cis* isomer transition during illumination.

In fluorinated azobenzene with ester terminal group, compound **N** gave 80.8 % of [*cis*] which was the highest among all four compounds, whereas compound **P** gave the lowest [*cis*] (64.46 %). For fluorinated azobenzene without ester terminal group, compound **M** gave 72.93 % of [*cis*] while compound **O** gave 70.26 % of [*cis*]. The reduced *cis* fraction observed in compound **N** (monofluoro) compared with compound **P** (difluoro), and also compound **M** (monofluoro) compared with compound **O** (difluoro) might be explicable in terms of the sterically hindered structure of the *cis* isomer having increased number of fluorine lateral groups on benzene ring. With an increasing number of fluorine atoms, the size of the molecules increased and this change resulted in an increasing free volume required for the photoisomerisation. So, it is clear that as the *cis* isomer was sterically crowded and thermodynamically unstable, it led to the reduced *cis* fraction in the photostationary state (Sasaki, Ikeda and Ichimura, 1993).

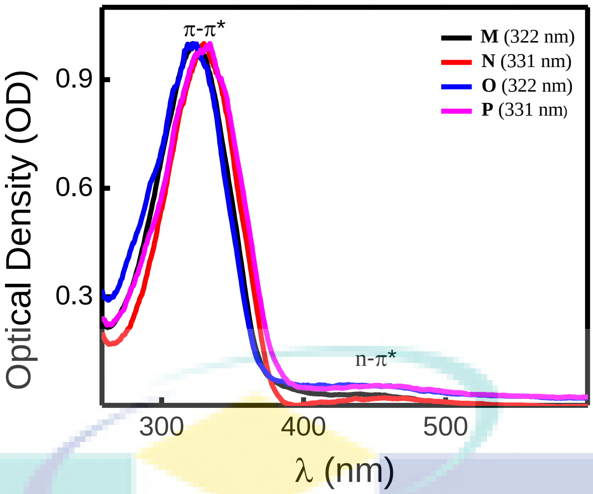

Figure 4.18: Absorption spectra of compound **M**, **N**, **O** and **P** before photoisomerisation studies.

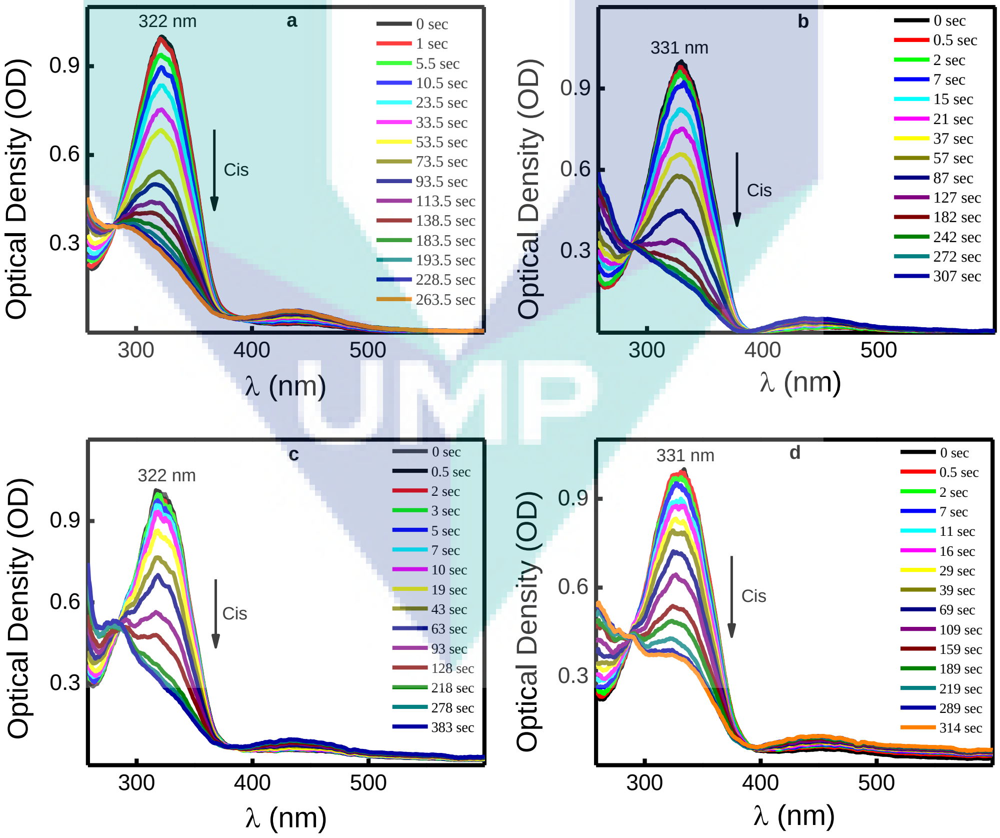

Figure 4.19: The changes in absorption spectra with different exposure time of UV light for: a) – compound **M**, b) – compound **N**, c) – compound **O** and d) – compound **P**.

Thermal back relaxation occurred when the molecules was left in the dark after attaining photostationary state, where the *cis* isomers transformed to *trans* isomers. The effect of structural modification could be observed in their thermal back relaxation time. The reverse isomerisation process of compound **M** and **N** as a function of recovery time is shown in figure 4.20. Monofluoro-substituted azobenzene **M**, took about 16.42 h to convert back to stable *trans* isomer whereas compound **N** with addition of ester terminal group took around 22.48 h. The reason for compound **N** took longer time for thermal back relaxation could be due to the liquid crystalline phases involve in *trans* configuration possess layered structure, in particular the smectic-A phase. Since the *trans* isomer exhibit the smectic-A and nematic phases, the *cis* isomer required more time to transform from isotropic to nematic phase before reaching *trans* configuration with the layered structure. In fact, a similar feature was observed in another case wherein the phase involved had a layer structure (Rahman et al., 2013).

After that, compound **M** and **N** were compared with difluoro-substituted azobenzenes. As shown in figure 4.21, the diflouro-substituted azobenzene **O** showed 13.08 h of thermal back relaxation whereas difluoro-substituted azobenzene with ester group, compound **P**, showed 11.55 h of thermal back relaxation. The presence of ester terminal group in difluoro azobenzene reduced the thermal back relaxation time from 13.08 h to 11.55 h. This is because, fluorine, the most electronegative element were thought to withdraw electron density from the bonding π-orbitals of –N=N– double bond. This negative mesomeric effect made the –N=N– double bond unstable and reduced the *cis–trans* barrier for inter-conversion, led to fast thermal back relaxation when more fluorine was added (Bronner and Tegeder, 2014). Interestingly, the monofluoro azobenzene containing ester group gave the longest *cis* lifetime compared to other compounds, almost double than that of difluoro-substituted azobenzene ester group.

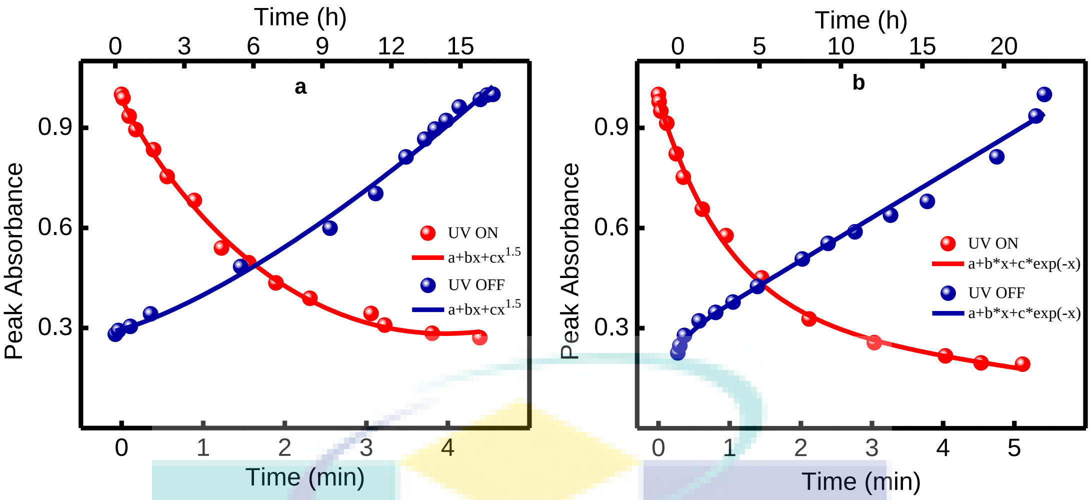

Figure 4.20: Thermal back relaxation process of a) – compound **M** and b) – compound **N** as function of time after illuminating the material to photostationary state.

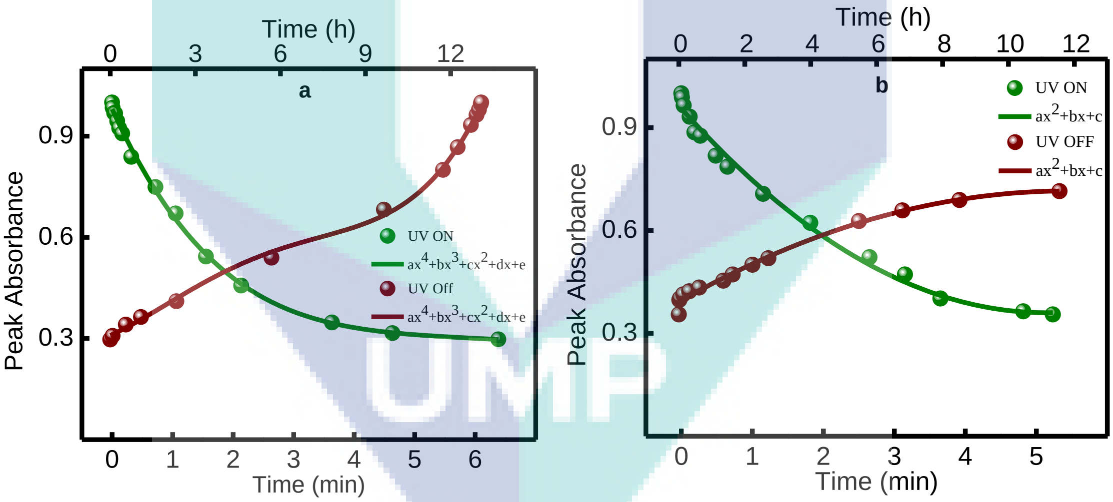

Figure 4.21: Thermal back relaxation process of a) – compound **O** and b) – compound **P** in the function of time after illuminating the material to photostationary state.

4.2.5 Azobenzene with olefinic terminal

Before UV irradiation, all compounds in chloroform solutions featured absorption bands between 358 nm to 364 nm and a relatively low absorption around 450 nm. The former band corresponds to a symmetry-allowed $\pi \rightarrow \pi^*$ transition whereas the later band corresponds to a symmetry-forbidden $n \rightarrow \pi^*$ transition appears as a weak band at 450 nm (Rau, 1990; Wei-Guang Diau, 2004; Bortolus and Monti, 1979; Pavia et al., 2008). There were no significant changes in the λ_{max} as the atoms are all from the same group-17 elements of periodic table.

Upon UV illumination, λ_{max} absorption at the UV region decreased due to *trans* –*cis* isomerisation, followed by a slight increase in the peak around 450 nm. The results revealed that compounds took around 73 sec to 91 sec for *trans–cis* conversion. The spectra data (figure 4.22) confirmed that photoisomerisation process led to a photostationary state. All the compounds gave more than 85 % of [*cis*]. For example, in compound **S**, 88.59 % of the *trans* isomers had been converted to *cis* isomer after exposed to UV radiation for 82 sec.

To observe the thermal back relaxation process after molecules attained photostationary state, samples were left in the dark to allow *cis*-*trans* transformation. The effect of structural modification could be observed in their thermal back relaxation time. Figure 4.23 shows the spectral changes of compound **S** to **W** during thermal back relaxation process. Among all, compound **S** without halogen showed the longest thermal back relaxation time of 45 h. The long thermal back relaxation could probably due to photo-crosslinking of olefin unit containing one double bond at α-position capable of efficient photoinitiated polymerization (Yagci et al., 2010). The double bond at the α-position enhanced the reactivity of the olefinic azobenzene molecules and formed intercrosslink bonds with nearby molecules after exposed to UV light (Burdick and Leffler, 2001). The photo-crosslinking might involve the production of singlet and triplet in excited state which then reacted with other azobenzene molecules (Yagci et al., 2010; Min and Boff, 2002; Burdick and Leffler, 2001; Bamford et al., 1978). As a consequence, the photo-crosslinking effect created a complicated network which made the *cis* isomers return to the original *trans* isomer more slowly.

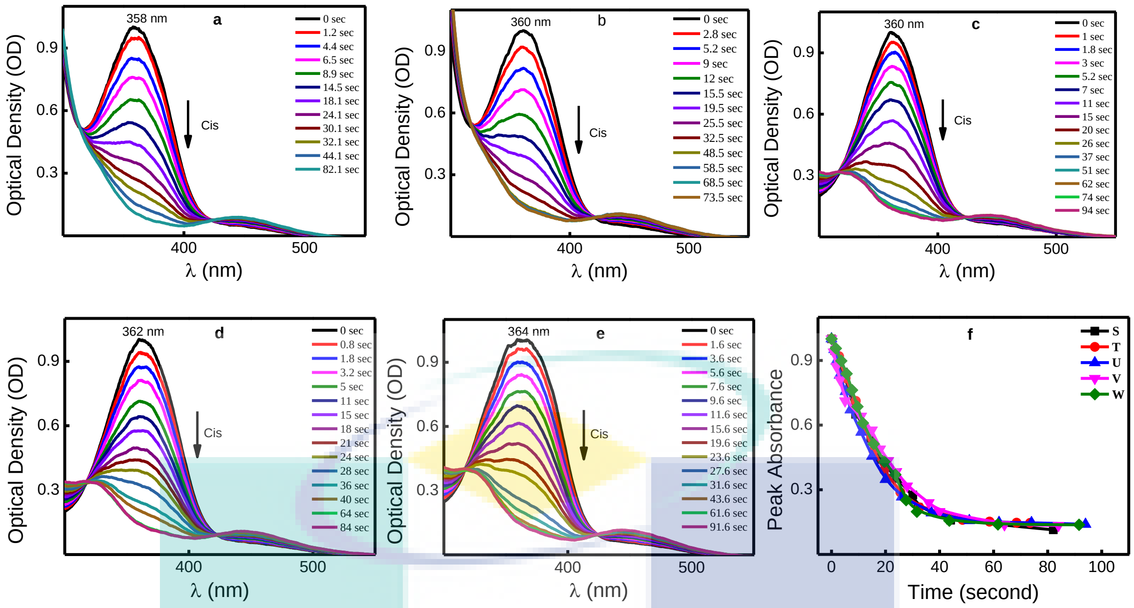

Figure 4.22: Changes of absorption spectra during UV exposure of compound: a) – **S**, b) – **T**, c) – **U**, d) – **V**, e) – **W** and f) the plot of peak absorbance vs. time extracted from a, b, c, d, and e.

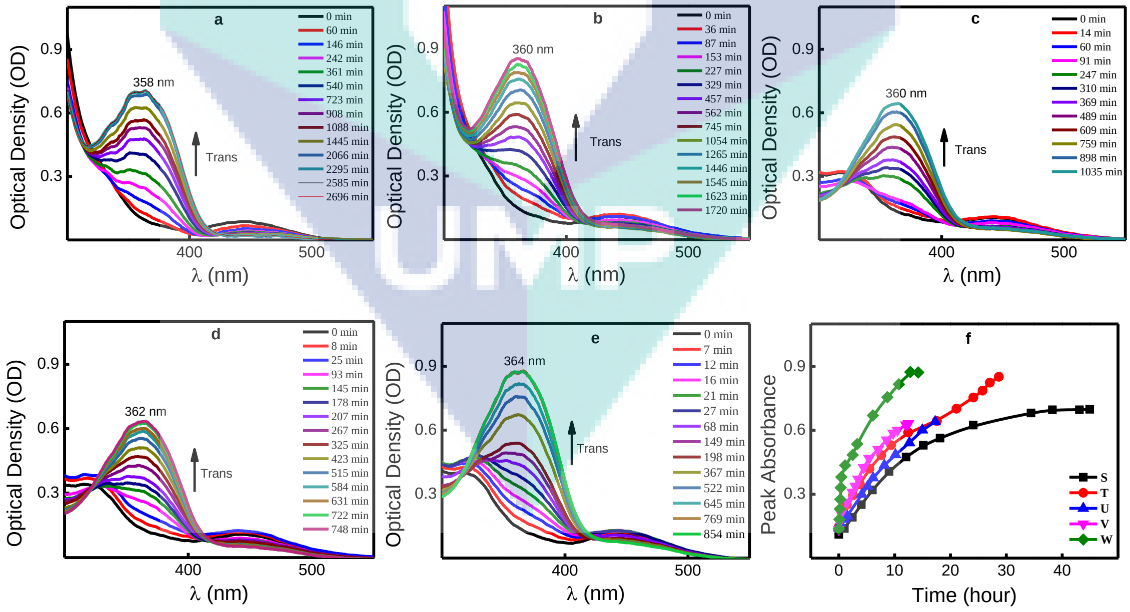

Figure 4.23: Changes of absorption spectra during thermal back relaxation of compound: a) – **S**, b) – **T**, c) – **U**, d) – **V**, e) – **W** and f) the plot of peak absorbance vs. time extracted from a, b, c, d, and e.

Table 4.7: Time taken for the five azobenzene derivatives for *trans–cis* and *cis–trans* isomerisation with calculated conversion efficiency (CE).

Compound designation	Substituent, R	*trans–cis* (sec)	*cis–trans* (h)	CE (%)
S	H	82	45	88.59
T	F	73	28.66	85.40
U	Cl	94	17.25	86.05
V	Br	84	12.46	86.58
W	I	91	14.23	86.25

In order to demonstrate the effect of electronegativity on photo-crosslinking property, a series of olefinic azobenzene bearing variable electronegative halogens was studied. Specifically, halogen with decreasing electronegativity of fluorine (F), chlorine (Cl), bromine (Br) and iodine (I) were attached as lateral group. In general, electronegativity is inversely related to atomic size. With increase in atomic size down the group-17 of periodic table, the electronegativity decreases from F (4.0) > Cl (3.0) > Br (2.8) > I (2.5). Compound **T** characterized by fluorine substituent, the most electronegative group, gave 28.66 h of thermal back relaxation. One can see from table 4.7, as the electronegativity of halogen increased, the thermal back relaxation extended significantly from 14.23 h to 28.66 h. However, the compounds did not show a linear increase in photoisomerisation behaviour with the increase of halogen electronegativity, which might be attributed to the impurity of the compounds. Nevertheless, these results lower considerably compared to compound **S** (without halogen). The possible reason for this might be due to the interaction of photo-crosslinking property with the electronegativity of halogen atoms which altered the electronic distribution of the molecular systems to make the reverse reaction preceded faster.

In brief, the photo-crosslinking effect with olefinic azobenzene can be a useful method to improve the thermal back relaxation. However, substitution of electronegative element as lateral group did not extend the thermal back relaxation although they exhibited smectic A and nematic phases. The studies showed that by proper tuning the azobenzene systems, one can able to achieve the desired storage time of optical storage devices.

4.3 FIRST-ORDER KINETICS

The rate constants for the thermal *cis–trans* isomerisation were studied in chloroform solution at room temperature and calculated from equation 3.2. Figure 4.24 shows the negative logarithmic plot with a linear fit, where the slopes determine the thermal rate constant. All of azobenzene derivatives behaved similarly, with first-order kinetic within the indicated time range, but fluctuated to non-first-order kinetic in the later stage of the reaction. This fluctuated kinetic of reaction might be attributed to the temperature changing as the thermal *cis–trans* isomerisation was a temperature dependence reaction. However, this could not be the possible reason as the environmental temperature was kept constant throughout the experiment. Eisenbach (1980) correlated the deviation from first-order kinetics to the fluctuation of free volume and this could be a logic reason as it was observable that the solutions were slowly evaporated during the experiments, and thus reduced in volume followed by restriction in free volume for azobenzene free motion. This might be one of the limitations of photoisomerisation studies in solution form where it could not provide sufficient and reliable data intended for creating optical storage devices. Therefore, in the following step, some of the compounds that showed good photochemical activities in solution form were studied in liquid crystal environment in order to obtain a better understanding of material's behaviour.

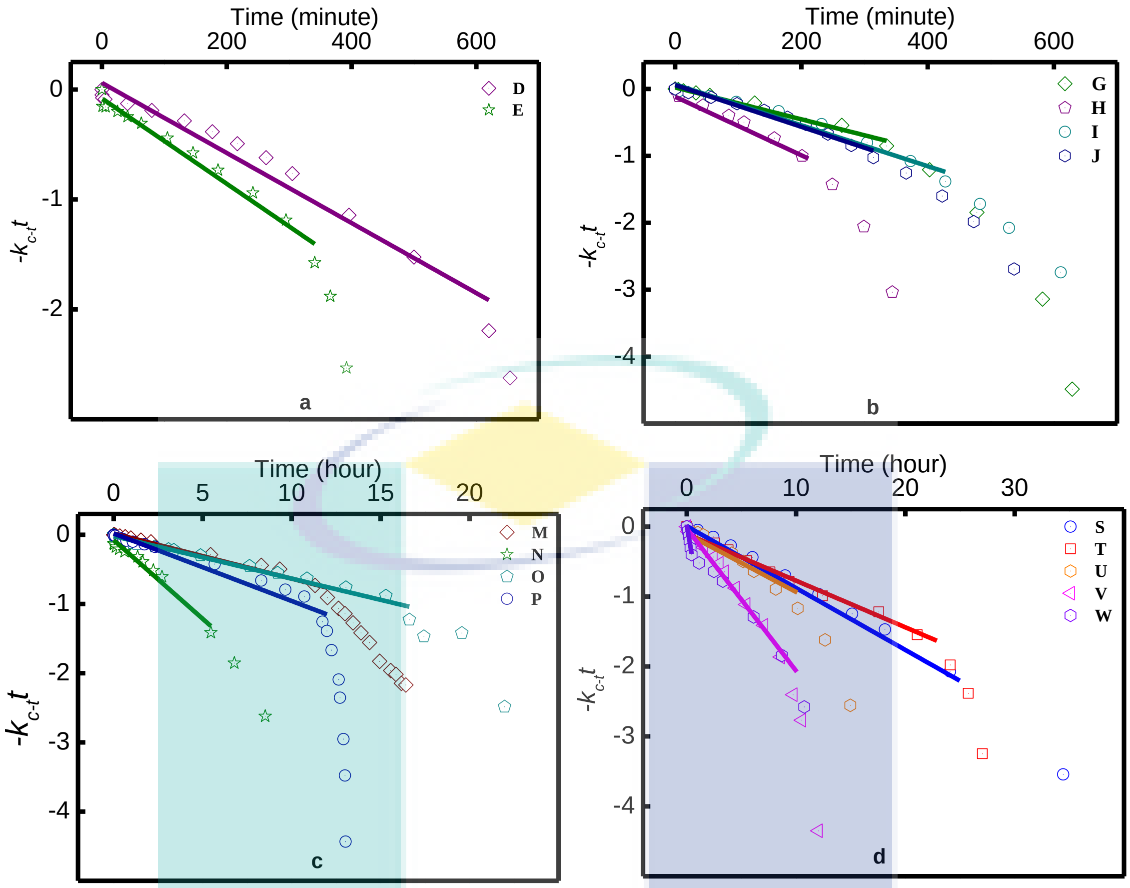

Figure 4.24: First-order plots for *cis–trans* thermal isomerisation for a) – azobenzene with aromatic/aliphatic spacer (**D** and **E**), b) – amide-based azobenzene (**G** – **J**), c) – azobenzene with fluorine addition (**M** – **P**) and d) – olefinic azobenzene (**S** – **W**) measured at room temperature.

4.4 DEVICE STUDIES

The optical storage device described in this project refers to a device for storing and processing optical images in recyclable manner. Liquid crystal cells was constructed with two clean glass slides, each coated with an alignment layer made from ITO, which after deposition on the substrates are unidirectionally rubbed (Elamain, Hegde, and Komitov, 2013). Spacer of desirable dimension and thinness was applied outside the active area in order to keep the two glass slides together at a fixed distance, which also determines the thickness of liquid crystal cell. The cell was then assembled by UV-hardened glue to fix the position of the two glass slides against each other. Next, the mixture 5 % of azobenzene in 95 % of commercial nematic liquid crystal MLC6873-100 was filled into the cell by capillary force at isotropic temperature (about 100 °C). After filling, the hole for the filling was sealed in the next step.

4.4.1 Photoisomerisation studies in liquid crystal host

The vast majority data obtained so far refers only to photoisomerisation in solution form. Given that in optical image storage application, the azobenzene photoisomerisation takes place in liquid crystal host, it is somehow necessary to study the behaviour of photoisomerisation of selected compounds in liquid crystal environment, where it was expected that the mechanism could be different. Thus, the incorporation of azobenzene which molecularly dispersed in liquid crystal cell was a useful method to study the photoisomerisation behaviour in liquid crystal host. In this regard, the measurement of the thermal back relaxation time of the azobenzene derivative was crucial since the rate of thermal back relaxation would reflect the storage time of the devices. That is to say, a long thermal back relaxation was an important parameter for creation of optical storage devices, which could be more advantageous if the same kind of thermal back relaxation obtained in solvent environment could also be achieved in liquid crystal cell.

The main difference in photoisomerisation in solution from photoisomerisation in liquid crystal host was the difference in the freedom of molecular motion due to the restriction of mobility. Consequently the thermal back relaxation time would be significantly different. Therefore, photoisomerisation studies initially performed in solutions were then studied in liquid crystal host. This could provide an idea of the behaviour of the azobenzene in the host material with respect to UV light and these results were indispensable for application in optical storage device (Rahman et al., 2014; Lutfor et al., 2013). Compound **D** and **J** were selected for this purpose because both showed good photoisomerisation behaviour in chloroform solution.

Though liquid crystallinity is not a necessary condition to induce photo-orientation of liquid crystalline phase, it made the photo-induced motion easier to achieve by azobenzene liquid crystals. The compound **D** and **J** dissolved well in the commercial nematic liquid crystal ascribed to their liquid crystalline phases. Before UV irradiation the *trans* isomers of compound **D** and **J** were in liquid crystalline phase. Once UV light at intensity 5.86 mW/cm^2 was irradiated, the molecules transformed into *cis* isomers and lost their mesomorphic nature (Ikeda and Tsutsumi, 1995).

Subsequently, the irradiation resulted in the formation of photostationary state. For compound **D**, photostationary state was obtained at 10 sec and complete thermal back relaxation was observed at 380 min (figure 4.25a). In the meantime, figure 4.25b shows the *trans–cis* photoisomerisation of compound **J** in liquid crystal cell. The photostationary state occurred at 40 sec and complete thermal back relaxation was observed at 90 min. The composition of photostationary state determined the rate of photo-induced phase transition (Legge and Mitchell, 1992). Compound **D** formed a photostationary state with 90 % of [*cis*] whereas compound **J** formed 61.4 % of [*cis*]. Therefore, compared with compound **J**, compound **D** showed better conversion efficiency in liquid crystal host and can be a good candidate for optical storage devices. Also, it is evident that the compound **D** can store images for a longer time due to its longer *cis* lifetime in liquid crystal host than compound **J**. Alternatively, due to short thermal recovery time in compound **J**, it can suitably be used for short-term optical storage devices with about 1.5 h of storage time.

Numerous cycles of photoisomerisation was performed on compound **D** with alternating UV light for *trans–cis* isomerisation and visible light for *cis–trans* isomerisation. As shown in figure 4.26, the system required relatively short time for

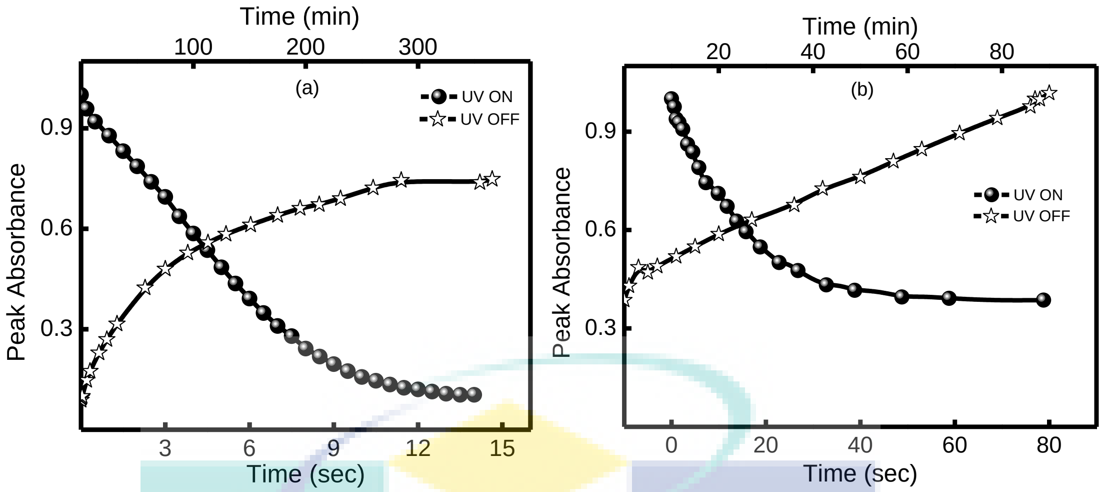

Figure 4.25: *Trans–cis* photoisomerisation and thermal *cis–trans* isomerisation of a) – compound **D**, b) – compound **J** in liquid crystal cell.

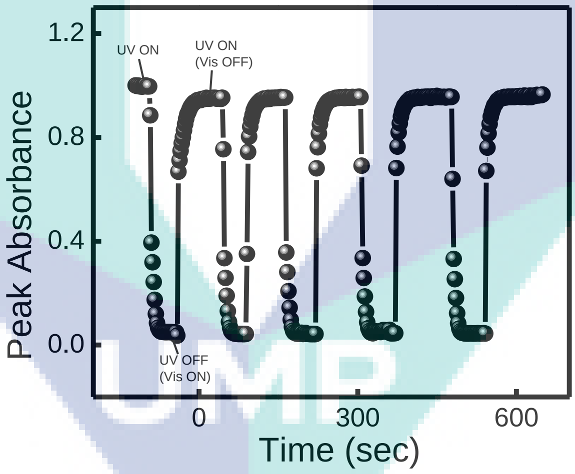

Figure 4.26: Photoswitching cycles of compound **D** when studied using UV light for *trans–cis* photoisomerisation and visible light for *cis–trans* isomerisation.

trans–cis isomerisation with UV illumination and the reverse transformation happen in few seconds by visible light illumination. The absorption showed no signs of decline in the peak absorbance even after five photoisomerisation cycles, which indicate the compound stability, capable of switching easily and rapidly. This study shows an excellent photoisomerisation performance of compound **D** which makes it possible to be applied for rewritable optical storage device in which UV light can be used to "write" while visible light can be used to "erase" information.

4.4.2 Fabrication of optical storage devices

In the last stage, to see the potential ability of the two materials, a prototype of optical storage devices was fabricated using mentioned materials. Similarly, two glass plates with ITO coated and rubbed were used for making the prototype. When alignment layer and the mixture of guest-host system were brought in contact, molecules at the surface adopt alignment; planar or vertical alignment, promoted by the surface anisotropy of the ITO alignment layer. This made liquid crystalline properties became apparent when it was contained in the flat thin cell.

The thickness of the cell was fixed at 5 μm. The narrow space between the two glass slides allowed the guest-host mixture to rise into the cell against the pull of gravity due to capillary force. After a photo-mask was placed on top of the device, UV light was shined for about 10 min. Here, the photo-mask was used to confine the photo-induced phase transition to image-forming region since the light could not pass through the masked area. Thus, images could be formed in this manner.

The formed images were observed using crossed polarisers. Figure 4.27 and 4.28 show the photographs taken when the mixture in liquid crystalline state exposed to UV irradiation through the photo-mask. The induction of azobenzene photochemical activity allowed director (*n*) in the bulk nematic to reorientation. Basically, this brought about photo-induced phase transition at the illuminated region, where nematic-to-isotropic transition took place, while the masked regions remained in nematic phase. The dark region belongs to the illuminated area, where materials had undergone photo-induced phase transition and therefore appear dark between crossed polarisers, indicating that they were in the isotropic phase. Beyond that regions were the masked areas, where the materials remained in the nematic phase and appeared bright when viewed by crossed polarisers. Hence, by shining UV light through a photo-mask, the sample mixtures transformed from the ordered state to the disordered state with the illumination of light giving high contrast between bright states and dark states. The image was erased once the system was shined by high intensity visible light at 450 nm.

In the guest-host system, the liquid crystal acted as host with azobenzene acted as guest molecules. The photo-induced phase transition behaviour can be understood better when the different molecular shape of the *cis* and *trans* isomers are considered. The *trans* configuration of the azobenzene possessed a rod-like shape, while the *cis* configuration had a bent shape. The disappearance of the liquid crystalline phase could take place at the same time scale as the *trans–cis* photoisomerisation, because the *cis* form showed no liquid crystalline phase and the bent configuration acted as impurities which disrupted the orientation order. As the azobenzene changed their molecular shape, the T_{N-I} of the mixture with the *cis* form was also lower than with the *trans* form (Ikeda and Tsutsumi, 1995; Shishido, 2010). So, *trans–cis* isomerisation induced a phase transition from the ordered liquid crystalline state to the isotropic phase. The *cis* isomers of compound **D** and **J** even when incorporated in a small amount (5 %) in liquid crystal system (95 %) able to reorient the entire sample (Eich and Wendorff, 1990). Since the photochemical phase transition accompanied a large change in birefringence of liquid crystal phase, compound **D** and **J** are obviously attractive for optical storage applications.

The photo-induced transition from nematic to isotropic represents a “write” mechanism in the optical storage devices. After irradiation termination, whether the disordered orientation is conserved or not, depends on the thermal back relaxation of azobenzene in the liquid crystal host. An optical image with a stable dark region corresponds to the “store” step, which can be observed through crossed polarisers (“read”). The disorder orientation can be completely erased by heating, or overwriting with visible light, or leaving in the dark. After that, the optical images can be re-written as many times as needed. This is how the optical storage devices work. In short, the devices can be use in a rewritable manner.

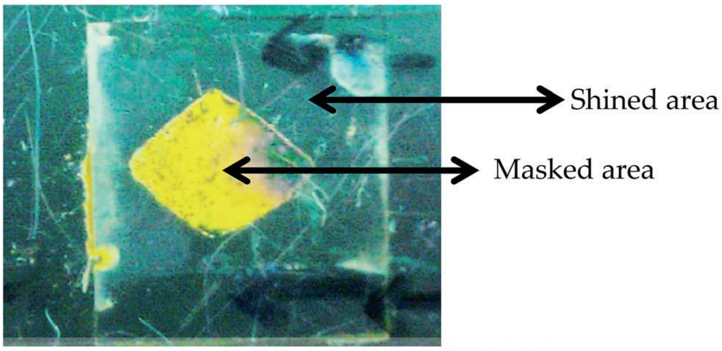

Figure 4.27: Demonstration of image stored in an optical storage device based on compound **D**.

Figure 4.28: Demonstration of image stored in optical storage device based on compound **J**.

CHAPTER 5

CONCLUSION AND RECOMMENDATIONS

5.1 CONCLUSION

Fifteen azobenzene derivatives with different structures were studied. Firstly, two bent-shaped dimeric azobenzene **D** and **E**, with different spacers exhibited nematic phase as evidenced by POM. It is clear that the effects of spacers on the optical properties of the compounds did not generate a dramatic change since both of the aliphatic and aromatic spacers were made up of six carbon atoms. The photoisomerisation properties of compound **D** and **E** showed *trans–cis* isomerisation at around 17 sec and 18 sec, respectively, whereas the reverse process took place at around 7.21 h for compound **E** and 13.25 h for compound **D** in solution. Photoisomerisation study of compound **D** in liquid crystal cell showed *trans–cis* photoisomerisation took around 382 min. Thus, **D** can be suitably exploited in the field of optical storage devices.

Next, amide-based azobenzene, **G** to **J**, having different terminal electron-withdrawing groups were studied. These materials showed *trans-cis* isomerisation in the range of 18 – 24 sec and the reverse process took place from 5 h to 10 h in solutions. The presence of intermolecular hydrogen bonding played an important role in photoisomerisation. Insertion of electron-withdrawing groups gave dramatic changes in the hydrogen bonding effect. With the weak electron-withdrawing group, the hydrogen bond was strengthen and resulted in long thermal back relaxation in the solution of compound **I** and **J**. Then, compound **J** in liquid crystal cell showed *trans–cis* photoisomerisation at around 40 sec and reverse process at 90 min. Due to short recovery time in liquid crystal cell, **J** may be suitably useful for making short-term optical data storage devices.

Thirdly, azobenzene with fluorine substitutions (compound **M** to **P**) were also studied. The presence of fluorine and ester group in azobenzene with fluorine at the terminal end proved to be an important structural factor determining the liquid crystallinity and thermal back relaxation time due to introduction of dipole moment in the molecular structure. Based on experimental results, materials with monofluoro-substituted azobenzene esters (compound **N**) exhibited longer thermal back relaxation in comparison with difluoro-substituted counterparts (compound **P**). Long thermal back relaxation nearly 22 h exhibited by compound **N** is a strong contender for creation of long-term optical information storage devices.

Lastly, olefinic azobenzene with an unsaturated double bond at terminal end was found to have the strongest influence on the thermal back relaxation, with the longest thermal back relaxation (45 h) obtained by compound **S**. The olefinic azobenzene was generally found to induce strong photoisomerisation without the addition of electron-withdrawing group. This study gave an important aspect to utilize the photochemically induced photo-crosslinking process; the olefinic terminal chain might form intercrosslink bond with nearby azobenzene molecules leading to long thermal back relaxation. This showed that by proper tuning of the azobenzene molecule one can able to get permanent crosslinking effect in which optical storage devices can last longer.

In a nutshell, by tuning azobenzene derivatives with different substitution it was found that different substitution had a significant effect on their liquid crystalline property as well as photoisomerisation behaviour. The thermal back relaxation had improved from about 5 h in dimeric bent-shaped azobenzene to 45 h by olefinic azobenzene. Data of photoisomerisation studies in solution form were summarized in in table 5.1. This research work provided several new photo-active materials along with mesophases so that one can able to make devices of different storage time based on the requirement using mentioned materials.

Table 5.1: The summary of data obtained from study of fifteen azobenzene derivatives.

Compound	Mesophases	*Trans–cis*	CE (%)	*Cis–trans*
D	Yes	17 sec	76	13.25 h
E	Yes	18 sec	55	7.21 h
G	No	18 sec	72	9.21 h
H	Yes	20 sec	52	5.73 h
I	Yes	22 sec	75	10.18 h
J	Yes	24 sec	75	10.58 h
M	No	4 min	72.93	16.42 h
N	Yes	4 min	80.8	22.48 h
O	No	4 min	70.26	13.08 h
P	Yes	4 min	64.46	11.55 h
S	Yes	82 sec	88.59	45.00 h
T	Yes	73 sec	85.4	28.66 h
U	Yes	94 sec	86.05	17.25 h
V	Yes	84 sec	86.58	12.46 h
W	Yes	91 sec	86.25	14.23 h

5.2 RECOMMENDATIONS AND FUTURE PROSPECT

Based on the results, discussion and data analysis done, some recommendations can be taken into consideration to upgrade future studies in azobenzene-liquid crystal composite for fabrication of long-term optical storage device. Since photo-crosslinking reactions between azobenzene molecules containing photo-crosslinkable units can be started or stopped at will by the simple expedient of turning on or off the light, it is suggested that the successful interlocking network formed between liquid crystal molecules with the photo-crosslinked azobenzene might provide a new strategy for creating long-term optical storage devices. If the effect of photo-crosslinking can be taken place in azobenzene–liquid crystal guest-host system, one can be able to obtain a stable photo-induced phase transition in the liquid crystal cell. This means that there are interlocking network formed between the photo-crosslinked guest azobenzene molecules and host liquid crystal molecules that prevent the excited disorder state of liquid crystalline system return to order state easily. This enables the optically patterned liquid crystal phase to be “frozen in” by subsequent interlocking effect between the guest and host molecules.

As shown in figure 5.1 before UV irradiation, the olefinic azobenzene may prefer to be in rod-shaped form. As UV light of wavelength 365 nm was shined, energetically stable *trans* molecules convert to *cis* molecules, in other words, it is possible for the system go from order to disorder state. But here, with the effect of UV light there may be the possibility of interlocking network between the photo-crosslinked azobenzene and liquid crystal molecules. Bringing them back to order state will be difficult due to the photocrosslink bonds between azobenzene molecules as well as interlocking effect form in the guest–host system. The system may be able to stay permanently in disorder state and give rise to a permanent optical storage device.

Another study can be done in future is by incorporating long chain alkane into mixture of azobenzene and liquid crystal molecules (figure 5.2). It is well-known that by increasing flexibility in the chain can increase the solubility of materials in the system. It has been reported by Nair and coworkers (2004) that long chain alkanes attain coiled-form in any system whereas liquid crystal molecules remain in rod shape. When these two systems are mixed together and subsequently shine with UV light, the rod-shaped molecules change to bent-shape. But the behaviour of coiled- form of long chain alkene after UV illumination is not clear. If the bent form is blocked from going back to rod form due to *cis–trans* isomerisation, then, the thermal back relaxation time increases. Long chain alkanes have only flexible units and thus do not support the formation of liquid crystalline phases. Structurally incompatible bent-shaped molecules of azobenzene and flexible long chain alkane may give rise to long or permanent optical storage devices when light of suitable wavelength is shined on them. In light of this, the project can provide a path for the exploration of systems for obtaining long-term or permanent optical storage devices.

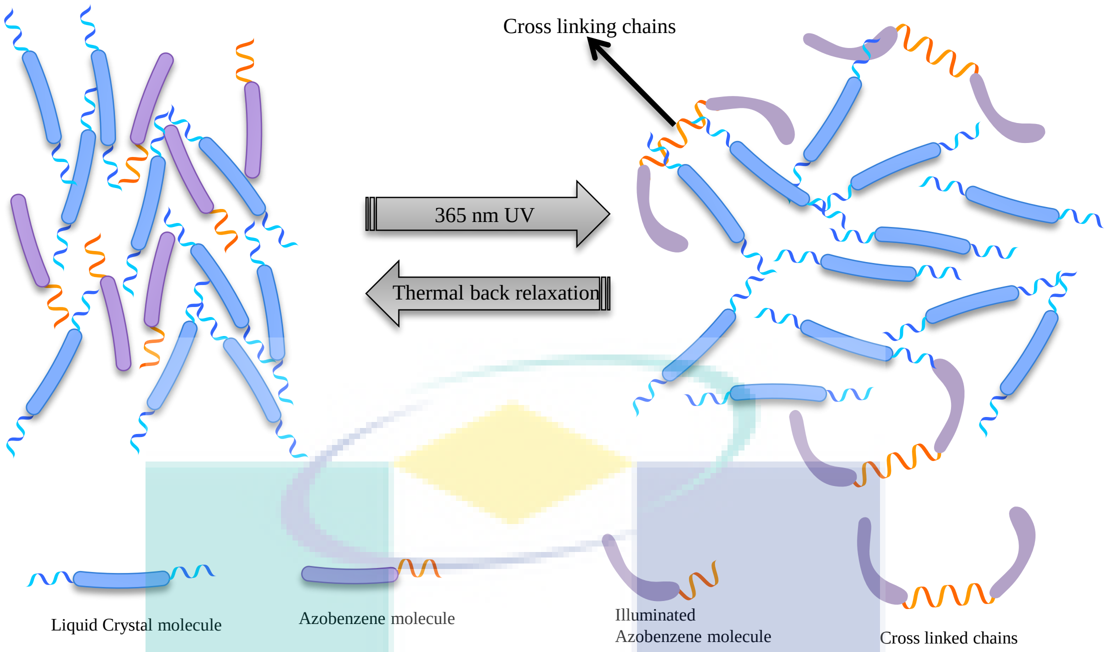

Figure 5.1: Mechanism of azobenzene photo-crosslinking in guest-host system. Due to the formation of intermolecular locking network between azobenzene and liquid crystal molecules, system takes longer time to reverse back to their original shape.

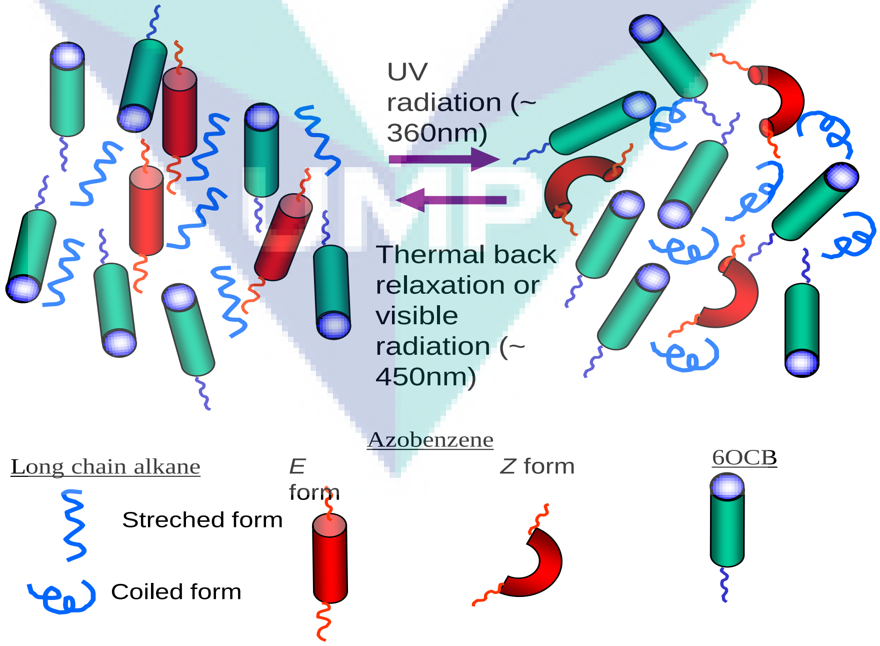

Figure 5.2: Composite materials made up of long chain alkane decorated with rod-shaped anisotropic molecules.

REFERENCES

Al-Hamdani, U. J., Gassim, T. E., Radhy, H. H. (2010). Synthesis and characterization of azo compounds and study of the effect of substituents on their liquid crystalline behavior. *Molecules*. **15**(8): 5620-5628.

Bamford, C. H., Ledwith, A., Yagci, Y. (1978). Synthesis and reactions of polymers with photoactive terminal groups: 2. New azo-initiator for the synthesis of polymers with N-acyldibenz [b, f] azepine terminal units. *Polymer*. **19**(3): 354-356.

Bandara, H. D., Friss, T. R., Enriquez, M. M., Isley, W., Incarvito, C., Frank, H. A., Burdette, S. C. (2010). Proof for the concerted inversion mechanism in the *trans→cis* isomerization of azobenzene using hydrogen bonding to induce isomer locking. *The Journal of organic chemistry*. **75**(14): 4817-4827.

Bandara, H. D., Burdette, S. C. (2012). Photoisomerization in different classes of azobenzene. *Chemical Society Reviews*. **41**(5): 1809-1825.

Barrett, C. J., Mamiya, J. I., Yager, K. G., Ikeda, T. (2007). Photo-mechanical effects in azobenzene-containing soft materials. *Soft Matter*. **3**(10): 1249-1261.

Barrett, C., Natansohn, A., Rochon, P. (1995). *Cis-trans* thermal isomerization rates of bound and doped azobenzenes in a series of polymers. *Chemistry of materials.* **7**(5): 899-903.

Biswas, N., Umapathy, S. (2003). Resonance Raman study of the solvent dynamics for ultrafast charge transfer transition in 4-nitro-4′-dimethylamino-azobenzene. *The Journal of chemical physics*. **118**(12): 5526-5536.

Bortolus, P., Monti, S. (1979). *Cis-trans* photoisomerization of azobenzene. Solvent and triplet donors effects. *Journal of Physical Chemistry*. **83**(6): 648-652.

Bronner, C., Tegeder, P. (2014). Photo-induced and thermal reactions in thin films of an azobenzene derivative on Bi (111). *New Journal of Physics*. **16**(5): 053004.

Burdick, D. L., Leffler, W. L. (2001). *Petrochemicals in nontechnical language*. Pennwell Books.

Chandrasekhar, S., Sadashiva, B. K., Suresh, K. A. (1977). Liquid crystals of disc-like molecules. *pramana*. **9**(5): 471-480.

Choe, D. H., Ban, S. Y. (2001). Effect of photopolymerization on the rate of photocrosslink in chalcone-based oligomeric compounds. *Bulletin of the Korean Chemical Society*. **22**(11): 1207-1212.

Coles, H. J., Walton, H. G., Guillon, D., Poetti, G. (1993). Photomechanically induced phase transitions in ferroelectric liquid crystals. *Liquid Crystals*. **15**(4): 551-558.

Collings, P. J., Hird, M. (1997). *Introduction to liquid crystals: chemistry and physics*. CRC Press.

Cvetinov, M., Obadović, D., Stojanović, M., Lazar, D., Vajda, A., Éber, N., Ristić, I. (2013). Mesophase behaviour of binary mixtures of bent-core and calamitic compounds. *Liquid Crystals*. **40**(11): 1512-1519.

Demus, D., Goodby, J. W., Gray, G. W., Spiess, H. W., Vill, V. (Eds.). (2011). *Handbook of Liquid Crystals, Low Molecular Weight Liquid Crystals I: Calamitic Liquid Crystals*. John Wiley & Sons.

Dokic, J., Gothe, M., Wirth, J., Peters, M. V., Schwarz, J., Hecht, S., Saalfrank, P. (2009). Quantum chemical investigation of thermal *cis*-to-*trans* isomerization of azobenzene derivatives: substituent effects, solvent effects, and comparison to experimental data. *The Journal of Physical Chemistry A*. **113**(24): 6763-6773.

Dou, Y., Allen, R. E. (2003). Detailed dynamics of a complex photochemical reaction: *Cis–trans* photoisomerization of stilbene. *The Journal of chemical physics*. **119**(20): 10658-10666.

Eich, M., Wendorff, J. (1990). Laser-induced gratings and spectroscopy in monodomains of liquid-crystalline polymers. *Journal of the Optical of America B*. **7**(8): 1428-1436.

Eisenbach, C. D. (1980). Relation between photochromism of chromophores and free volume theory in bulk polymers. *Berichte der Bunsengesellschaft für physikalische Chemie*. **84**(7): 680-690.

El Halabieh, R. H., Mermut, O., Barrett, C. J. (2004). Using light to control physical properties of polymers and surfaces with azobenzene chromophores. *Pure and applied chemistry*. **76**(7-8): 1445-1465.

Elamain, O., Hegde, G., Komitov, L. (2013). Alignment and alignment transition of bent core nematics. *Applied Physics Letters*. **103**(2): 023301.

Feringa, B. L., Jager, W. F., de Lange, B. (1993). Organic materials for reversible optical data storage. *Tetrahedron*. **49**(37): 8267-8310.

Fujii, T., Kuwahara, S., Katayama, K., Takado, K., Ube, T., Ikeda, T. (2014). Molecular dynamics in azobenzene liquid crystal polymer films measured by time-resolved techniques. *Physical Chemistry Chemical Physics*. **16**(22): 10485-10490.

García-Amorós, J., Velasco, D. (2012). Recent advances towards azobenzene-based light-driven real-time information-transmitting materials. *Beilstein journal of organic chemistry*. **8**(1): 1003-1017.

Hampp, N. (2000). Bacteriorhodopsin as a photochromic retinal protein for optical memories. *Chemical Reviews*. **100**(5): 1755-1776.

Henderson, R., Schertler, G. F. X. (1990). The structure of bacteriorhodopsin and its relevance to the visual opsins and other seven-helix G-protein coupled receptors. *Philosophical Transactions of the Royal Society B: Biological Sciences*. **326**(1236): 379-389.

Hird, M. (2005). Banana-shaped and other bent-core liquid crystals. *Liquid Crystals Today*. **14**(2): 9-21.

Ho, M. S., Natansohn, A., Rochon, P. (1995). Azo polymers for reversible optical storage. 7. The effect of the size of the photochromic groups. *Macromolecules*. **28**(18): 6124-6127.

Hu, D., Zhang, Z., Hu, Y., Luo, Y., Zhang, Q., Huang, W. (2011). Study on the rewritability of bisazobenzene-containing films in optical storage based on two-photon process. *Optics Communications*. **284**(3): 802-806.

Ikeda, T. (2003). Photomodulation of liquid crystal orientations for photonic applications. *Journal of Materials Chemistry*. **13**(9): 2037-2057.

Ikeda, T., Tsutsumi, O. (1995). Optical switching and image storage by means of azobenzene liquid-crystal films. *Science*. **268**(5219): 1873-1875.

Jákli, A., Chien, L. C., Krüerke, D., Sawade, H., Heppke, G. (2002). Light shutters from antiferroelectric liquid crystals of bent-shaped molecules. *Liquid crystals*. **29**(3): 377-381.

Jánossy, I. (2000). Dye-assisted optical reorientation of nematic liquid crystals. In *Multiphoton and Light Driven Multielectron Processes in Organics: New Phenomena, Materials and Applications* (pp. 225-236). Springer Netherlandsz.

Janossy, I., Csillag, L., Lloyd, A. D. (1991). Temperature dependence of the optical Freedericksz transition in dyed nematic liquid crystals. *Physical Review A*. **44**(12): 8410.

Javani, M., Khorasani, S. N., Abdolmaleki, A., Nouri Khorasani, A. (2014). Photocrosslinking of styrene–isoprene–styrene; effect of benzoin and ethylene glycol dimethacrylate on physical properties. *Journal of Adhesion Science and Technology*. **28**(10): 975-985.

Jayalakshmi, V., Hegde, G., Nair, G. G., Prasad, S. K. (2009). Photo-controlled conformation-assisted permanent optical storage device employing a polymer network liquid crystal. *Physical Chemistry Chemical Physics*. **11**(30): 6450-6454.

Jayalatha, D., Balamurugan, R., Kannan, P. (2009). Synthesis and characterization of benzylidene and azobenzene based photochromic liquid-crystalline polymers. *High Performance Polymers*. **21**(2): 139-154.

Jørgensen, K. B. (2010). Photochemical oxidative cyclisation of stilbenes and stilbenoids – the Mallory-reaction. *Molecules*. **15**(6): 4334-4358.

Keith, C., Lehmann, A., Baumeister, U., Prehm, M., Tschierske, C. (2010). Nematic phases of bent-core mesogens. *Soft Matter*. **6**(8): 1704-1721.

Kojima, M., Nebashi, S., Ogawa, K., Kurita, N. (2005). Effect of solvent on cis-to-trans isomerization of 4-hydroxyazobenzene aggregated through intermolecular hydrogen bonds. *Journal of physical organic chemistry*. **18**(10): 994-1000.

Legge, C. H., Mitchell, G. R. (1992). Photo-induced phase transitions in azobenzene-doped liquid crystals. *Journal of Physics D: Applied Physics*. **25**(3): 492.

Li, X., Fang, L., Hou, L., Zhu, L., Zhang, Y., Zhang, B., Zhang, H. (2012). Photoresponsive side-chain liquid crystalline polymers with amide group-substituted azobenzene mesogens: effects of hydrogen bonding, flexible spacers, and terminal tails. *Soft Matter*. **8**(20): 5532-5542.

Lutfor, M. R., Hegde, G., Kumar, S., Tschierske, C., Chigrinov, V. G. (2009). Synthesis and characterization of bent-shaped azobenzene monomers: guest–host effects in liquid crystals with azo dyes for optical image storage devices. *Optical Materials*. **32**(1): 176-183.

Lutfor, M. R., Yusoff, M. M., Hegde, G., Fazli, M. N., Malek, A., Samah, N. A., Srinivasa, H. T. (2013). Synthesis of banana-shaped liquid crystals for photoswitching properties. *Molecular Crystals and Liquid Crystals*. **587**(1): 41-53.

Matsuzawa, Y., Kato, H., Ohyama, H., Nishide, D., Kataura, H., Yoshida, M. (2011). Photoinduced dispersibility tuning of carbon nanotubes by a water-soluble stilbene as a dispersant. *Advanced Materials*. **23**(34): 3922-3925.

Mahimwalla, Z., Yager, K. G., Mamiya, J. I., Shishido, A., Priimagi, A., Barrett, C. J. (2012). Azobenzene photomechanics: prospects and potential applications. *Polymer bulletin*. **69**(8): 967-1006.

Merino, E., Ribagorda, M. (2012). Control over molecular motion using the *cis–trans* photoisomerization of the azo group. *Beilstein journal of organic chemistry*. **8**(1): 1071-1090.

Min, D. B., Boff, J. M. (2002). Chemistry and reaction of singlet oxygen in foods. *Comprehensive reviews in food science and food safety*. **1**(2): 58-72.

Miao, X., Cheng, Z., Ren, B., Deng, W. (2012). Hydrogen bonds induced supramolecular self-assembly of azobenzene derivatives on the highly oriented pyrolytic graphite surface. *Surface Science*. **606**(15): L59-L63.

.

Modi, V. P., Patel, N. P., Hasmukh, Patel, S. (2012). Studies on synthesis, characterization and solvatochromic effect of novel tris(heteroaryl)bisazo dyes for dyeing polyester fabric. *Elixir Organic. Chemistry*. **4**: 7192-7201.

Nägele, T., Hoche, R., Zinth, W., Wachtveitl, J. (1997). Femtosecond photoisomerization of *cis*-azobenzene. *Chemical physics letters*, **272**(5): 489-495.

Nair, G. G., Prasad, S. K., Hegde, G. (2004). Influence of a long-chain alkane on the photoinduced nematic-isotropic transition. *Physical Review E*. **69**(2): 021708.

Nair, G. G., Prasad, S. K., Yelamaggad, C. V. (2000). Opto-dielectric effect on a nematic liquid crystal doped with a photoactive azo mesogen. *Journal of Applied Physics*. **87**(5): 2084-2089.

Namazian, M., Coote, M. L. (2009). Gas-phase acidity, bond dissociation energy and enthalpy of formation of fluorine-substituted benzenes: A theoretical study. *Journal of Fluorine Chemistry*. **130**(7): 621-628.

Nayek, P., Ghosh, S., Roy, S., Majumder, T. P., Dabrowski, R. (2012). Electro-optic and dielectric investigations of a perfluorinated compound showing orthoconic antiferroelectric liquid crystal. *Journal of Molecular Liquids*. **175**: 91-96.

Niori, T., Sekine, T., Watanabe, J., Furukawa, T., Takezoe, H. (1996). Distinct ferroelectric smectic liquid crystals consisting of banana shaped achiral molecules. *Journal of materials Chemistry*. **6**(7): 1231-1233.

Nishimura, N., Sueyoshi, T., Yamanaka, H., Imai, E., Yamamoto, S., Hasegawa, S. (1976). Thermal *cis*-to-*trans* isomerization of substituted azobenzenes II. Substituent and solvent effects. *Bulletin of the Chemical Society of Japan*. **49**(5): 1381-1387.

Pal, K., Maiti, U. N., Majumder, T. P., Dash, P., Mishra, N. C., Bennis, N., Otón, J. M. (2011). Ultraviolet visible spectroscopy of CdS nano-wires doped ferroelectric liquid crystal. *Journal of Molecular Liquids*. **164**(3): 233-238.

Pavia, D., Lampman, G., Kriz, G., Vyvyan, J. (2008). *Introduction to spectroscopy*. Cengage Learning.

Pelzl, G., Diele, S., Weissflog, W. (1999). Banana-shaped compounds – a new field of liquid crystals. *Advanced materials*. **11**(9): 707-724.

Prasad, S. K., Nair, G. G. (2001). Effects of photo-controlled nanophase segregation in a re-entrant nematic liquid crystal. *Advanced Materials*. **13**(1): 40-43.

Prasad, S. K., Nair, G. G., Sandhya, K. L., Rao, D. S. (2004). Photoinduced phase transitions in liquid crystalline systems. *Current Science*. **86**(6): 815-823.

Prasad, S. K., Sandhya, K. L., Nair, G. G., Hiremath, U. S., Yelamaggad, C. V. (2002). Spacer parity dependence of photo-induced effects in liquid crystalline dimers. *Journal of applied physics*. **92**(2): 838-841.

Pu, X., Wong, N. B., Zhou, G., Gu, J., Tian, A. (2005). Substituent effects on the *trans*–*cis* isomerization and stability of diazenes. *Chemical physics letters*. **408**(1): 101-106.

Rahman, M. L., Hegde, G., Azazpour, M., Yusoff, M. M., Kumar, S. (2013). Synthesis and characterization of liquid crystalline azobenzene chromophores with fluorobenzene terminal. *Journal of Fluorine Chemistry*. **156**: 230-235.

Rahman, M. L., Yusoff, M. M., Hegde, G., Malek, M. N. F. A., Samah, N. A., Srinivasa, H. T., Kumar, S. (2014). Synthesis and characterization of naphthalene-based banana-shaped liquid crystals for photoswitching properties. *Journal of the Chinese Chemical Society*. **61**(5): 571-577.

Rau, H. (1990). Photochromism: molecules and systems. *Photochromism, Molecules and Systems* (pp. 165-192).

Rau, H. (1990). *Photoisomerization of azobenzenes* (Vol. 2, pp. 119). CRC Press: Boca Raton, FL.

Samanta, S., Qureshi, H. I.,Woolley, G. A. (2012). A bisazobenzene crosslinker that isomerizes with visible light. *Beilstein journal of organic chemistry*. **8**(1): 2184-2190.

Santamato, E., Daino, B., Romagnoli, M., Settembre, M., Shen, Y. R. (1986). Collective rotation of molecules driven by the angular momentum of light in a nematic film. *Physical review letters*. **57**(19): 2423.

Sasaki, T., Ikeda, T., Ichimura, K. (1993). Photoisomerization and thermal isomerization behavior of azobenzene derivatives in liquid-crystalline polymer matrixes. *Macromolecules*. **26**(1): 151-154.

Sato, M., Kinoshita, T., Takizawa, A., Tsujita, Y. (1988). Photoinduced conformational transition of polypeptides containing azobenzenesulfonate in the side chains. *Macromolecules*. **21**(6): 1612-1616.

Schulze, F. W., Petrick, H. J., Cammenga, H. K., Klinge, H. (1977). Thermodynamic properties of the structural analogues benzo [c] cinnoline, *trans*-azobenzene, and *cis*-azobenzene. *Zeitschrift für Physikalische Chemie*. **107**(1): 1-19.

Shishido, A. (2010). Rewritable holograms based on azobenzene-containing liquid-crystalline polymers. *Polymer journal*. **42**(7): 525-533.

Simoni, F., Francescangeli, O. (1999). Effects of light on molecular orientation of liquid crystals. *Journal of Physics: Condensed Matter*. **11**(41): R439.

Stuart, J. A., Marcy, D. L., Wise, K. J., Birge, R. R. (2002). Volumetric optical memory based on bacteriorhodopsin. *Synthetic metals*. **127**(1): 3-15.

Tazuke, S., Kurihara, S., Ikeda, T. (1987). Amplified image recording in liquid crystal media by means of photochemically triggered phase transition. *Chemistry Letters*. (5): 911-914.

Tiberio, G., Muccioli, L., Berardi, R., Zannoni, C. (2010). How does the *trans–cis* photoisomerization of azobenzene take place in organic solvents? *ChemPhysChem*. **11**(5): 1018-1028.

Tilton, M. (1992). *Liquid crystals: applications and uses* (Vol. 3, pp. 68-199). B. Bahadur (Ed.). Singapore: World Scientific.

Vorländer, D. (1929). The direction of the carbon-valenz in benzol-progeny. *Berichte der deutschen chemischen Gesellschaft (A and B Series)*. **62**(10): 2831-2835.

Waldeck, D. H. (1991). Photoisomerization dynamics of stilbenes. *Chemical Reviews*. **91**(3): 415-436.

Wazzan, N. (2009). *Cis-trans* isomerisation of azobenzenes studied by NMR spectroscopy with in situ laser irradiation and DFT calculations.

Wei-Guang Diau, E. (2004). A new *trans*-to-*cis* photoisomerization mechanism of azobenzene on the S_1 (n, π^*) surface. *The Journal of Physical Chemistry A*. **108**(6): 950-956.

Yagci, Y., Jockusch, S., Turro, N. J. (2010). Photoinitiated polymerization: Advances, challenges, and opportunities. *Macromolecules*. **43**(15): 6245-6260.

Yang, C. A., Xie, H., Zhong, G., Zhang, H. (2013). The effects of para-, meta-and ortho-monosubstituted azobenzene moiety in the side chain on phase behavior of mesogen-jacketed liquid crystalline polymers. *Polymer*. **54**(13): 3238-3247.

Yari, M., Sedaghat, S., Hekmati, M. (2008). Synthesis of some new azo disperse dyes and investigation of their solvatochromic effect. *Journal of Physical & Theoretical Chemistry*. **5**(1): 25-30.

APPENDIX A

FT-IR Spectra for Compound D

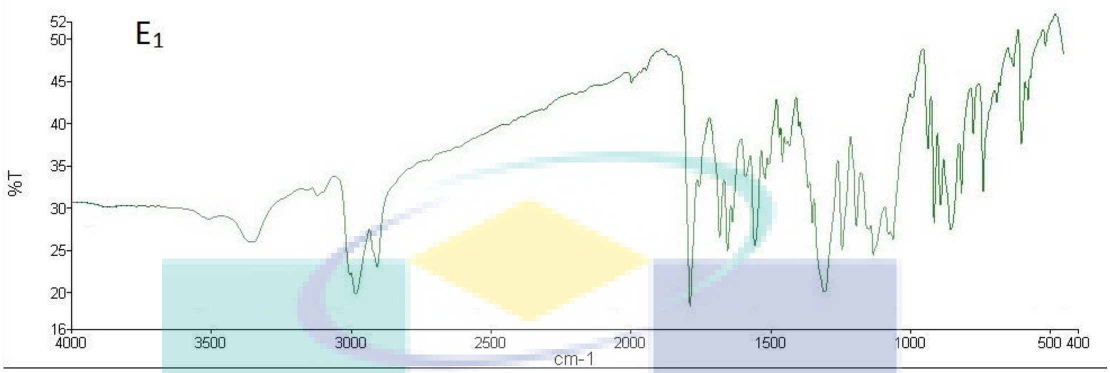

FT-IR Spectra for Compound E

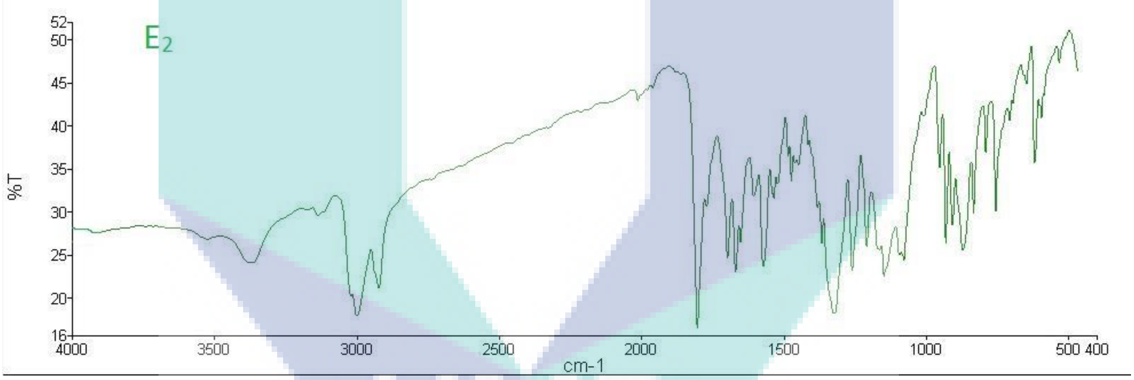

^{1}H-NMR Spectra for Compound D

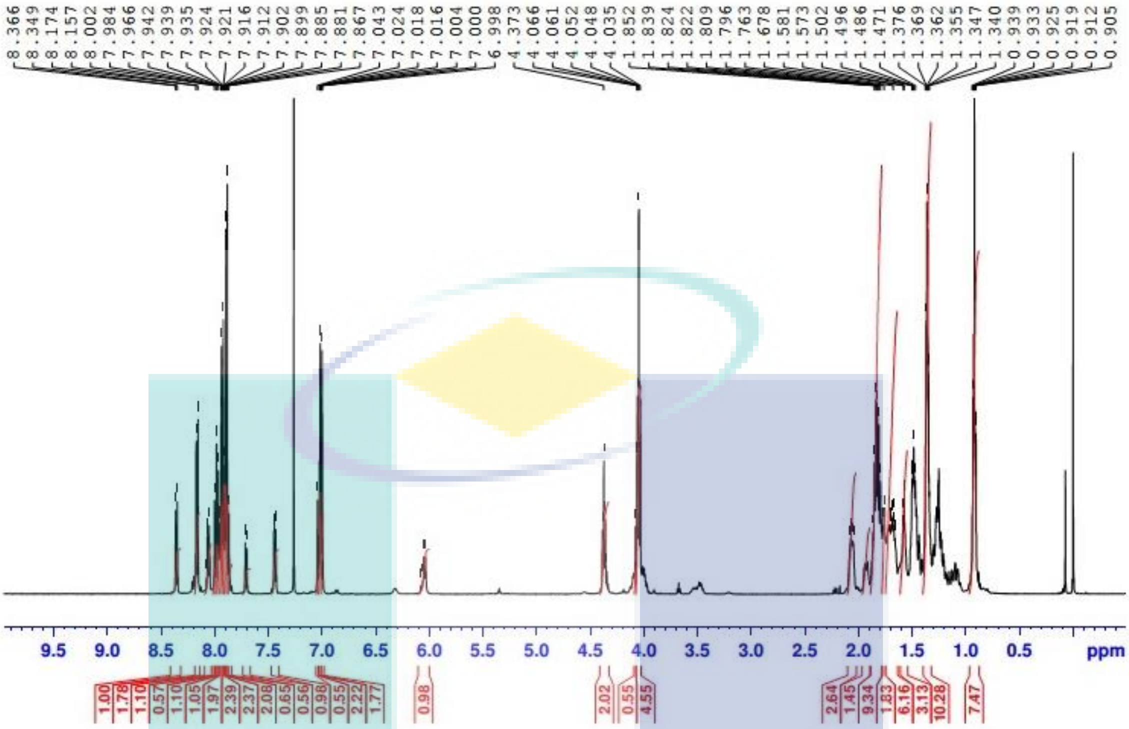

^{1}H-NMR Spectra for Compound E

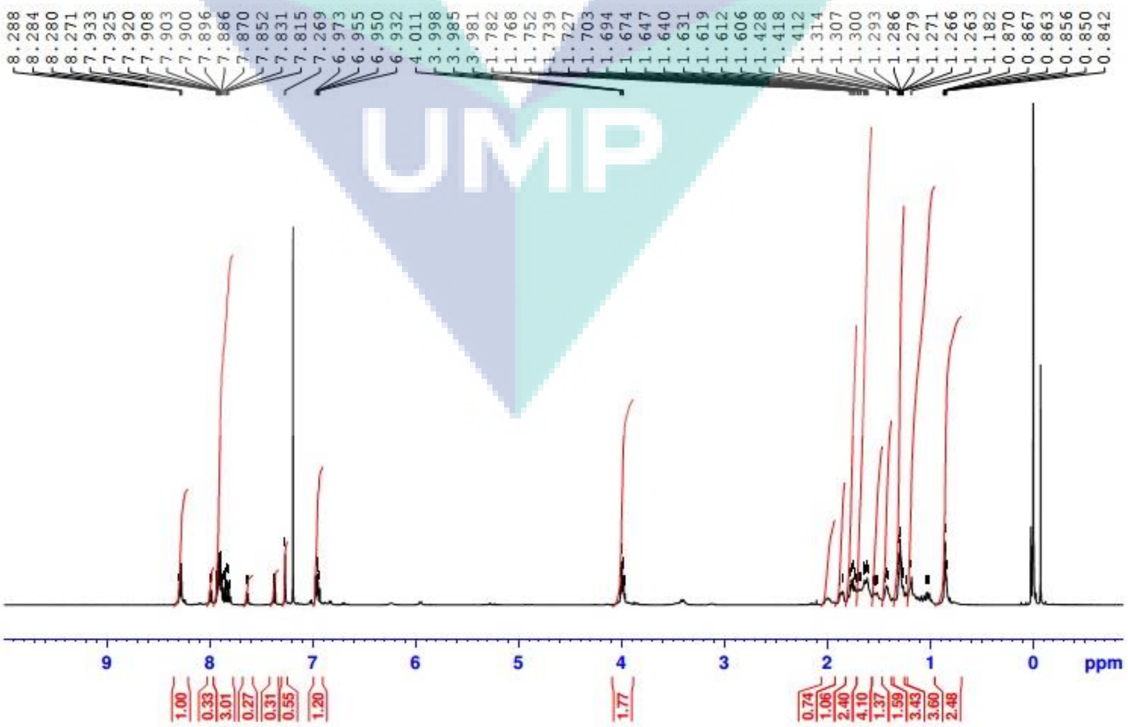

^{13}C-NMR Spectra for Compound D

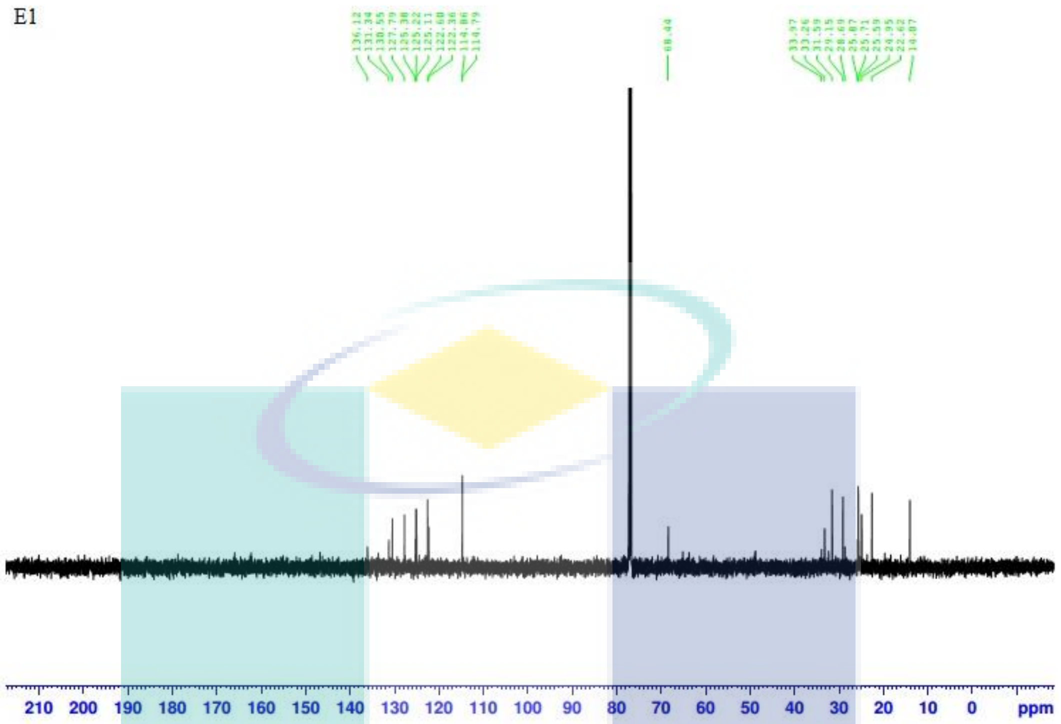

^{13}C-NMR Spectra for Compound E

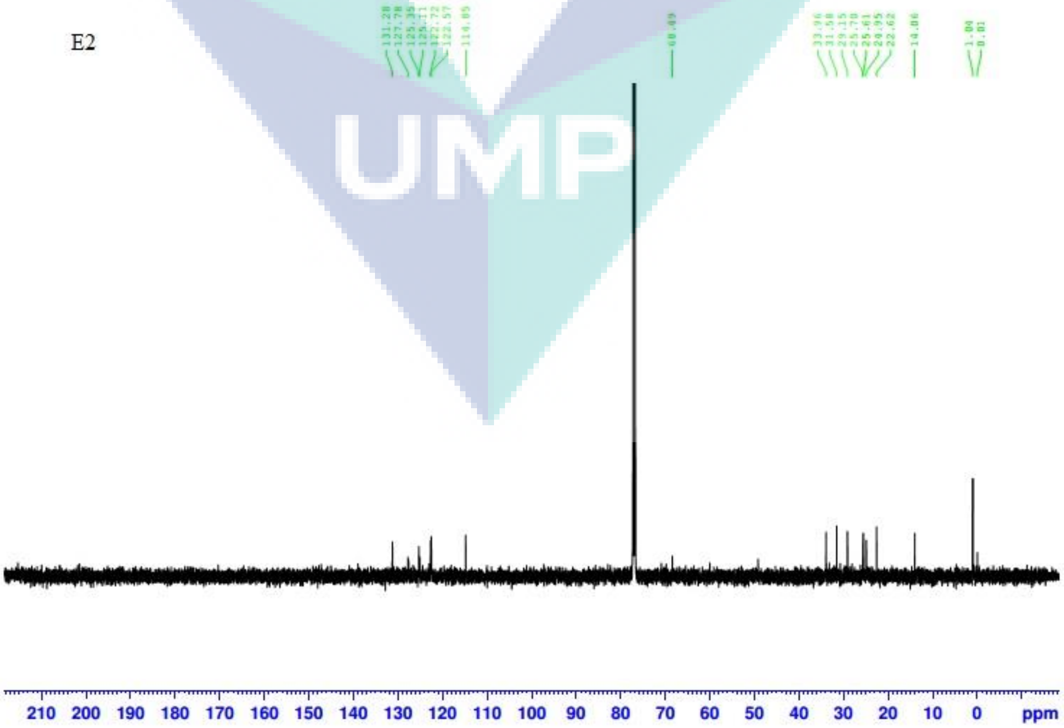

APPENDIX B

^{1}H-NMR Spectra for Compound G

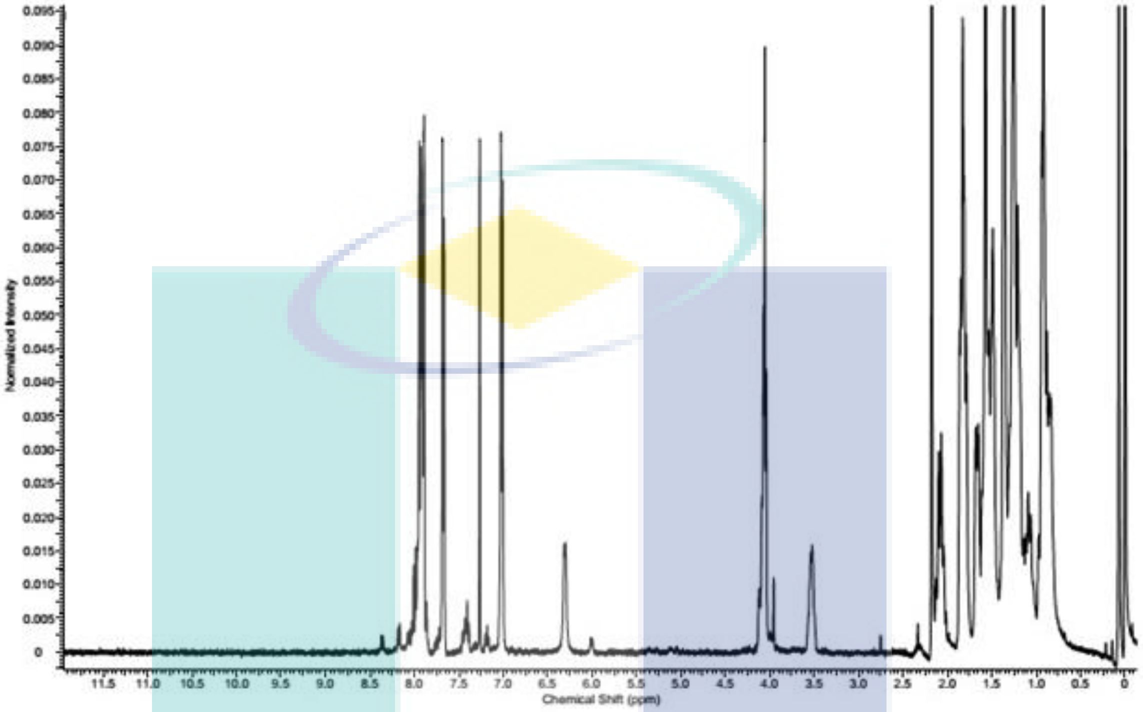

^{1}H-NMR Spectra for Compound H

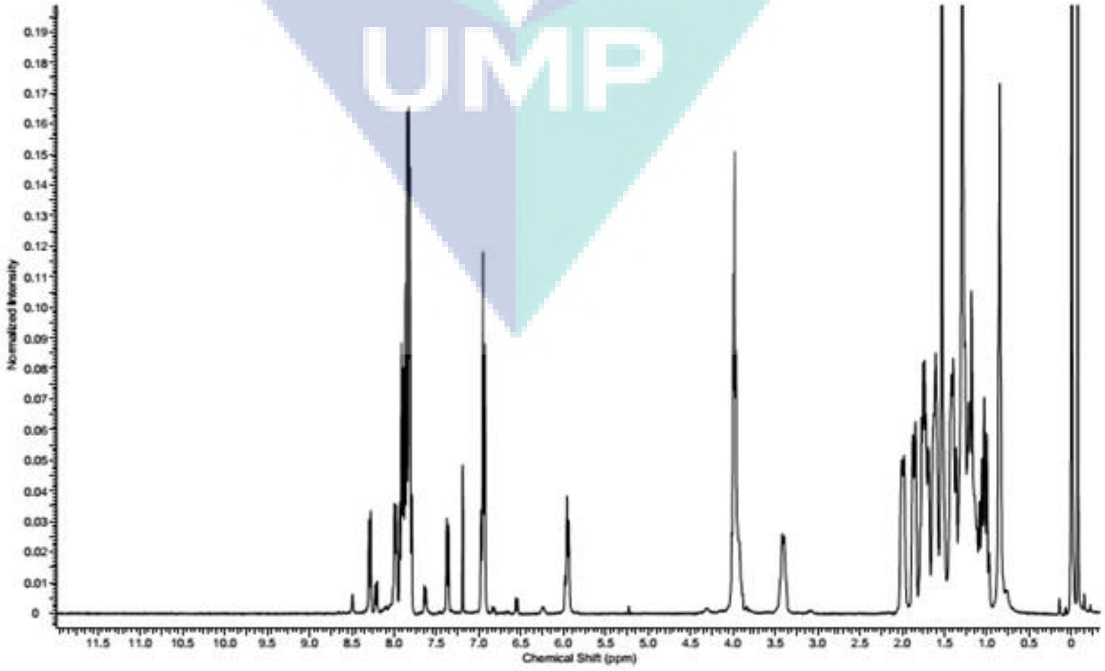

^{1}H-NMR Spectra for Compound I

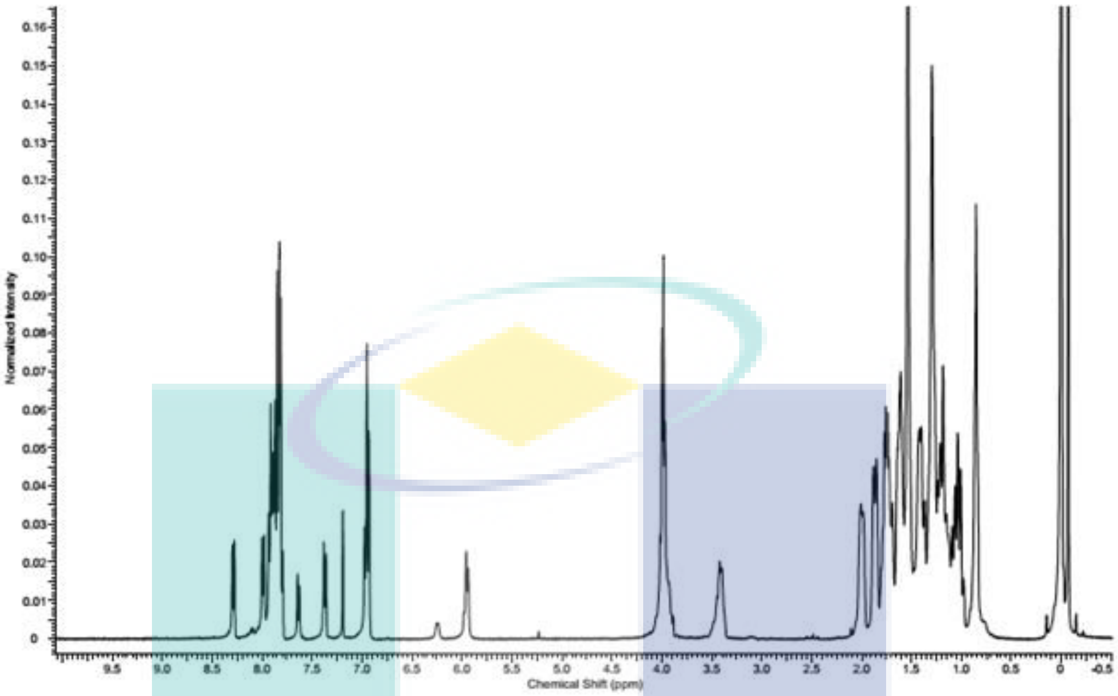

^{1}H-NMR Spectra for Compound J

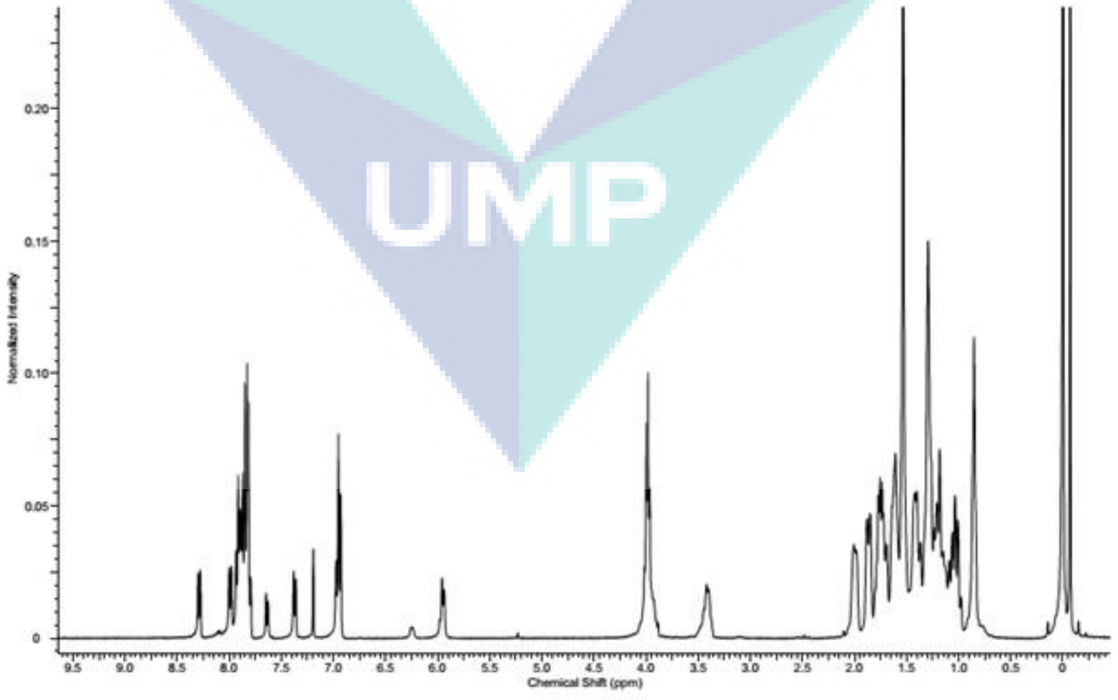

^{13}C-NMR Spectra for Compound H

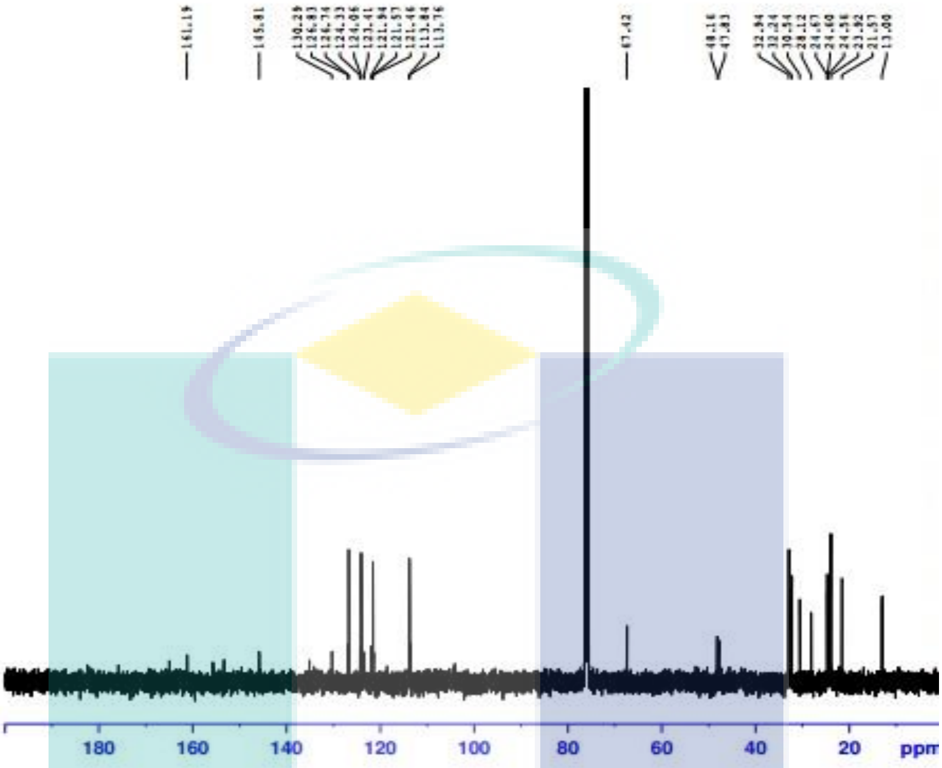

^{13}C-NMR Spectra for Compound I

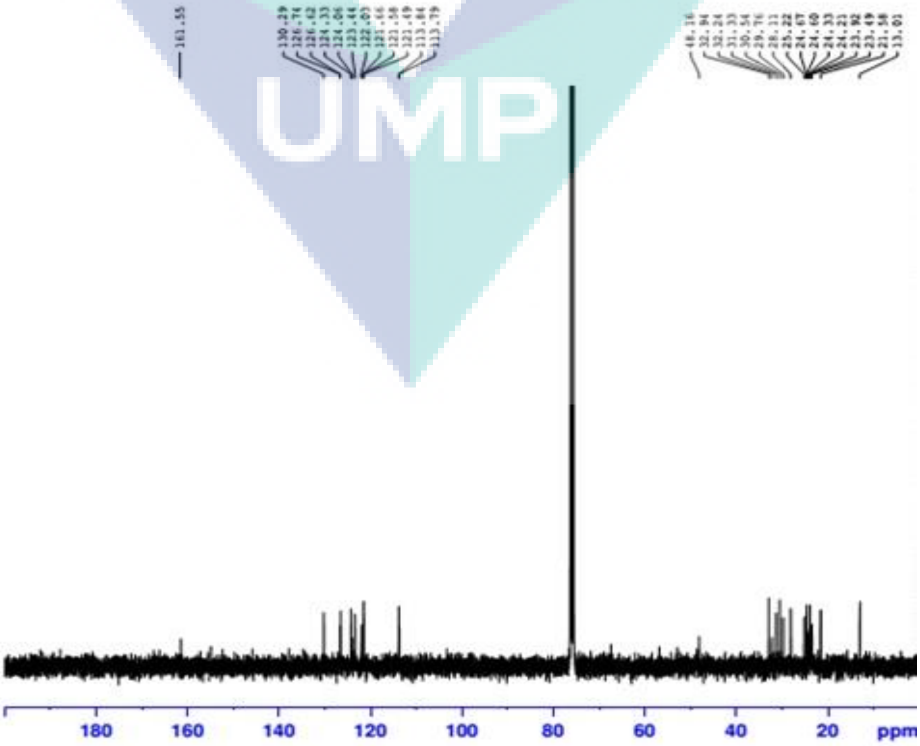

^{13}C-NMR Spectra for Compound J

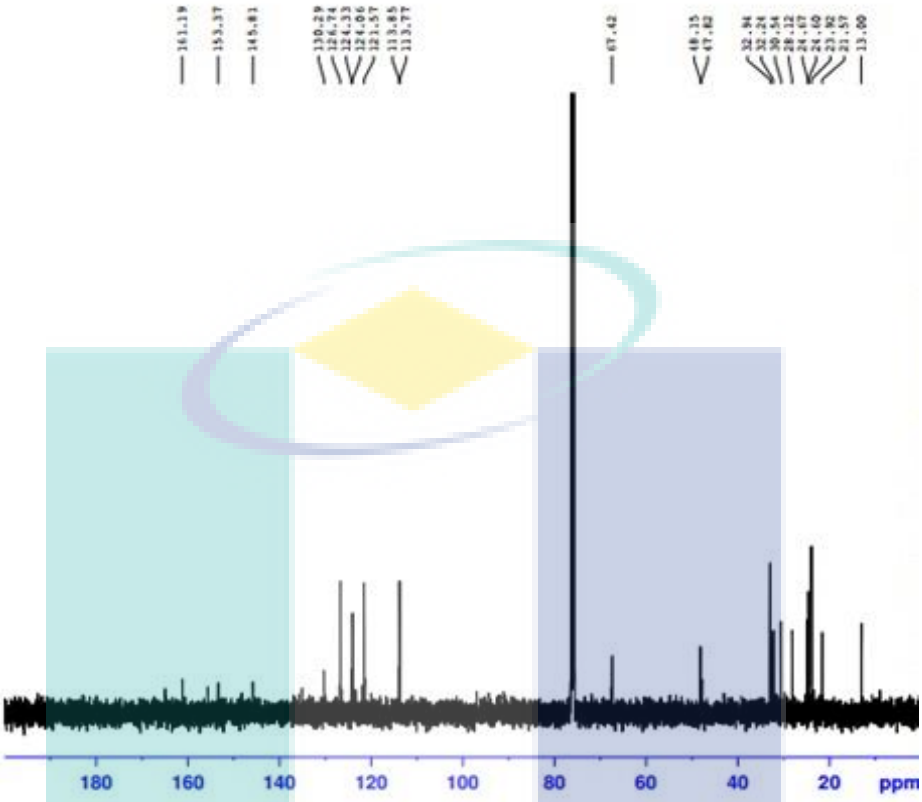

APPENDIX C

^{1}H-NMR Spectra for Compound M

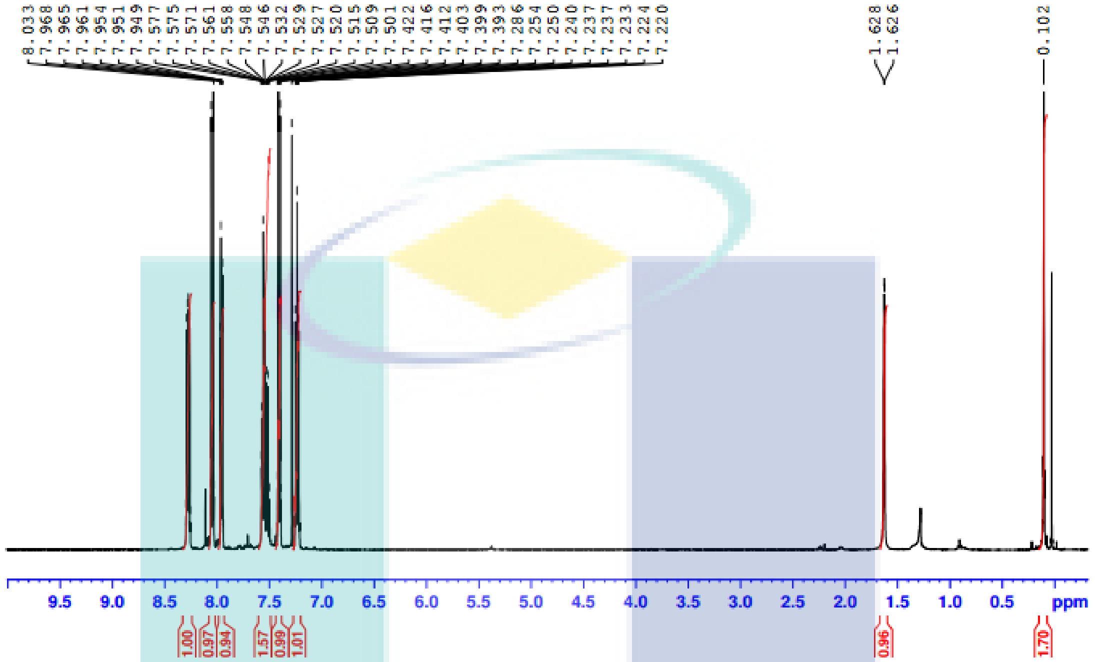

^{1}H-NMR Spectra for Compound N

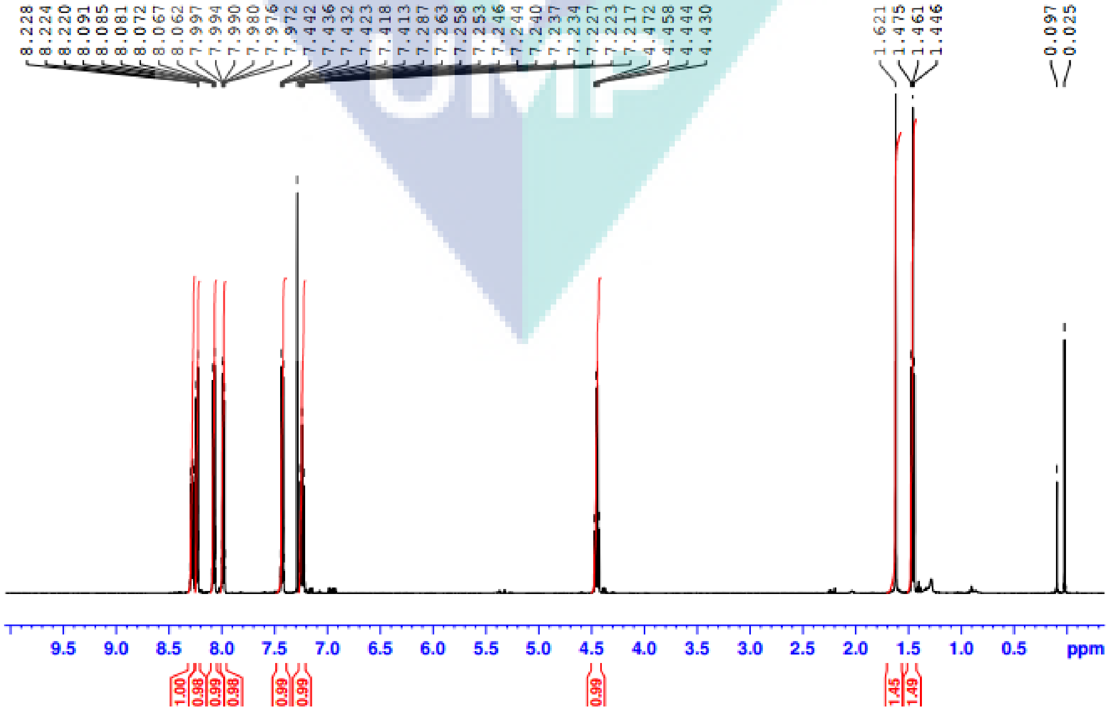

^{13}C-NMR Spectra for Compound M

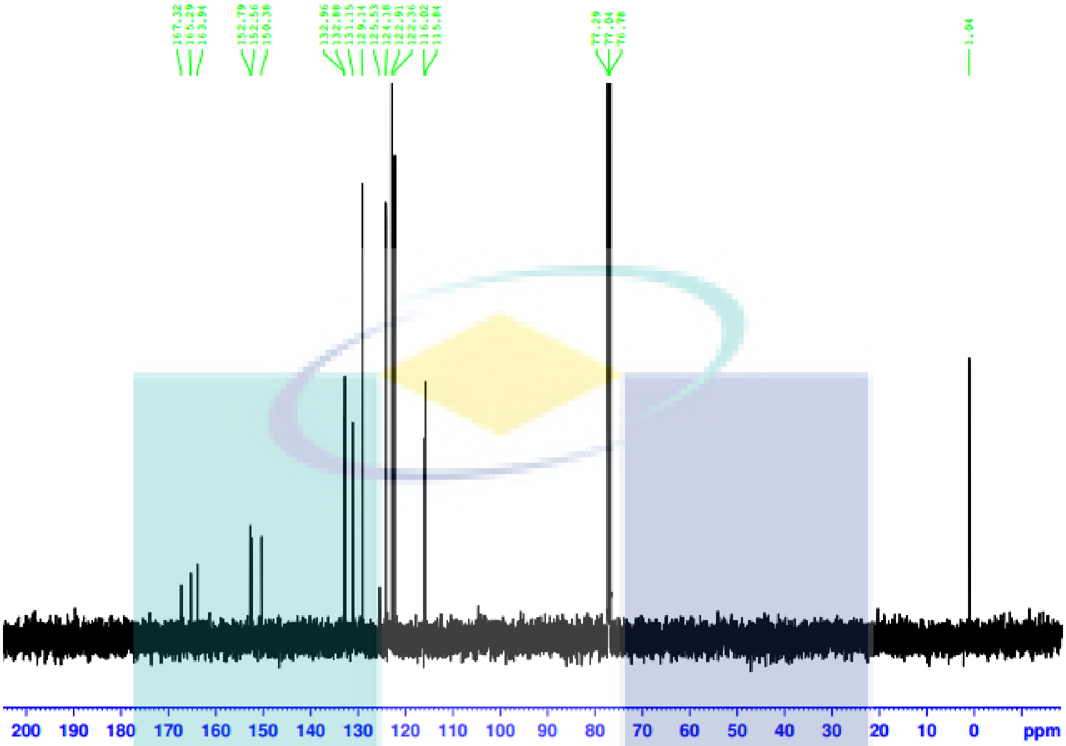

^{13}C-NMR Spectra for Compound N

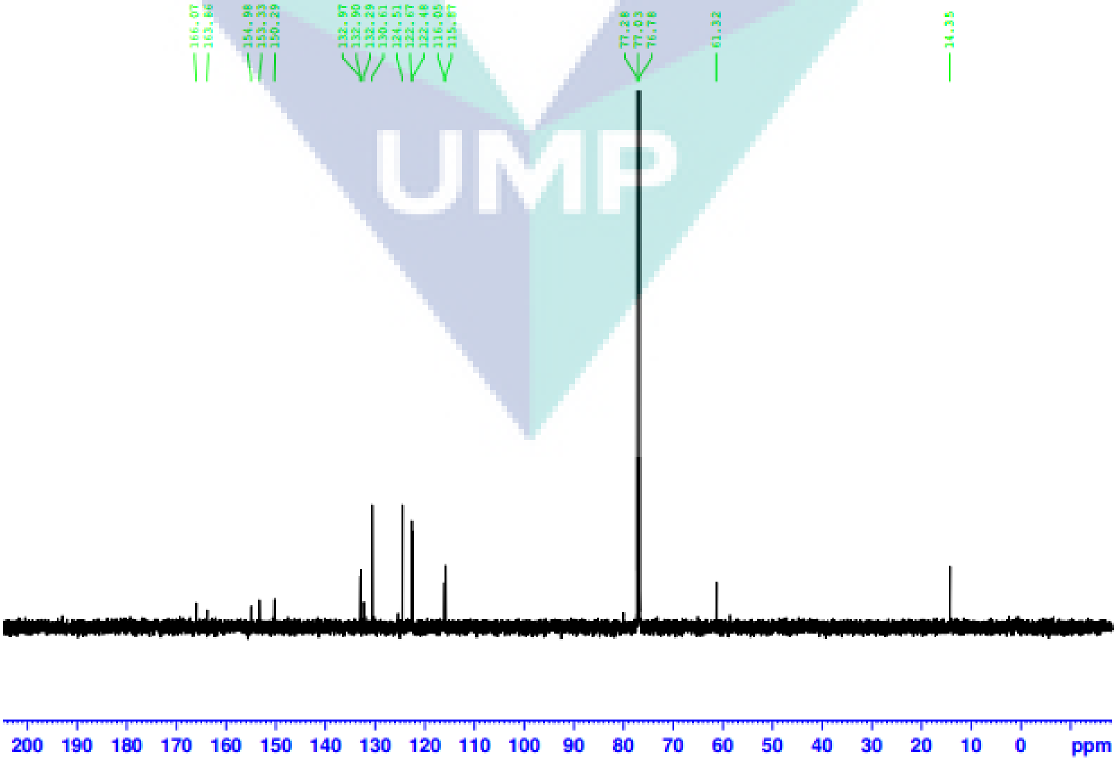

APPENDIX D

FT-IR Spectra for Compound S

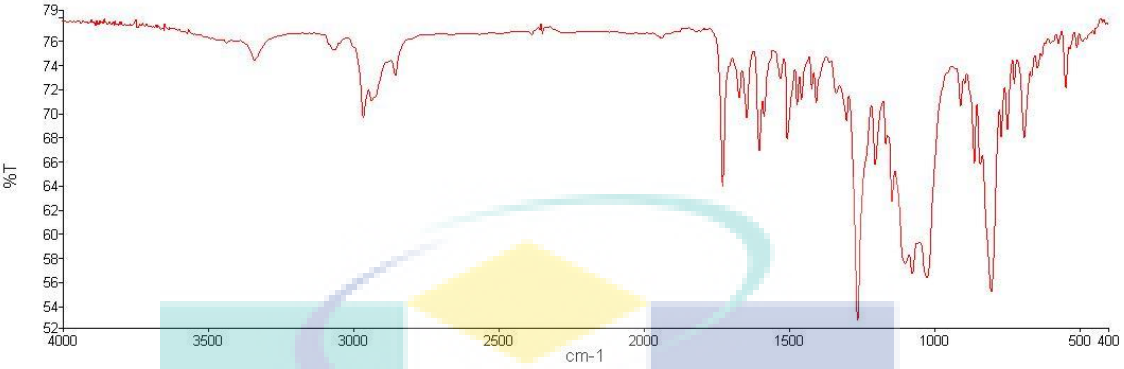

FT-IR Spectra for Compound V

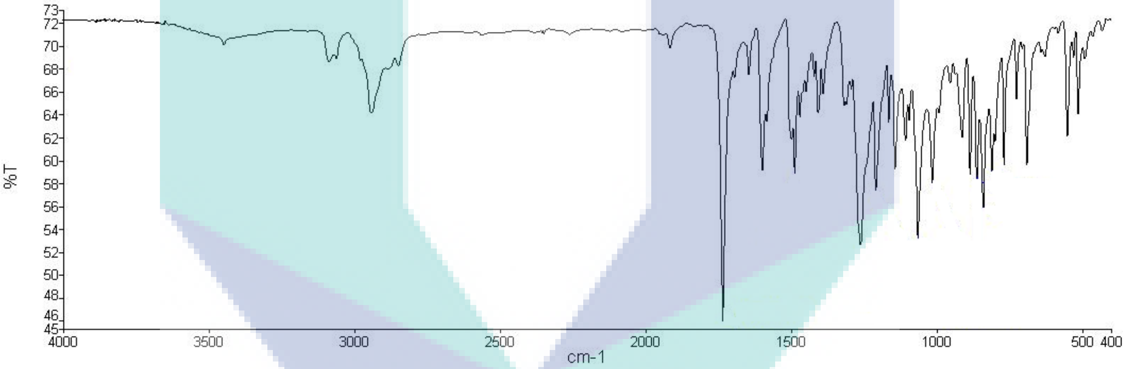

^{1}H-NMR Spectra for Compound S

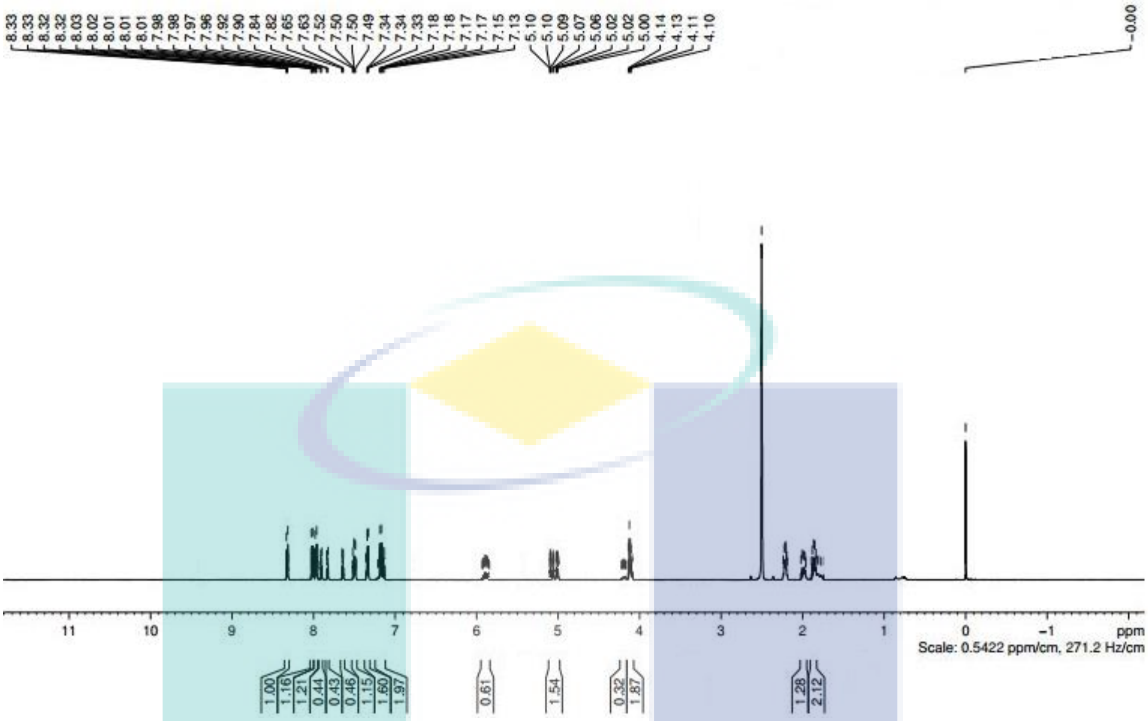

^{13}C-NMR Spectra for Compound S

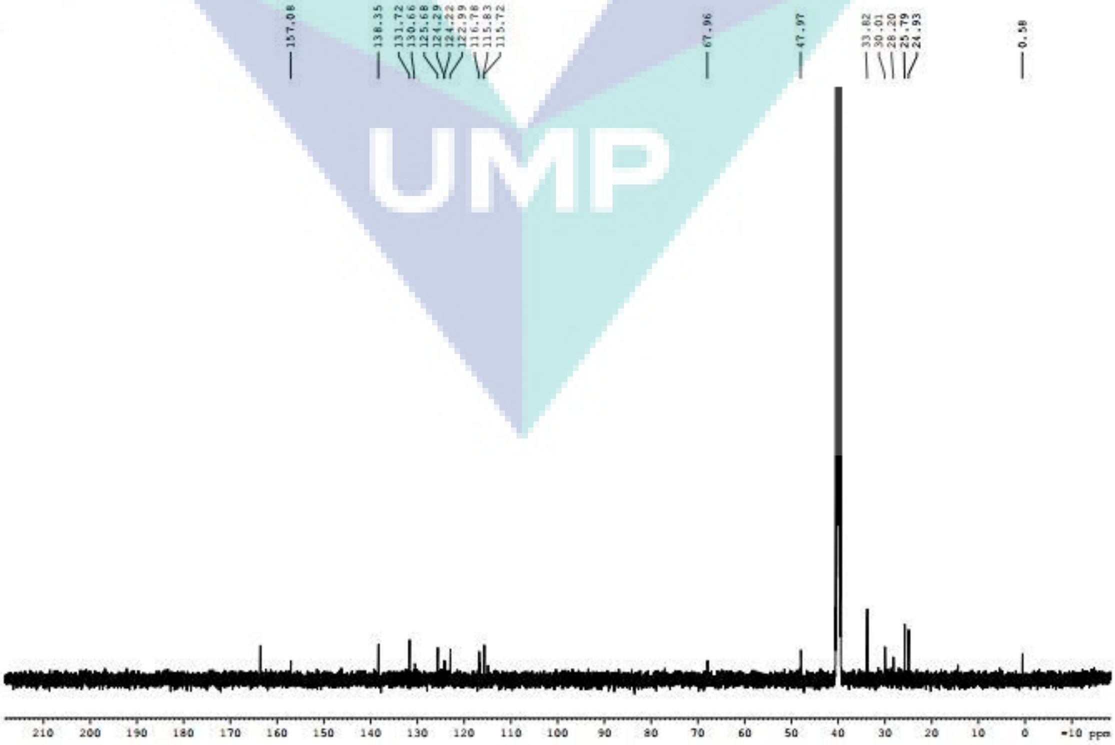

^{13}C-NMR Spectra for Compound V

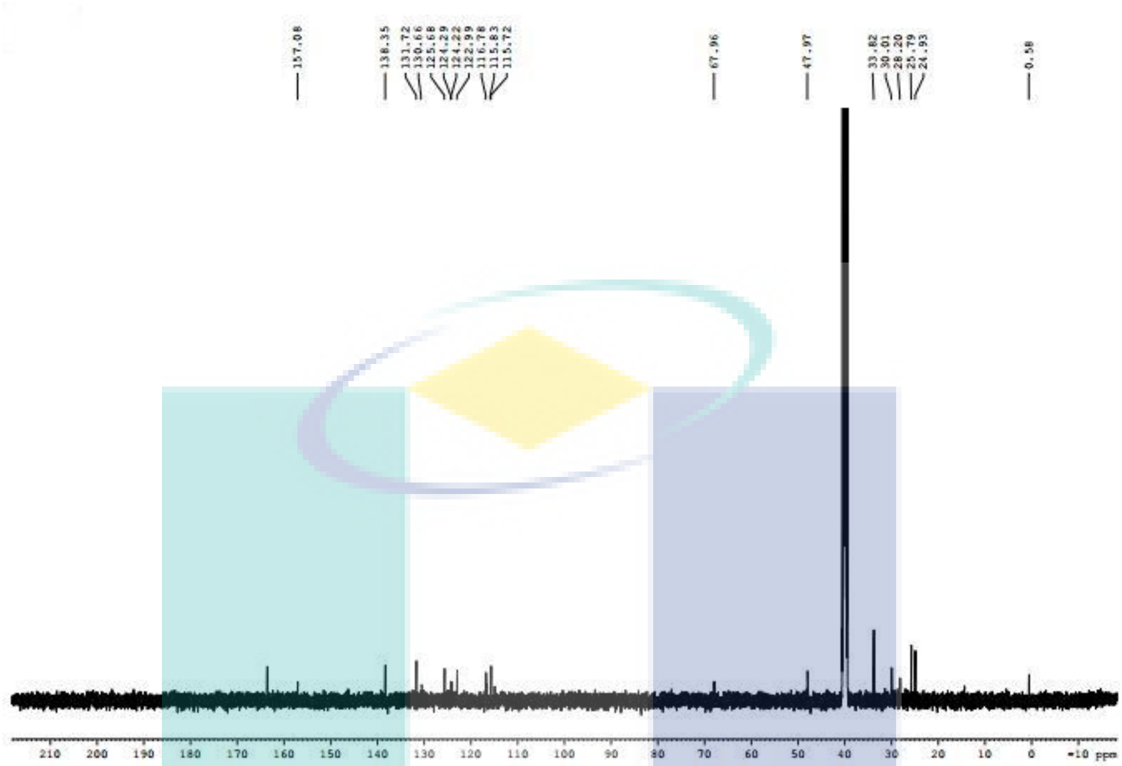

ACHIEVEMENTS

Achievements	Award Authority	Venue	Year
Best Invention of the Asia Pacific Rim	The Invention & New Product Exposition (INPEX)	USA	2014
Winner for Best Poster Competition	28th Regional Conference on Solid State Science and Technology (RCSSST)	Cameron Highland	2014
Gold Medal, Best Award, and Green Technology Award	Malaysia Technology Expo (MTE)	PWTC	2014
Gold Medal	22th Internaltional Invention, Innovation & Technology Exhibition (ITEX)	KLCC	2014
2 Gold Medals	National Innovation and Invention Competition Through Exhibition (iCompEx)	POLIMAS	2014
Silver Medal	The 2nd International Innovation, Design and Articulation (I-IDeA)	UiTM, Perlis	2014
Gold Medal and Silver Medal	Creation, Innovation, Technology & Research Exposition (CITREX)	UMP	2014
Bronze Medal	Malaysia Technology Expo (MTE)	PWTC	2015
Silver Medal	26th Internaltional Invention, Innovation & Technology Exhibition (ITEX)	KLCC	2015

PUBLICATIONS

1. S. M. Gan, A. R. Yuvaraj, M. R. Lutfor, M. Y. Mashitah, Hegde G, (2015). Synthesis, liquid crystal characterization and photo-switching studies on fluorine substituted azobenzene based esters. *RSC Advances*. **5**: 6279.

2. Yuvaraj, A. R., Mei, G. S., Kulkarni, A. D., Mashitah, M. Y., Hegde, G. (2014). Aliphatic/aromatic spacers based azo dye dimers: synthesis and application for optical storage devices. *RSC Advances*. **4**(92): 50811-50818.

3. Mei, G. S., Yuvaraj, A. R., Kabeb, S. M., Yusoff, M. M., Chigrinov, V. G., Hegde, G. (2014). Biocompatible Polymer Embedded In Light-Sensitive Materials: Investigation Of Structural Properties. *International Journal of Automotive and Mechanical Engineering (IJAME)*. **10**: 2025-2033.

4. Gan, S. M., Pearl, Z. F., Yuvaraj, A. R., Lutfor, M. R., Gurumurthy, H. (2015). Polarity dependent photoisomerization of ether substituted azodyes: Synthesis and photoswitching behavior. *Spectrochimica Acta Part A: Molecular and Biomolecular Spectroscopy*. **149**: 875-880.

CONFERENCES

1. Hegde, G., Yuvaraj, A. R., Mei, G. S., Mustapha, S. A., Yusoff, M. M., Chigrinov, V. G. (2014). Biocomposite polymer embedded with light-sensitive molecules for plastic displays. In *SPIE OPTO* (pp. 90050B-90050B). International Society for Optics and Photonics.

2. Gan Siew Mei, Yuvaraj AR, Lutfor MR, Mashitah Yusoff, Gurumurthy Hegde, Amide based azodyes and their behavior with light, ICPVS-2014.

3. Mei, G. S., Yuvaraj, A. R., Lutfor, M. R., Yusoff, M. M., Hegde, G. Photosensitive Bent Core Liquid Crystals for Optical Storage Devices. MUCET 2013.

4. Gurumurthy Hegde, Gan Siew Mei, Shu Ting Chua, Yuvaraj A R, Mashitah M Yusoff, Zainab bt Ngaini, Ainaa Nadiah bt Abd Halim, Carolynne Sie. Photo-crosslinking Permanent Optical Storage Devices Using Biocompatible Kojic Acids. MUCET 2014.

PATENT

A composition for the use of WORM display: PI2014701167, 2014.